© 2010

Anushree Karnik

ALL RIGHTS RESERVED

AN ADAPTIVE SENSORIMOTOR REPRESENTATION FOR REACHING IN THE INFERIOR PARIETAL LOBULE OF BEHAVING MONKEYS

By Anushree Karnik

A dissertation submitted to the

Graduate School – Newark

Rutgers, The State University of New Jersey

in partial fulfillment of the requirements

for the degree of

Doctor of Philosophy

Graduate Program in Integrative Neuroscience

written under the direction of

Professor Ralph M. Siegel

and approved by

_____

_____

_____

_____

_____

Newark, New Jersey

October, 2010

ABSTRACT

An Adaptive Sensorimotor Representation for Reaching in

the Inferior Parietal Lobule of Behaving Monkeys

By Anushree Karnik

Thesis director: Professor Ralph M. Siegel

Primates use visual guidance in order to interact with their environment. For several decades, the inferior parietal lobule (IPL) has been known to contain neurons that respond to visual stimulation and motor behavior. While the neural activity during the reaching behavior has been shown in area 7a of IPL, reach related neural responses have never been tested in the dorsal prelunate area (DP) of IPL, which is adjacent to area 7a. Furthermore, neural response prior to the reaching movement has not been assessed in DP and area 7a. The first aim was to investigate the tuning properties of single neurons in DP and area 7a. The second aim was to assess the influence of eye position signal on reaching behavior. Third, the temporal evolution of sensorimotor transformation in area 7a and DP neurons was investigated by comparing neural signals throughout the reaching task. Lastly, cortical plasticity was tested using Fresnel prisms, which displaced the visual field by 12º in one of four directions: contralateral, ipsilateral, upwards, or downwards. Foveal and peripheral reaching tasks and reaching under perceptually distorted conditions were used. Neurons in area 7a and DP were observed to have differential tuning properties during the planning phase and the initiation of the reach, in addition to being selective for eye position and retinal visual stimulation. The response properties of the neurons in areas 7a and DP changed as the trial progressed in time.

Differential preparatory and reach responses were observed during foveal and peripheral reaching. This implies that both eye position and retinal signals modulated the reach related responses. Alterations in spatial tuning of the neurons during all phases of the task were observed upon insertion of the Fresnel prisms imply that neural plasticity occurs as the cortex swiftly adapts to the mismatch between sensory input and motor output. The spatial tuning of the neurons did not merely compensate for the eye position shift implying that signals other than eye position affect the neural response during reaching. These combined results strongly support the claim that crucial aspects of sensorimotor transformation occur in areas 7a and DP.

ACKNOWLEDGMENTS

The completion of this thesis would have been impossible without the contribution of all the people mentioned below. I extend my greatest gratitude to each and every one of them.

First and foremost, I would like to thank my thesis advisor, Prof. Ralph M. Siegel, for providing me with the best guidance, advice, support, and resources. He always encouraged me to set higher goals and just when I thought I had reached my limit, he helped me realize I could extend myself even further. Thank you Ralph for believing in me and allowing me countless opportunities to expand my horizons. Thank you for introducing me to many other leading scientists in our field and providing me with an opportunity to complete a research rotation at Salk! I cannot imagine being able to do that without your support and faith. Thank you for your excellent technical training and your patience when it came to data analysis and especially programming. I cannot thank you enough for your help with securing a post-doctoral position at the Salk Institute!!! Most importantly, thank you for showing me how interesting and intriguing research is. You are absolutely right – asking questions and coming up with ways to answer them is far more interesting than being in a classroom. Thank you! Thank you! Thank you!

I would also like to thank Dr. Barbara Heider for providing me the excellent training in electrophysiology. Thank you, Barbara, for showing me the proper way to conduct experiments (from setup to completion). Thank you for training me in other techniques (e.g.: rat perfusions) and building my confidence even when I made many errors. Thanks a ton for being so patient and for all of your time providing input and advice throughout my thesis project. I also can't thank you enough for the numerous

reviews of this dissertation and all of your suggested edits. You have become more than a colleague, but also a friend. Thank you for all those Swiss chocolates – I will surely miss them.

I would also like to thank Jasmine Siegel. You were the best over the past five years. Thank you for teaching me the basics of working with monkeys and training me to handle them. Your confidence in me allowed to me progress even though; I was apprehensive about working with monkeys at times. All those conversations during monkey-business and coffee breaks were awesome. They definitely set a good balance between work and fun while I was in the lab. You have helped me to grow not only as a researcher, but also as a person. I have learned a great deal about culture, psychology, politics, and many other important things in life. I cannot thank you enough for the friendship and the balance that you provided me with throughout graduate school.

I would like to thank all the members of the Siegel Lab – past and present. Dr. Milena Raffi: Even though you and I never really worked together, communicating with you about experiments was very helpful. Thank you very much Milena, for providing me with support, advice and understanding that I needed during the initial years of my graduate career. Thank you for hosting me in Italy and giving me an opportunity to present a talk at the University of Bologna. Reuben Meltzer, Sam Kallus, Adam Butensky, and Danny Michaelis– thank you very much for your excellent technical assistance. I cannot imagine completing my experiments without your help. Adam, thank you for providing me with an opportunity to mentor a student; I have learned a great deal from you.

I would like to thank my thesis committee chair, Prof. Bart Krekelberg, for providing me with important advice when I needed it and a lab away from my own. Thank you, Bart, for providing me with encouragement, support, advice, and resources. In addition, thank you for making sure that I performed to the best of my abilities when it came to writing journal club reports and presenting papers. Thank you also for providing a class for which learning MATLAB was a must. Although programming was not my cup of tea, getting me familiarized with coding in MATLAB was one of the most important skills I learned. Mostly, thank you for all your advice.

I would like to thank my thesis committee: Prof. Denis Pare, Prof. Elizabeth Abercrombie, Prof. Esther Gardner, and Prof. Bart Krekelberg for their advice and guidance throughout my graduate studies. All of you have given me extremely valuable input on my thesis project. Your advice was priceless.

I would also like to thank the animal facility and the veterinary staff. Larry Barbour and Juan Rodriguez, thank you very much for your assistance and overseeing the wellbeing of our monkeys. Drs. Elizabeth Dodemaide and David Reimer: In addition to your excellent veterinary support, I would like to thank you for providing me with education regarding starting an I.V. and intubation during each surgery. I learned a lot each time. Jason Presutti, Robert Stonaker, Robert Goodwin, and Manuel Montero: Thank you very much for taking care of the monkeys by giving them food, water, and clean cages to live in. I always found them very happy; my project would not have been successful without your help.

I would like to thank the Newark crew. Amanda Fakira, Sona Goswami, Amber Ziegler, Katie Dickerson, Olga Rodriguez – my fellow TA, Kurt Fakira – my other fellow

TA, Bengi Altinbilek, Till Hartmann, Adam Morris, and Jacob Duijnhouwer: Thank you very much for having random science and non-science conversations with me. You all definitely destressed me from my work. Sona, what will I do without my twin? Till, thank you very much for helping me out with MATLAB issues and I will never forget the days on South Orange Ave!!! Adam, thank you for all the discussions we have had about my project; thank you for your input and statistics advice.

Jessica Wright and Samhita Dasgupta – I am going to miss all the crazy times and our coffee breaks!!! Thank you for being my turf when I needed to fall back on something. Thank you very much for all your time that you devoted for my whine sessions. Those were very therapeutic. Our dinners are very memorable. Thank you both for listening to my talks numerous times on numerous occasions and giving me valuable feedback. Jess and Sam, you guys are the best – don't know how I would sort out my personal life without you. Thank you so much for your irreplaceable friendship.

Arielle Schmidt, my roommate of four years!!! Thank you a ton and more for always being there. I cannot imagine how I would have done the 40 minute daily commute without your company; in fact I am not sure if I could function normally had you not been there with me in graduate school. Our politically incorrect zone proved to be the perfect destressor. Thank you so much on various occasions for staying at school until the very late hours for me and reducing my parents' worries in half. Thank you for motivating me to go to the gym – something I had been putting off for about five years. Most importantly, thank you very much for the irreplaceable friendship. Thank you for everything!!!

Now for the people who have always been with me every step of the way, who have cheered with me for my accomplishments and provided a shoulder to lean on when the stress of everything got just a little overwhelming. My greatest debt is to my parents, Smita and Prashant Karnik, for their encouragement, support, and faith in me and my abilities. You never doubted that I could accomplish anything and I thank you for that and making me believe in myself. I thank you for making sure that I reached home safely, staying up during very late night hours, and waiting for me to have dinner just so I would not have to eat alone. Thank you for caring. My brother, Ankush Karnik, has been the best role model for me for my entire life. Thank you for setting a good example and expecting nothing but the best from me. I would also like to thank my sister-in-law, Sameeta Karnik, for being the sister that I never had. Your company at home is something I will miss tremendously once I move. Thank you also for helping me with the images and movies for this dissertation. I would like to thank my parents-in-law, Jyotsna and Sudhakar Karkhanis for giving me the added motivation that I needed to finish. I would also like to thank my grandparents on both sides for having faith in me that I will be able to write the salutation “Dr.” in front of my name one day! Finally, a very special thanks to Nikhil, for his love, faith, and patience. Nikhil, you set my life in balance and provided me with extra energy to complete my dissertation. Our weekends spent together were a perfect break from work which energized me when I returned. Thank you for believing in me when I thought I wouldn’t be able to write my thesis. Thank you very much for being supportive of my decision to go to Salk! Thank you for understanding me. Most importantly thank you for always being there for me!!!

TABLE OF CONTENTS

Abstract ii

Acknowledgements iv

List of tables xiii

List of illustrations xiv

Chapter 1: General introduction 1

OVERVIEW 1

ANATOMICAL LOCATION OF AREA 7A AND THE DORSAL PRELUNATE (DP) AREA IN NON-HUMAN PRIMATES 3

FUNCTIONAL ANATOMICAL CONNECTIONS OF DP AND AREA 7A 3

Dorsal Prelunate area (DP) 3

Area 7a 6

FUNCTIONAL SIGNIFICANCE OF THE ANATOMICAL CONNECTIONS IN IPL 8

DP 8

Area 7a 10

Combined functional properties of DP and area 7a 13

REACHING AND RELATED PROPERTIES OF PARIETAL AND PREFRONTAL AREAS 16

Inferior parietal lobule (IPL) 17

Superior parietal lobule (SPL) 20

The premotor areas 22

Summary 24

CORTICAL PLASTICITY 25

Summary 28

RATIONALE 29

Chapter 2: General Methods 31

ANIMAL PREPARATION 31

EXPERIMENTAL SETUP 32

VISUAL STIMULI 33

BEHAVIORAL TASK 34

NEURAL RECORDINGS 36

SPIKE ANALYSIS 37

Statistical analysis 40

Chapter 3: Neural representation of visually guided reaching in macaque posterior parietal cortex 46

INTRODUCTION 46

MATERIALS AND METHODS 48

Behavioral task 48

Statistical analysis 49

RESULTS 50

Behavioral data 50

Electrophysiological data 52

SUMMARY 69

DISCUSSION 70

Behavioral data 70

Caveats 72

Chapter 4: Spatial effects of shifting prisms on neuronal properties of posterior parietal cortex 73

INTRODUCTION 73

MATERIALS AND METHODS 75

Behavioral task 75

Statistical analysis 76

RESULTS 77

Behavioral data 77

Electrophysiological data *82*
SUMMARY 112
DISCUSSION 113
Behavioral data *113*
Caveats *114*

Chapter 5: General Discussion 117

OVERVIEW 117
WHY USE A RADIAL REACHING MOVEMENT? 123
EVOLUTION OF THE NEURAL SIGNAL DURING FOVEAL REACHING 125
Baseline and visual response *125*
Preparatory response *126*
Reach response *127*
EVOLUTION OF THE NEURAL SIGNAL DURING PERIPHERAL REACHING 128
Baseline and visual response *128*
Preparatory response *128*
Reach response *129*
REACH RELATED RESPONSE IN DP 130
DIFFERENTIAL NEURAL RESPONSE FOR FOVEAL AND PERIPHERAL REACH 131
MODULATION OF VISUAL, PREPARATORY, AND REACH RESPONSES DUE TO PRISMATIC DISTORTION 133
Baseline response *133*
Visual response *134*
Preparatory response *134*
Reach response *135*
EFFECT OF PRISMATIC DISTORTION ON BEHAVIORAL ADAPTATION AND CHANGES IN SPATIAL TUNING RESULTING IN CORTICAL PLASTICITY 136
Behavioral adaptation *136*
Cortical plasticity *137*
Do the tuning properties return to the original tuning properties after removing the Fresnel prism? *141*
SENSORIMOTOR TRANSFORMATION 143

SUMMARY 149
FUTURE DIRECTIONS 150

Appendix A: Abbreviations 152

Appendix B: Complete description of categorical regression analysis 153

OBJECTIVE 153
BENEFIT OF STEPWISE REGRESSION 153
GENERAL PROCEDURE 153
CRITERIA TO CHOOSE THE BEST MODEL 154
R-squared criterion 154
Mallow's C_p criterion 155
AN EXAMPLE OF THE STEPWISE REGRESSION ANALYSIS FOR ONE NEURON 156

Appendix C: Two way analysis of variance 163

References 167

Curriculum vitae 177

LIST OF TABLES

Chapter 1: General introduction

TABLE 1.1 5

Chapter 4: Spatial effects of shifting prisms on neuronal properties of posterior parietal cortex

TABLE 4.1: DISTRIBUTION OF CXP TYPE NEURONS DURING THE BASELINE EPOCH 94
TABLE 4.2: DISTRIBUTION OF CXP TYPE NEURONS DURING THE VISUAL EPOCH 95
TABLE 4.3: DISTRIBUTION OF CXP TYPE NEURONS DURING THE PREPARATORY EPOCH 98
TABLE 4.4: DISTRIBUTION OF CXP TYPE NEURONS DURING THE REACH EPOCH 100
TABLE 4.5: DISTRIBUTION OF CXP TYPE NEURONS WITH SPATIAL TUNING SHIFTS IN VARIOUS DIRECTIONS 107

LIST OF ILLUSTRATIONS

Chapter 1: General introduction

FIGURE 1.1: IMAGE OF A MACACA MULATTA BRAIN 3
FIGURE 1.2: CORTICAL CONNECTIONS OF DP AND AREA 7A 10

Chapter 2: General Methods

FIGURE 2.1: RECORDING CHAMBERS 32
FIGURE 2.2: TEMPORAL PROGRESSION OF A TRIAL OF THE VISUALLY GUIDED REACHING TASK 34
FIGURE 2.3: EXAMPLE OF A SORTED NEURON USING PLEXON 37
FIGURE 2.4: EXAMPLE OF A PERI-STIMULUS TIME HISTOGRAM (PSTH) WITH SUNCHRONIZED EVENTS AND EPOCHS OF INTEREST 38

Chapter 3: Neural representation of visually guided reaching in macaque posterior parietal cortex

FIGURE 3.1: ILLUSTRATIONS OF THE EYE POSITION VARYING (EVAR) AND THE RETINAL VARYING (RVAR) CONDITIONS 48
FIGURE 3.2: REACH ENDPOINTS OF ONE TYPICAL EXPERIMENT DURING THE EVAR AND RVAR CONDITIONS 50
FIGURE 3.3: DISTRIBUTION OF MEAN BEHAVIORAL TIMES FOR THE RVAR AND THE EVAR CONDITIONS 51
FIGURE 3.4: RESPONSE OF AN AREA 7A NEURON EVAR CONDITION 54
FIGURE 3.5: RESPONSE OF A DP NEURON DURING EVAR CONDITION 56
FIGURE 3.6: RESPONSE OF AN AREA 7A NEURON DURING RVAR CONDITION 59
FIGURE 3.7: RESPONSE OF A DP NEURON DURING RVAR CONDITION 61
FIGURE 3.8: POPULATION DISTRIBUTION OF EPOCH BASED COMPARISON 62
FIGURE 3.9: PREPARATORY RESPONSE DURING EVAR AND RVAR CONDITIONS 64
FIGURE 3.10: REACH RESPONSE DURING EVAR AND RVAR CONDITIONS 67
FIGURE 3.11: POPULATION DISTRIBUTION OF CONDITION BASED COMPARISON 67

Chapter 4: Spatial effects of shifting prisms on neuronal properties of posterior parietal cortex

FIGURE 4.1: REACH ENDPOINT ACCURACY AND RAPID ADAPTATION TO PRISMS 78

FIGURE 4.2: DISTRIBUTION OF MEAN BEHAVIORAL TIMES FOR THE PRE-PRISM AND THE PRISM CONDITIONS..... 81

FIGURE 4.3: A NEURON'S RESPONSE DURING THE PRE-PRISM CONDITION 84

FIGURE 4.4: A NEURON'S RESPONSE DURING THE PRISM CONDITION..... 87

FIGURE 4.5: A NEURON'S RESPONSE DURING THE POST-PRISM CONDITION 89

FIGURE 4.6: POPULATION DISTRIBUTION OF EPOCH BASED COMPARISON..... 90

FIGURE 4.7: RESPONSE OF A NEURON DURING BASELINE AND VISUAL EPOCHS OF THE PRE-PRISM AND PRISM CONDITIONS 93

FIGURE 4.8: RESPONSE OF A NEURON DURING PREPARATORY EPOCH OF THE PRE-PRISM AND PRISM CONDITIONS..... 97

FIGURE 4.9: RESPONSE OF A NEURON DURING REACH EPOCH OF THE PRE-PRISM AND PRISM CONDITIONS..... 99

FIGURE 4.10: POPULATION DISTRIBUTION OF PRE-PRISM VS. PRISM COMPARISON 101

FIGURE 4.11: RESPONSE OF A NEURON DURING PRE-PRISM AND PRISM CONDITIONS 103

FIGURE 4.12: POPULATION OVERVIEW OF SPATIAL TUNING MODULATION.....105

FIGURE 4.13: DIFFERENT TUNNING PROPERTIES OF A NEURON DURING PRE-PRISM AND POST-PRISM CONDITIONS.....110

FIGURE 4.14: POPULATION DISTRIBUTION OF PRE-PRISM VS. POST-PRISM COMPARISON.....111

Chapter 1:
General introduction

Overview

Reaching under visual guidance involves multiple modalities. One needs to visually identify the reaching target relative to one's body in space or relative to an external reference point. This must be followed by the proprioceptive input of the hand location relative to the object in space. The visual and the proprioceptive information must be then integrated in order to compute a motor plan to successfully initiate and execute the reaching action. In order to do this, multiple neural areas are recruited. Many electrophysiology studies in non-human primates have identified areas in the parietal lobe that are involved in the execution of a successful reach. Human and non-human lesion studies exemplify the importance of the parietal lobe in the planning, initiation, and execution of the reaching behavior.

For example, the Bàlint syndrome, defined by a set of three visuospatial and visuomotor deficits (optic ataxia, optic apraxia, simultaneous agnosia), affects mostly *visually guided* reaching, that is, patients can reach properly without visual guidance with tactile control, but are impaired when reaching to a visually presented object. The Bàlint syndrome is caused by bilateral lesions of posterior parietal cortex in humans (Bàlint, 1909; Pisella et al., 2000; Battaglia-Mayer and Caminiti, 2002). Transcranial magnetic stimulation (TMS) of the posterior parietal cortex (PPC) of humans disrupted the ability to correct or alter the path of the reaching movement when the reach behavior was goal directed and visually guided (Desmurget et al., 1999).

In non-human primates, unilateral lesions of area 7a, an area of the PPC, resulted in gross inaccuracies in reaching for an object with the contralateral hand (Lamotte and Acuna, 1978). These inaccuracies in reaching intensified while grasping an object in the contralateral visual field (Faugier-Grimaud et al., 1985). Lesions of different areas of the PPC can have distinct effects on reaching behavior (Rushworth et al., 1997b, a). Bilateral lesions of area 7a (along with areas 7b and the lateral intraparietal area – LIP) disrupted reaching to visual targets in light, whereas lesions of areas 7b, 5, and medial intraparietal (MIP) mostly affected reaching movements in the dark (Rushworth et al., 1997b).

The PPC, being a part of the association cortex, receives multimodal input explaining the heterogeneity of its functional properties. The areas of the PPC are involved in the analysis of visual information needed for planning and execution of saccades (rapid and ballistic eye movements), reaching, and other body movements. Thus, the cells of the PPC respond to visual, proprioceptive and somatosensory stimulation, and to motor behavior. These modalities are thought to be combined into a sensorimotor efferent signal. Furthermore, the heterogeneity and interconnectivity of the parietal lobe increases its ability to be plastic.

This introduction will address the anatomical location and connections, and the physiological properties of two areas of the PPC: area 7a and the dorsal prelunate area (DP). Additionally, it will discuss the rationale for the experiments conducted for the dissertation.

Anatomical location of area 7a and the dorsal prelunate (DP) area in non-human primates

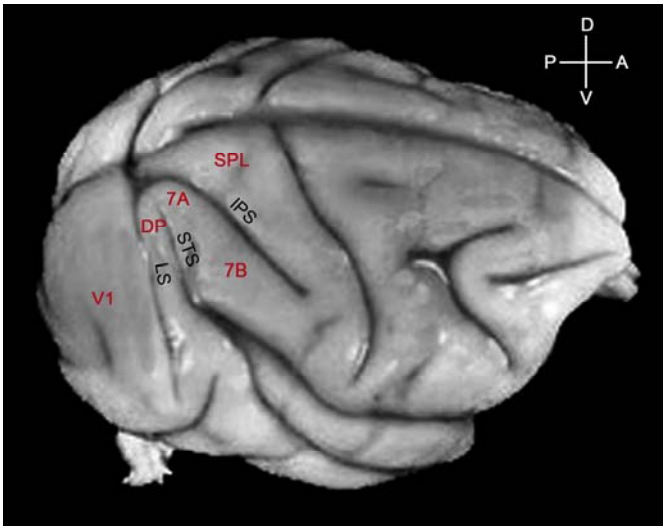


Figure 1.1: **Image of a Macaca mulatta brain**. Cortical areas are labeled in red: SPL, superior parietal lobule; 7a, area 7a; 7b, area 7b; DP, dorsal prelunate area; V1, primary visual area. Area 7a, 7b, and DP are part of the inferior parietal lobule (IPL). The sulci bordering the IPL are labeled in black: IPS, intraparietal sulcus; STS, superior temporal sulcus; LS, lunate sulcus. The IPS marks the boundary between the SPL and the IPL. The LS marks the boundary between V1 and DP. The STS runs through the IPL. Modified from: http://brainmuseum.org/Specimens/primates/rhesusmonkey/brain/Rhesusmonk6.jpg

The intraparietal sulcus (IPS) divides the PPC into two main regions: the superior parietal lobule (SPL) and the inferior parietal lobule (IPL; Fig. 1.1). The SPL includes the medial intraparietal area (MIP), parieto-occipital area (PO), and area 5. The IPL includes area 7a, and adjacent area 7b, DP, LIP, and anterior intraparietal area (AIP) (Rizzolatti and Matelli, 2003). IPL is bordered by the IPS and the lunate sulcus (LS) (Fig. 1.1).

Functional anatomical connections of DP and area 7a

Dorsal Prelunate area (DP)

DP predominantly receives visual information via extrastriate areas: V2 (Stepniewska et al., 2005), V3A, and V4 (Andersen et al., 1990; Tanaka et al., 1990). Projections from V2 and V3A arise from regions that represent the peripheral visual field

(Baizer et al., 1991). Similarly, the reciprocal projections that DP receives from V4 arise from the peripheral representation regions of V4 (Ungerleider et al., 2008).

The middle superior temporal (MST) area and DP are reciprocally connected (Andersen et al., 1990). Connections between middle temporal area (MT) and DP, and inferotemporal cortex (IT) and DP have also been observed (Stepniewska et al., 2005). Both MST and MT contain motion selective neurons, therefore explaining the motion sensitivity of DP (Raffi and Siegel, 2007).

LIP and DP have reciprocal connections (Andersen et al., 1990; Blatt et al., 1990; Baizer et al., 1991; Rozzi et al., 2006). In addition to LIP, the ventral intraparietal area (VIP) also has connections with DP (Baizer et al., 1991; Lewis and Van Essen, 2000). DP projects predominantly to area 7a and receives input from parieto-occipital area (PO; both areas V6 and V6A). Area 7a has efferent connections with DP (Andersen et al., 1990).

Retrograde and anterograde tracer studies have shown that the posterior cingulate cortex (PCC) has reciprocal connections with DP (Kobayashi and Amaral, 2007 2007). There are equal feedback and feedforward projections between PCC and DP. Since the neurons in PCC respond to orbital eye position signals (Olson et al., 1996) these reciprocal connections may explain the eye position signal observed in DP (Siegel et al., 2003). The frontal eye fields (FEF) and DP are also connected (Stepniewska et al., 2005), which may also explain the eye position signal observed in DP.

Even though there have been a number of anatomical studies investigating the connections of DP, these connections have not been tested for functionality. Area 7a has a strong feedback projection to DP implying that DP is involved in reaching. However there is no study that investigates the reach related activity in DP.

Area	Eye position		Visual		Preparatory		Reach		Spatial	
	DP	7a	DP	7a	DP	7a	DP	7a	DP	7a
V1										
V2	***		***							
V3/V3A	***		***							
V4			***							
MT			***							
STS			***	***						
IT			***							
MST			***	***						
STP				***				***		
PO			***	***	***	***	***	***		
V6/V6A	***	***	***	***	***	***	***	***		
MIP			***	***	***	***	***	***		
LIP	***	***	***	***						
VIP			***	***			***	***		
AIP			***	***			***	***		
DP		***		***		***				
7a	***		***		***		***			
SEF		***								
FEF	***	***								
PMd						***		***		
PCC	***	***								
CA1										***
pulvinar				***						

Table 1.1: Cortical connections of DP and area 7a. Reciprocal connections between various cortical areas and DP; and those between various cortical areas and area 7a are listed. The connections are separated based on the functional importance. A list of abbreviations is included in Appendix A. The asterisks denote a bidirectional connection. The "visual" column includes signals regarding retinotopy and other visual information such as for example, a signal for motion detection in DP and area 7a that may arise from MST. The "spatial" column includes connections that may enable neurons in area 7a to encode the extrapersonal space.

Area 7a

Anatomical studies have shown that extrastriate areas have feedforward connections to 7a via cortico-cortical connections (Pandya and Seltzer, 1982; Cavada and Goldman-Rakic, 1989b, a; Andersen et al., 1990; Felleman and Van Essen, 1991). Two areas in the temporal lobe, the superior temporal sulcus (STS) and the parahippocampal gyrus, receive a dense projection from area 7a (Andersen et al., 1990). The projections from area 7a to the STS dominate the anterior bank of the STS, which includes the superior temporal polysensory area (STP) (Bruce et al., 1981) and the medial superior temporal area (MST); fundus of the STS; and the rostral aspect of the STS which is within the inferotemporal cortex (IT; Andersen et al., 1990). Rizzolatti and Matelli (2003) demonstrated that area 7a receives inputs from the STP. Since STP encodes information regarding visual space and action (Bruce et al., 1981), it is possible that area 7a responds to reaching to specific locations. Furthermore, STP neurons show high selectivity to motion stimuli (Anderson and Siegel, 1999). Since area 7a receives efferents from MST, which receives extensive projections from MT, this may be the reason for motion selectivity of area 7a neurons (Read and Siegel, 1997; Siegel and Read, 1997; Raffi and Siegel, 2007).

Areas within the parietal lobe are reciprocally interconnected; parieto-occipital area (PO), LIP, MIP, AIP, and DP have visual efferents to area 7a and receive an afferent

signal from area 7a (Pandya and Seltzer, 1982; Colby et al., 1988; Cavada and Goldman-Rakic, 1989b, a; Andersen et al., 1990; Felleman and Van Essen, 1991). The eye position signal in LIP can explain the eye position dependent visual response modulation (gain field) observed in area 7a (Siegel et al., 2003).

A monosynaptic bidirectional connection is present between area 7a and the dorsolateral prefrontal cortex (Cavada and Goldman-Rakic, 1989a) which is involved in motor planning (Andersen and Cui, 2009). Specifically, the dorsal premotor area (PMd) receives direct projections from area 7a (Tanne et al., 1995). The supplementary eye fields (SEF) also have monosynaptic bidirectional connections with area 7a (Andersen et al., 1990). The SEF and the FEF consist of neurons that are spatially tuned to eye movement. However there are only weak connections between the FEF and area 7a (Andersen et al., 1990; Lewis and Van Essen, 2000; Clower et al., 2001). The caudal portion of the cingulate gyrus also had monosynaptic bidirectional connections with area 7a (Andersen et al., 1990). Area 7a has equal strength of ipsilateral and contralateral connections with the posterior cingulate cortex (PCC). Laminar pattern of projection suggests that the posterior cingulate cortex and area 7a have equal proportion of feedback and feedforward projection (Andersen et al., 1990).

Area 7a receives topographical afferents from the medial pulvinar. The medial pulvinar consists of disk-like aggregates of neurons (Asanuma et al., 1985). Rostrally and caudally located neurons project to the rostral and caudal parts of area 7a respectively; whereas, laterally and medially located neurons project to medial and lateral parts of area 7a (Asanuma et al., 1985). The visual signal in area 7a may be partially attributed to the pulvinar (Asanuma et al., 1985) in addition to DP and other areas. Area 7a has no

connections with the superior colliculus (Andersen et al., 1990; Lewis and Van Essen, 2000; Clower et al., 2001).

The CA1 area of the hippocampal formation sends a disynaptic efferent signal to area 7a. This projection to area 7a arises from the pyramidal cell layer within the central strip of the CA1 region. This connection is bidirectional however it does not create a closed loop. Monosynaptic efferents from area 7a terminate in a region that is rostral and distal to the region of CA1 that sends efferents to area 7a (Clower et al., 2001). Lesions of both, the hippocampus and the PPC result in increased difficulty for spatial navigation (Barrash, 1998; Barrash et al., 2000).

Functional significance of the anatomical connections in IPL

Physiological studies provide information about the functions of the anatomical connections. The IPL is a multimodal area considering the cortico-cortical and the subcortico-cortical connectivity.

DP

Neurons in DP are driven by motion stimuli (Siegel and Read, 1997). DP is reciprocally connected to areas that respond selectively to motion stimuli: MT (Stepniewska et al., 2005) and MST (Andersen et al., 1990).

Electrophysiological studies have shown that the response of the neurons in DP is modulated by gain field (Andersen et al., 1985; Andersen et al., 1990; Read and Siegel, 1997; Siegel et al., 2003). That is, the visual response of the neurons varies depending on the angle of gaze (position of the eye). An intrinsic imaging study revealed that DP

contains a topographic map of the gain field representation; DP represents the upper eye positions (Siegel et al., 2003). These topographical gain field maps were reproduced over days. The eye position responses in DP are a result of the projection from LIP (Andersen et al., 1990; Blatt et al., 1990; Baizer et al., 1991; Rozzi et al., 2006); or feedback projections from area 7a (Andersen et al., 1990); FEF (Stepniewska et al., 2005), and PCC (Kobayashi and Amaral, 2007 2007). Of these areas, the strongest reciprocal connection is between area 7a and DP, followed by connections between LIP and DP; FEF and DP; PCC and DP.

An intrinsic imaging study has shown that neurons in DP have retinotopic fields (Heider et al., 2005). Unlike the gain field maps, the retinotopic field maps were not constant over days in DP; these maps altered from day to day. DP receives projections from the periphery representing regions within early visual areas V2, V3A (Baizer et al., 1991), and V4 (Ungerleider et al., 2008). Feed forward projections from these periphery representing regions likely contribute to the retinotopic representation in DP.

Optical imaging has also revealed the presence of topographic representation of attention over DP (Raffi and Siegel, 2005), albeit this representation was bilateral. These attentional maps, which appeared in patches, altered over days. The spatial locations of these patches altered over days however the frequency of the patches remained constant. Lastly, the attention patches were observed to be embedded within the constant eye position gain field maps in DP. It is likely that the attentional signal observed in DP is due the indirect connection of DP to the pulvinar via area 7a. Area 7a is innervated by projections form the pulvinar (Asanuma et al., 1985), which is known to be involved in

the attention circuitry (Shipp, 2004; Reep and Corwin, 2009). DP and area 7a have extensive reciprocal connections (Andersen et al., 1990).

There have been no studies investigating the reach related responses in DP. DP receives projections from V6A (Andersen et al., 1990). Area V6A is involved in reach movement planning (Fattori et al., 2005). Neurons in area V6A are spatially tuned to the direction of the arm movement. Moreover, DP and area 7a have extensive reciprocal connections (Andersen et al., 1990). Thus it is hypothesized that neurons in DP also selective respond to visually guided reaching. The behavioral paradigms are designed to investigate the spatial tuning of the neurons in DP during the reaching phase of the task.

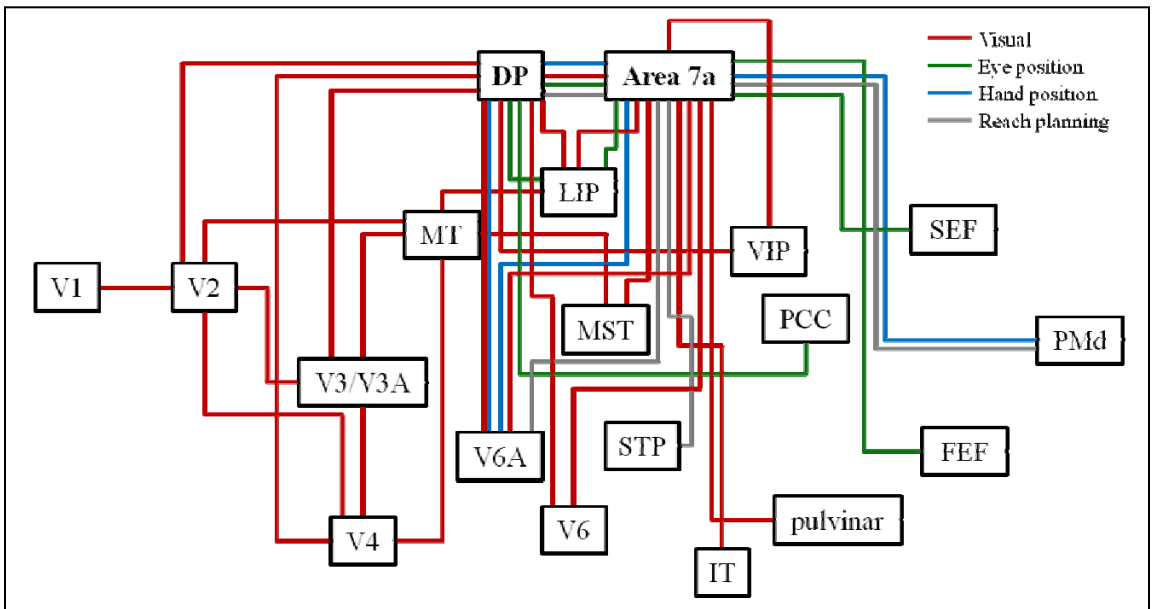


Figure 1.2: Cortical connections of DP and area 7a. Cortical connections that provide information regarding the signals investigated in the current experiments are shown here. Connections shown in red provide visual information; green provide eye position information; blue provide information regarding the hand position; gray provide information regarding planning of the reaching behavior. All Abbreviations are included in Appendix A.

Area 7a

Area 7a neurons prefer the translational optic flow displays over the rotational optic flow stimuli (Siegel and Read, 1997; Read and Siegel, 1997). More specifically,

these neurons have an even greater preference to expanding optic flow stimuli compared to the compression optic flow stimuli (Siegel and Read, 1997; Read and Siegel, 1997). This is likely due to the apparent motion observed as one walks in the environment. The selective response to motion stimuli could also be due to the reciprocal connections between area 7a and MST (Andersen et al., 1990). Additionally, DP and area 7a have extensive reciprocal connections (Andersen et al., 1990); DP received projections from the motion selective area, MT (Stepniewska et al., 2005). Therefore, due to the indirect connection with MT, perhaps area 7a neurons posses motion selective properties.

The gain of the neural response in area 7a is modulated differentially by the position of the eyes in the orbit; these neurons therefore, have gain fields (Andersen et al., 1985; Andersen et al., 1990; Read and Siegel, 1997; Siegel and Read, 1997; Siegel et al., 2003). An optical imaging experiment revealed that area 7a contains a topographical gain field map; lower eye positions are represented over area 7a (Siegel et al., 2003). Area 7a has reciprocal connections with areas that contain spatial eye position signals: LIP (Andersen et al., 1990; Blatt et al., 1990; Baizer et al., 1991; Rozzi et al., 2006), SEF (Andersen et al., 1990), FEF (Andersen et al., 1990; Lewis and Van Essen, 2000; Clower et al., 2001), and PCC (Andersen et al., 1990). PCC and area 7a and SEF and area 7a have equal feedback and feedforward projections. DP and area 7a have extensive bidirectional projections, efferents from DP innervate area 7a (feedforward projection) whereas area 7a sends a feedback projection to DP (Andersen et al., 1990).

Electrophysiology studies (Andersen et al., 1985; Andersen et al., 1990; Read and Siegel, 1997; Siegel and Read, 1997; Siegel et al., 2003) have shown that neurons in area 7a are driven differentially by the retinal location of the visual stimulus. Optical imaging

while monkeys detected change in stimulus motion in the periphery revealed that retinotopy is topographically mapped over area 7a (Heider et al., 2005). Area 7a receives a majority of its visual input from DP and LIP. It is likely that the peripheral representing regions in the early visual cortical areas that project to DP indirectly influence the visual properties of the neurons in area 7a. The retinotopic maps observed in area 7a were not reproduced from day to day (Heider et al., 2005). Therefore, retinotopic representation in area 7a is plastic.

Attention modulation has been observed in area 7a using electrophysiology (Bushnell et al., 1981; Quraishi et al., 2007) and optical imaging (Raffi and Siegel, 2005). Topographical representation of spatial attention was observed in area 7a however, the attention maps were not reproducible within the regions of area 7a (Raffi and Siegel, 2005). The maps were observed to be embedded within the gain field topography; attention maps altered in cortical location however the frequency was maintained. Area 7a receives topographical afferents from the medial pulvinar (Asanuma et al., 1985). Output from the SC innervates the pulvinar prior to proceeding to the cortical areas (Shipp, 2004). This pathway is a part of the attention circuitry (Shipp, 2004; Reep and Corwin, 2009). It is therefore likely that the projection from pulvinar to area 7a drives attentional modulation in area 7a and is responsible for the topographical organization.

It has been known for decades that the neurons in area 7a respond to visually guided reaching (Hyvarinen and Poranen, 1974; Mountcastle et al., 1975; Blum, 1985; MacKay, 1992; Battaglia Mayer et al., 1998; Battaglia-Mayer et al., 2005; Battaglia-Mayer et al., 2007). Electrophysiology experiments testing the reach-related responses in area 7a have observed that neurons in area 7a are spatially tuned to arm movements

(Battaglia-Mayer et al., 2005; Battaglia-Mayer et al., 2007). Area 7a has reciprocal connections with regions of the SPL that are involved in the reaching behavior: MIP and PO (Pandya and Seltzer, 1982; Colby et al., 1988; Cavada and Goldman-Rakic, 1989b, a; Andersen et al., 1990; Felleman and Van Essen, 1991). Projections from PO to area 7a are of the feedforward type and those from area 7a to PO are of feedback type (Andersen et al., 1990). Area MIP and the dorsal aspect of the PO, which is on the rostral wall of the parieto-occipital sulcus, are a part of what is defined as the "parietal reach region" (PRR) (Cohen and Andersen, 2002). PRR is known to respond to the planning of a visually guided reach (Batista and Andersen, 2001; Scherberger and Andersen, 2007). It is likely that the reach properties of area 7a neurons are a result of projections from the combined regions within the PRR.

Although neurons with spatially tuned reach responses have been observed in area 7a, the paradigms used to test this involved a constant visual feedback of the reaching arm. This may have confounded the neural response observed during the reaching phase. In the current study, a reach paradigm excluding the visual feedback of the hand is used to test the reach response of the neurons. Furthermore the eye positions and the endpoint locations of the reach hand are varied systematically to investigate the spatial properties of the neurons. The reach paradigm and the reach related properties of the neurons in area 7a are discussed in greater detail in the subsequent sections of the thesis.

Combined functional properties of DP and area 7a

Response to visual stimuli: Neurons in area 7a and DP receive afferent information from areas that are implicated in motion and spatial analysis (Baizer et al., 1991) which explains why these areas are selective to motion (Siegel and Read, 1997)

and highly spatially tuned (Andersen et al., 1985; Andersen et al., 1990). The DP neurons receive inputs from the peripheral field representation of V2, V3A, and V4 (Neal et al., 1988; Baizer et al., 1991). This explains the distributed representation of space observed in area 7a and DP.

Sensorimotor properties: Based upon an early study the connectivity between area 7a and area 5, a predominantly somatosensory area in the SPL, explains the visual and somatic convergence in area 7a (Hyvarinen and Poranen, 1974). In addition to the attentional, visual, and somatic convergence, neurons in area 7a have visuomotor properties, i.e., the response of these neurons is correlated with reaching behavior (Hyvarinen and Poranen, 1974; Mountcastle et al., 1975; Blum, 1985; MacKay, 1992). These neurons have the ability to command the movement of the limbs in immediate extrapersonal space (Mountcastle et al., 1975). Neurons in area 7a encode spatial visuomotor signals for the eye and the hand (Battaglia-Mayer et al., 2005).

The bidirectional projections between area 7a and the PCC and between DP and PCC might explain the neural response elicited by the eye position and eye movements. An increase in neural activity in the PCC was observed at the onset of the saccade and dependent on the orbital position of the eye (Olson et al., 1996). Thus it is suggestive that PCC monitors the eye position and may be involved in assigning spatial coordinates to retinal images. The connectivity of area 7a and the premotor cortex (Kurata, 1991; Tanne et al., 1995; Wise et al., 1997; Stepniewska et al., 2006) possibly influence the reach related activity observed in area 7a.

Neurons in area 7a respond to reaching to specific spatial locations. Neurons of the hippocampal area CA1 project to area 7a. These neurons are known to encode spatial

localization and navigation. Thus the connectivity between CA1 and area 7a may partially explain the visuomotor spatial representation in area 7a, for example during reaching behavior to specific locations in space.

The spatially tuned reaching activity observed in area 7a largely follows an eye-centered coordinate system (Battaglia-Mayer et al., 2007). Both LIP (Stricanne et al., 1996) and PRR (Batista et al., 1999; Cohen and Andersen, 2002) have been shown to follow an eye-centered reference frame during planning of an eye or reach movement. Since both LIP and parts of PRR have strong projections to area 7a, it is likely that neurons in area 7a also follow an eye-centered reference frame.

Both LIP and PRR neurons have a gain field modulation (Cohen and Andersen, 2002) and thus are claimed to be the locus of reference frame transformations. Gain field modulation is defined as the eye position dependency of the change in neural activity (Andersen et al., 1985; Cohen and Andersen, 2002). Neurons in area 7a also show gain field modulation (Andersen et al., 1985). Thus it can be hypothesized that the IPL including areas 7a and DP are involved in the reference frame transformation.

Attentional modulation: Bushnell and Robinson (1981) conducted single unit recordings in area 7a while the monkeys were required to attend peripherally and foveally. Under both conditions the visual response was modulated, showing that attention influences the neural response in area 7a. Attentional maps (Raffi and Siegel, 2005) and attentional modulation of receptive field structures (Quraishi et al., 2007) have been observed in area 7a and DP. The projection from the medial pulvinar is one probable source for selective attention resulting in overall attentional modulatory effects. A human study shows a correlation between increased attention and increased activation

of the medial pulvinar (Coull et al., 2004). Additionally, PCC neurons' response is altered by attentional demands and visual stimuli, for example, they signal the saliency of stimuli over large visual space (Dean et al., 2004). A decrease in response amplitude was observed when monkeys were required to divide their attention between targets (Dean et al., 2004). Area 7a shares these properties which may have come from the reciprocal connections between the two areas.

In summary, the reciprocal connectivity of areas 7a and DP with areas expressing specific and combined sensory and motor modalities explains the heterogeneity of the neural responses. Area 7a and DP both respond to visual stimulation, motor behavior, and visually guided reaching. Both areas contain a distributed representation of space. The visuomotor signals follow an eye centered frame of reference. Thus there is reason to hypothesize that these areas are involved in sensorimotor transformation leading to a successful completion of a reaching behavior. Based on the reciprocal connections between area 7a and DP and DP's connections to other reach-related areas within the PPC, there is reason to hypothesize that DP neurons are involved in visually guided reaching.

Reaching and related properties of parietal and prefrontal areas

The reaching action requires multiple levels of processing. Once an object of interest is spatially located, the visual (sensory) input needs to be transformed into a goal directed motor output. This process recruits multiple cortical networks or cortical areas. Extracellular single unit recording is the main method used to study the cortical areas involved in different aspects of reaching in non-human primates. These electrophysiology

studies have shown that the areas involved in reaching include: Areas 7a (Hyvarinen and Poranen, 1974; Mountcastle et al., 1975; Blum, 1985; MacKay, 1992; Battaglia Mayer et al., 1998; Battaglia-Mayer et al., 2005; Battaglia-Mayer et al., 2007) of the IPL, the PRR (specifically area V6A of the SPL) (Batista and Andersen, 2001; Scherberger and Andersen, 2007), and the PMd (Jouffrais and Boussaoud, 1999; Gregoriou and Savaki, 2003) of the prefrontal cortex. Areas that are related to reaching but not directly involved will not be discussed. These areas include: LIP in the IPL; AIP and VIP in the SPL; FEF, SEF and PCC in the prefrontal cortex. Each section below addresses the reaching and related properties in IPL, SPL, and the premotor areas.

Inferior parietal lobule (IPL)

In general, areas of the IPL respond to eye positions (area 7a and DP), saccades (LIP), retinotopic field, somatosensory stimulation (area 7b), visually guided reaching (area 7a and DP), grasping (area 7b), and attention. Taken together the IPL is thought to encode information regarding spatial localization of objects and reaching behavior since 1953 (Critchley, 1953). However, systematic investigation regarding the integration of multimodal inputs and the spatial tuning properties of the neurons is only being done recently (Battaglia-Mayer et al., 2005; Battaglia-Mayer et al., 2007). It has been suggested that area 7a is involved in computing the location of the visual target (Shadmehr and Wise, 2005). Area 7a neurons have been observed to respond to the actual action of reaching and the initiation of reaching (Battaglia-Mayer et al., 2005; Battaglia-Mayer et al., 2007). “Intentional” reach related response (Snyder et al., 1997) and reach related activity during the memory period during the delayed reaching task (Battaglia-

Mayer et al., 2007) have been reported in area 7a. Studies in which the neural response in area 7a during reaching was explored are considered next.

Area 7a: Area 7a neurons have the ability to relay information regarding the movement of the limbs in immediate extrapersonal space (Mountcastle et al., 1975). Reach related responses were first observed by Hyvarinen and Poranen (1974) and Mountcastle et al. (1975). In both studies, area 7 neurons were observed to respond to arm projections and reaching when the monkeys reached for desired objects that they were fixating either to the right or the left of the midline. Reaching blindly in the dark to previously visually identified object elicited no response in these neurons (Mountcastle et al., 1975). However, a task requiring reaching in the periphery was not used in this study, thus peripheral reaching responses were not tested. Furthermore, the variation in the response of these neurons as the monkeys reached to different spatial locations was not systematically tested.

Blum (1985) characterized the neurons in the IPL that responded to reach as visually sensitive or insensitive. This study considered area 7, which contains areas 7a and 7b, and tested whether these neurons respond to reaching with or without visual guidance. Both types of cells were found in area 7. To test visually guided reaching, the monkeys were required to fixate a spot of light in the center of the monitor. Moreover, the monkeys were required to reach to only one location. Thus the characteristics of the neural response as a result of spatial variation were not tested.

MacKay (1992) observed that about 50% of area 7a neurons that responded to the reaching behavior were spatially tuned for both arms. The spatial tuning for both arms was identical, suggesting the neurons have bilateral response fields. Neurons that

responded to movements of only one of the two arms often preferred the contralateral response field. Area 7a neurons were also observed to respond to visual stimuli. Although this study showed that area 7a neurons were bimodal, the relationship between the visual and the motor signal was not assessed.

Other studies have shown that neurons in area 7a encode spatial visuomotor signals for both eye and hand (Battaglia Mayer et al., 1998; Battaglia-Mayer et al., 2005; Battaglia-Mayer et al., 2007) suggesting that sensorimotor transformation occurs in the IPL. Battaglia-Mayer et al. (2005) recorded neural responses from area 7a while the monkeys were required to perform a multitude of tasks including, memory reach, memory saccade, memory reach and saccade, reaching in the periphery, saccade and reach, and no-go task. It was observed that neurons in area 7a responded to both, eye and hand signals. Moreover, the eye and the visual signals were found to influence the hand signal. Both eye and hand movements elicited directionally selective activity in area 7a. Differential neural responses observed during the pre-reach interval of the memory reach task and the no-go task suggest that neurons in area 7a respond to the planning of the reaching behavior. Area 7a neurons overrepresented the contralateral workspace; the overall response of the units during all tasks was greater when the monkeys made a saccade and/or a reach in the contralateral workspace.

Battaglia-Mayer et al. (2007) observed that neural activity in area 7a was modulated by the retinal location of the visual stimulus, the eye position, the eye movement, and the hand movement. Neurons in area 7a responded to the onset of the visual stimulus as well as to the motor cue for just the hand movement, saccade, and a coordinated eye-hand movement. The observed activity was the greatest when the

monkeys reached to a foveated location, reached to a peripheral location, and maintained fixation during a delayed reach task. This suggests that area 7a is involved in the processing of visually guided reaching.

DP: There have been no studies to date in which visually guided reaching response was measured in this area. The eye position signals have been demonstrated in DP by intrinsic optical imaging (Siegel et al., 2003). DP was observed to consistently represent the upper eye positions using the hemodynamic signal in superficial cortical layers. The current experiments will investigate the reach responses in DP.

Superior parietal lobule (SPL)

The SPL consists of areas 5, MIP, and PO. Area PO is further divided into area V6A and V6 based on functional (Galletti et al., 1995; Galletti et al., 1996) and cytoarchitectural (Luppino et al., 2005) differences. The ventral area V6 is a purely visual area and consists of eye position signals (Galletti et al., 1995; Galletti et al., 1996), whereas the dorsal area V6A consists of visuomotor signals specific to visually guided reaching and grasping (Galletti et al., 1995; Galletti et al., 1996; Galletti et al., 1997; Fattori et al., 2001; Fattori et al., 2005). Area MIP and the dorsal aspect of the PO (area V6A) together form the PRR (Cohen and Andersen, 2002). Neurons of the SPL show strong activation during visually guided reaching behavior (Caminiti et al., 1996). Studies suggest that area 5 and PRR play a critical role in the transformation between the eye and hand centered representations (Batista et al., 1999; Burnod et al., 1999; Xing and Andersen, 2000).

Area 5: During the memory period of a delayed reach task, neurons in area 5 were observed to encode the location of the reach target in both eye and hand centered

reference frames (Buneo et al., 2002; Buneo et al., 2008). Neural response of area 5 was observed to increase at the onset of the arm movement, the final endpoint of the arm movement, or a combination of the two (Lacquaniti et al., 1995). This neural response was derived to be in a body centered frame of reference. Neurons in area 5 that encode information in an eye centered reference frame are distinct from those that encode information in hand centered reference frame. This implies that area 5 is critical in reference frame transformation.

PRR: This area shows neural activation during the planning stage of reach movements (Batista and Andersen, 2001; Scherberger and Andersen, 2007). It encodes the location of reach targets in an eye centered reference frame during the memory phase of a delayed reach task (Batista et al., 1999). Neural response in PRR is strongly modulated by visual input (Snyder et al., 2000; Buneo et al., 2003; Buneo et al., 2008). Area V6A of the SPL and a part of the PRR (Shipp et al., 1998) contain neurons that encode direction of the arm movement (Fattori et al., 2005). Direction of gaze modulated the reach response of about two-thirds of the neurons in area V6A (Fattori et al., 2005; Marzocchi et al., 2008).

Studies have also shown that the PRR is active during the perisaccadic time period in a delayed saccadic task (Snyder et al., 2000). Eye position signals for PRR are likely to come from areas V6 and V6A. Area V6 has feedforward connections to area V6A; eye position signals have been observed in area V6 (Galletti et al., 1995; Galletti et al., 1996; Luppino et al., 2005). Area V6A neurons are sensitive to eye position (Galletti et al., 1995) and respond to saccades (Nakamura et al., 1999; Kutz et al., 2003). Proprioceptive eye position signals might also originate from primary somatosensory

cortex (Wang et al., 2007). This anatomical organization explains the perisaccadic response in the PRR. While the PRR is crucial during the planning of the reaching behavior, planning of saccadic activity does not occur in the PRR; the activity is seldom pre-saccade (Snyder et al., 2000). The presence of both the eye position signal and the reach response suggest that this area is involved in integrating multiple signals to derive a motor behavior. The fact that the eye position signal modulates that pre-reach response implies that the sensorimotor transformation occurs in an eye-centered reference frame.

The premotor areas

The IPL (including area 7a) and the premotor areas are connected via bidirectional projections (Kurata, 1991; Wise et al., 1997; Stepniewska et al., 2006) resulting in a direct input of visual information. This visual information can be used to generate visually guided reaching movements (Caminiti et al., 1996; Wise et al., 1997; Jouffrais and Boussaoud, 1999) or for object identification to produce accurate grasping movements (Fogassi et al., 2001; Raos et al., 2006). The dorsal aspect of the premotor cortex (PMd) and the ventral aspect of the premotor cortex (PMv) have distinct functional properties (Tanne-Gariepy et al., 2002). The PMd is involved in visually guided reaching (Boussaoud et al., 1998) whereas the PMv generates accurate arm positioning and grasping behavior (Fogassi et al., 2001).

PMd: The neurons in the dorsal premotor area (PMd) respond to limb movements that are guided by sensory information, including visually guided reaching (Caminiti et al., 1996; Wise et al., 1997; Jouffrais and Boussaoud, 1999). The pre-movement activity in the PMd area implies that this region is involved in movement planning (Boussaoud and Wise, 1993; Hoshi and Tanji, 2000, 2006). Boussaoud et al (1998) observed

differential neural responses which were linearly dependent on the eye position in the PMd. In general, PMd neurons encode the eye position, hand position, and the reach target location in space (Pesaran et al., 2006; Batista et al., 2007).

When monkeys were required to reach to foveated targets and peripheral targets, the neural response differed further confirming that the PMd encodes hand movements based on the eye-position (Jouffrais and Boussaoud, 1999). Forelimb reaching activity and saccade related activity was reported in the PMd area (Gregoriou and Savaki, 2003). The ventral aspect of PMd can be associated with visually guided reaching as neurons in these regions responded when the monkeys reached under illuminated conditions and did not respond when reaching was done in the dark. These neural responses were greater when the monkey reached during fixation compared to reaching while performing saccades (Gregoriou and Savaki, 2003). Thus, the neural response in the ventral aspect of the PMd area is modulated by angle of gaze (Boussaoud et al., 1993; Mushiake et al., 1997; Boussaoud et al., 1998; Gregoriou and Savaki, 2003). The dorsal aspect of PMd, on the other hand, responded to reaching behavior in both light and dark conditions. This property can be attributed to response to reaching activity under somatosensory or motor-memory (non-visual) guidance (Gregoriou and Savaki, 2003).

The gaze signal was persistent during the reaching movement suggesting that the eye position modulated the reach response (Boussaoud et al., 1998). Since the gaze direction or the eye position modulated the reach response, it was thought that the eye position signal was persistent throughout the trial, from identifying the target location to the completion of a reach (Boussaoud and Bremmer, 1999). In general it was observed that the retinal influence deceases, movement representation increases and the eye

position signal was maintained throughout the reach task in PMd (Boussaoud and Bremmer, 1999). This implies that the arm movement signal in the PMd is strongly modulated by the eye position.

PMv: The neural response in PMv was modulated by sensory stimuli (Boussaoud et al., 1993; Fogassi et al., 1996) and this activity increased upon the initiation of a reaching movement (Kurata and Hoshi, 2002). The strong connectivity between the parietal cortex and PMv (Cavada and Goldman-Rakic, 1989a; Kurata, 1991), and the primary motor cortex and PMv (Muakkassa and Strick, 1979) together result in the visually guided reaching activity in the PMv. Inactivation of the ventral premotor area (PMv) resulted in an inappropriate hand posture and an inaccurate hand shape preceding the grasping action (Fogassi et al., 2001). Neurons in the PMv responded to both the grasping action as well as to a visual object presentation (Raos et al., 2006). Neural response in the PMv reflects the spatial localization of the visual targets (Hoshi and Tanji, 2000, 2006). Many neurons have visual receptive fields that are fixed to certain body parts and are modulated by attention (Graziano and Gross, 1998).

Summary

The parietal and premotor areas are discussed due to their reciprocal projections to and from areas 7a and DP and their involvement in the reach circuitry. Parts of the parietal lobe and the premotor cortex are involved in the reach: the PRR, area 7a, and PMd. There are strong bidirectional connections between the IPL and the SPL and PMd. Therefore neurons in area 7a may respond to the computation involved in reaching to a specific spatially located visual stimulus. Area 7a could serve as the source for the PRR signals or vice versa. Both the PRR and the PMd are active during the planning stage of

the reaching behavior. Most reaching studies in area 7a so far have focused on responses at the onset or during the visually guided reaching movement, and less is known about reach planning activity in 7a.

Cortical plasticity

Cortical plasticity is known to occur in the adult brain. For example, changing the attentional demands alters the cortical activation in parietal cortex. An intrinsic imaging study showed that area 7a and DP contain attentional map which alter from day to day (Raffi and Siegel, 2005). At the single cell level, attentional modulation was demonstrated across various areas (Bender and Youakim, 2001; Quraishi et al., 2007). The attentional state can even alter the structure of receptive fields in area 7a (Quraishi et al., 2007). Covert attentional demands modulated the neural response in the IPL (Bushnell and Robinson, 1981). A decrease in neural response of neurons in V4 and IT when the unattended visual stimulus was in the receptive field of the neuron was demonstrated (Moran and Desimone, 1985). Alteration of retinotopic maps over days was demonstrated in areas 7a and DP (Heider et al., 2005). Shifting the position of the attended target resulted in a partial shift of the center of mass of the visual receptive fields of the neurons in MT towards the shifted attention target (Connor, 2006; Womelsdorf et al., 2006).

Cortical plasticity has been demonstrated in early sensory cortex by inducing gross experimental changes in sensory input, for example fusing the digits of the hand (Allard et al., 1991) which altered representation in somatosensory cortex over months. Focal lesions of the retina resulted in alteration in the systematic retinotopic

representation in V1 and V2 (Kaas et al., 1990); the altered cortical representations now represented the area surrounding the focal lesions of the retina (Darian-Smith and Gilbert, 1995). The orientation tuning properties of V1 neurons showed short-term shifts when exposed to an orientation that is orthogonal to the preferred orientation (Schummers et al., 2005).

Not only does change in sensory input alter the cortical representation; but perceptual learning can also induce plasticity. Monkeys that were trained on an orientation discrimination task for a particular retinal location improved their performance over time. With an improvement in the performance, cortical plasticity was observed. Neurons in V4 that had receptive field overlapping the trained retinal location had narrower tuning curves compared to other neurons (Yang and Maunsell, 2004; Raiguel et al., 2006). Orientation adaptation and orientation discrimination training resulted in altered tuning curves for V1 neurons (Teich and Qian, 2010).

These studies show that cortical representations are not always stable and can change when cognitive demands vary or sensory input alters as a result of experimental perturbation further confirming that neural plasticity occurs even in the adult brain. In the studies mentioned above, cortical representation was altered via daily changes and changes in cognitive state, attention, gross experimental changes, adaptation, and perceptual learning. Below is an overview of cortical malleability resulting from a combination of alteration of sensory input, attentional modulation, adaptation, and perceptual learning.

Neural plasticity of V1 neurons occurred when monkeys were required to wear horizontally inverting prisms continuously as the responses of V1 neurons were

monitored (Sugita, 1996). The inverting prisms resulted in enlarged receptive fields of V1 neurons, that is, contralateral receptive fields expanded into the ipsilateral visual field. The enlargement in the receptive field properties i.e. cortical plasticity occurred in conjunction with behavioral adaptation. The monkeys perceptually learned and therefore adapted to their altered (horizontally reversed) environment.

Similar results were observed for the tuning properties of PMv neurons (Kurata and Hoshi, 2002). In this study, the visual field was displaced by 10º either to the left or right. Monkeys were trained to reach to the physical location of the reaching target and not the perceived location (perceived to be displaced due to the prismatic distortion). Prism adaptation was very rapid in this experiment. Differential neural response was observed when the monkeys were required to reach to the target under different prism conditions. Visual targets were always along the same coordinates however the maintaining fixation was not mandatory and eye position was not recorded for one out of three monkeys.

Prism adaptation in humans induced long-term alterations in cortical representation of space (Luaute et al., 2009). Differential cortical activation was observed during the baseline (pre-prism condition), prism condition and the post exposure condition (post-prism condition). After prism exposure, short-term behavioral plasticity was also observed.

Behavioral plasticity occurs along with cortical plasticity. Upon inserting a prism and perturbing the visual field, both human and non-human primates initially missed the target but adapted to the distortion and increased reach accuracy over time (Flook and McGonigle, 1977; McGonigle and Flook, 1978; Kurata and Hoshi, 2002; Marotta et al.,

2005; Kurata, 2007; Luaute et al., 2009). This adaptation occurred due to the error feedback that was received while the subject attempted to reach under prismatic distortion (Healy et al., 1973; Redding and Wallace, 1996). Visual feedback from a previous trial was used to increase reaching accuracy for the next trial (Rossetti et al., 1993). Thus, prism adaptation occurred rapidly over a few trials. Once the prism was removed, subjects initially reached incorrectly in the opposite direction of the prism shift (Redding et al., 2005). Again, the reaching accuracy was increased as subjects performed more and more trials. The feedback timing was determined to be critical for adaptation to occur; reach accuracy did not increase if the feedback was delayed for more than 500 ms (Kitazawa and Yin, 2002).

Summary

Cortical plasticity occurs as a result of a wide range of alterations. Minor cognitive changes can result in alteration of neural response. Likewise, attentional modulation can alter topographical maps and the receptive fields of the neurons. Gross experiment changes such as suturing digits or retinal lesions can remap the cortical representation of body parts. Adaptation or perceptual learning can alter behavior and neural properties. Perturbing the sensory visual input, for example, using prisms to displace or invert the visual field, results in modification of cortical representation of visual space which may occur as a result of enlarged receptive fields.

Rationale

Goal directed reaching performed under visual guidance requires identifying the location of the object in the extrapersonal space and then designing a motor plan to reach to it. There are multiple reference frames that this can occur in. First, the object can be identified in retinal coordinates (retinotopic), eye-centered frame of reference, or in head-centered frame of reference. Second, the limb position must be encoded either in eye centered, body centered, or head centered frames of reference. Third, the object location must be identified with respect to the limb position used to complete the reaching movement. Therefore, an accurate reaching movement can only occur, with successful reference frame transformations.

Multiple areas of the parietal lobe and the prefrontal cortex are involved in goal directed reaching. It is important to investigate and identify the transformations occurring in individual areas. Previous studies have conducted detailed experiments in the SPL (parietal lobe) and the PMd (prefrontal cortex), however natural reaching, that is, a radial movement made towards an object in the extrapersonal space, has not been studied in areas 7a and DP systematically. The current experiments investigate the dependence of eye position on the reach response of single neurons in area 7a and DP using a foveal and peripheral reaching task. Studying the neural response to naturally occurring reaching behavior will enable us to build upon the reaching literature for area 7a and introduce reach related activity in DP. Investigating the multimodal inputs in these two areas will enable us to add to the reference frame transformation literature.

In order to adapt to an ever-changing environment during reaching, the cortex is expected to be plastic. However, there have been no studies thus far that have

investigated whether areas 7a and DP are plastic during reaching. Is the representation of extrapersonal space “hardwired” within these two areas or can they adapt to changing demands? Prisms are used to perturb the visual field in order to test the cortical plasticity of spatial representation and to further investigate the dependence of eye position signal on the reach signal.

Together with the foveal and peripheral reaching task, and the prism adaptation task, it is possible to address the sensorimotor transformation occurrence in areas 7a and DP. These experiments provide a rigorous analysis of the neural signals in areas 7a and DP and their interactions thus leading to an improved understanding of reaching based on sensorimotor transformation.

Chapter 2:
General Methods

Animal preparation

Two male rhesus monkeys (M1R 11 kg, M3R 8.5 kg; both approximately 10 years of age) were trained on a visually guided reaching task. All experimental and surgical procedures were in accordance with the National Institute of Health Guidelines on the Care and Use of Animals in Research and approved by the Rutgers University Review Board for the Use and Care of Animals. Two separate surgeries were done in both animals to implant the head post and the optical chamber. In the first surgery, a stainless steel head post was implanted. In the second surgery, a stainless steel optical chamber (20 mm outside diameter) was implanted over the right hemisphere in each animal. All surgical procedures were performed under sterile conditions. Prior to the current study, both animals were used for intrinsic optical imaging of the posterior parietal cortex (Siegel et al., 2003; Heider et al., 2005). This allowed visual identification of areas 7a and DP based on anatomical landmarks that were visible through the artificial dura. Prior to electrophysiological recordings, the transparent artificial dura was removed and the natural dura was allowed to grow back. A stainless steel adapter was attached to the optical chamber in order to secure the stage and the microdrive. This setup permitted precise penetrations with the electrode in both monkeys (Fig. 2.1A M1R; Fig. 2.1B M3R). Recordings were conducted in the right hemisphere of both animals. Both animals performed the visually guided reaching task using their left hands (contralateral to the recording chamber).

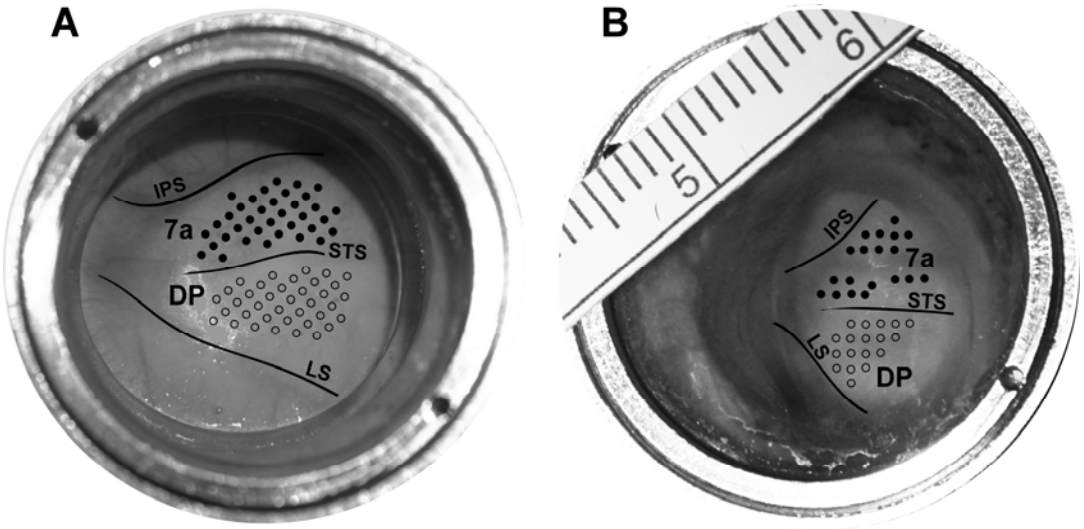


Figure 2.1: **Recording chambers**. Photograph of the recording chambers of M1R (A) and M3R (B). Both chambers were placed over the right hemispheres. The black solid lines mark the sulci, which can be seen through the transparent silicon artificial dura. The hydrolic microdrive contained a grid for the exact placement of the electrode. The penetrations made in area 7a (filled circles) and DP (open circles) were therefore targeted. IPS, intraparietal sulcus; STS, superior temporal sulcus; LS, lunate sulcus; 7a, area 7a; DP, dorsal prelunate area.

Experimental setup

The animal was seated in a primate chair and his head was immobilized using the implanted custom head holder. A touch screen monitor (Elo TouchSystems, Menlo Park, CA), which provided a touch surface of 36º X 36º of visual angle and recorded the animal's reaching endpoint, was positioned 29 cm or 35 cm (depending on the monkey's arm length) away from the monkey's eyes. A capacitive proximity sensor (touch sensor; KD5041, IFM Electronic Inc., Exton, PA) was placed on the primate chair close to the monkey's torso at the waist level. This touch sensor was used to position the monkey's hand at a constant starting position for every trial. The sensor provided a touch sensitive surface area of 49 cm^2. Distance from the starting position of the hand to the touch screen was 34 cm to 40 cm (depending on the position of the visual stimulus).

An infrared eye tracking camera (RK-416, ISCAN, Cambridge, MA) was used to track the monkey's eye position throughout the trial and ensured that fixation was maintained within 4º of the control eye position. If the eye movement exceeded 4º, the trial was aborted. This value is in accordance with previous reaching studies (Batista and Andersen, 2001; Battaglia-Mayer et al., 2005; Snyder et al., 2006). The infrared camera along with the NIMH Cortex system monitored and recorded the eye movements at 60 Hz. The stimulus display and collection of behavioral measures was programmed using the NIMH Cortex software (http://www.cortex.salk.edu). The NIMH cortex software was also synchronized with the analog spike collection system. The experiments were performed in as close to complete darkness as possible; however, some luminance from the touch screen monitor was observed at the lowest brightness and black background settings. The animal was thus able to see his hand when it was very close to the endpoint of his reach and partially occluded the visual stimulus.

Visual stimuli

The fixation point was a small red square (diagonal 0.8°). The visual stimuli used were optic flow circular patches (diameter, 12° of visual angle) of 128 dots (diameter 0.1°) moving in an expanding motion. The dots moved in the outward direction with the fixation point as the reference point at a velocity of 6°/s and had a point life of 532 ms. An optic flow stimulus was chosen as areas 7a and DP represent an architectural map representing rotational and radial optic flows (Raffi and Siegel, 2007). A radial optic flow was chosen over the rotational optic flows as area 7a neurons respond optimally to radial

optic flows (Siegel and Read, 1997). Moreover, a majority of area 7a neurons respond preferentially to the expanding optic flow (Merchant et al., 2001).

Behavioral task

For all the experiments described in this thesis, the monkeys performed a visually guided reaching task. Each trial lasted for a maximum of 8000 ms (Fig. 2.2A and B). Both monkeys were highly trained on various versions of the reaching task before recording began.

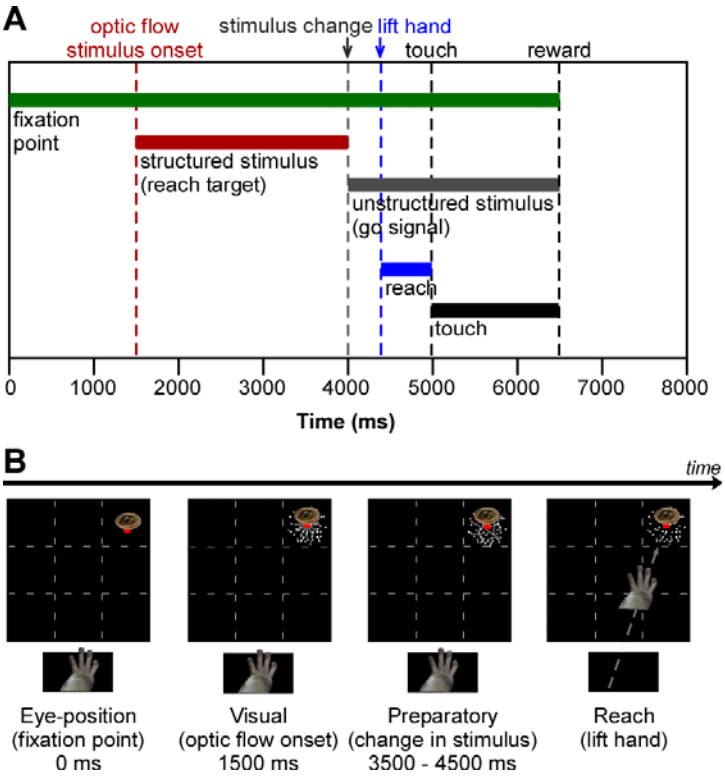


Figure 2.2: **Temporal progression of a trial of the visually guided reaching task**. (A) Marks the time when each event occurs and the time it lasts for. Solid lines: green – fixation point; red – structured expanding optic flow stimulus; gray – unstructured stimulus; blue – reach movement; black – touch and hold. The vertical dotted lines mark the time when an event occurs. (B)The black square illustrates the touch sensitive monitor used to detect the reach endpoint. The gray dotted lines on the black squares divide the screen to show the nine possible locations of the fixation point and the visual stimuli. The red dot illustrates the fixation point. The white dots behind the fixation point resemble the optic flow stimulus. The small rectangle illustrates the touch sensitive panel which is used by to the monkeys to their hands at the beginning of each trial. This touch sensitive panel marks the starting position of the hand.

Basic visually guided reaching task (foveal reach): Each trial began with the monkeys' hand resting on the touch sensor that was placed on the primate chair adjacent to the monkeys' waist. This touch sensor marked the starting position of the hand. Once the touch sensor was activated by

the monkeys' hand, a red fixation point appeared on the touch screen. This fixation point was systematically varied in one of nine positions on the screen. The monkeys were required to fixate the fixation point throughout the trial. After 1500 ms, the expanding optic flow stimulus (visual stimulus) appeared centered behind the fixation point. After 2000 ms to 3000 ms (3500 ms to 4500 ms absolute time in the trial), the expanding motion of the optic flow became unstructured (Siegel and Read, 1997). The change from structured to unstructured motion cued the monkeys to reach to the foveated visual stimulus. Thus the eye position and the reach position were always congruent resulting in a "foveal" reach. The monkeys were required to make a movement as fast as possible closely detailing a ballistic movement. Behavioral requirements of a ballistic reach (Vercher et al., 1994; Desmurget and Grafton, 2000) ensured that the monkeys received as little visual feedback as possible during the reach. Additionally, reaching in a dark room and the placement of the starting position of the hand, which was placed on the proximity sensor close to the monkeys' torso, minimized the visual feedback. The monkeys were able to visually perceive the hand only when it was close to the reach endpoint. The reaction time (RT) to lift the hand off of the sensor and the movement time (MVT) to reach the screen were set to total maximal value of 1000 ms.

The monkeys were required to hold the hand to the visual stimulus for 1500 ms during which the visual stimulus remained on the screen. A juice reward and the offset of the visual stimulus marked the end of a successful trial.

If at any time during the trial (a) the fixation was lost, (b) the hand was launched outside the given time, or (c) an erroneous reach was made (either by reaching outside the visual stimulus radius or by not holding the hand to the visual stimulus for sufficient time

– 1500 ms), the trial was aborted immediately. A new trial was initiated once the monkeys' hand was again on the proximity sensor. The missed location was repeated in a pseudo-randomized order. Each block consisted of 90 trials, ten trials per position. Both monkeys were required to complete at least 90% of the trials correctly in each block in order to proceed to the next block.

Neural recordings

Extracellular single unit recordings were conducted by electrical measurements from DC to 20 KHz using platinum-iridium, glass coated microelectrodes (UEPSEGSG2N5G, FHC, Bowdoinham, ME) with an impedance of 0.5 MΩ – 2.5 MΩ. The electrode was advanced through the dura using a hydraulic motor microdrive (650, David Kopf Instruments, Tujunga, CA). The microdrive was attached to the recording chamber via a stainless steel adapter.

The coordinate system on the microdrive and the prior optical images of the brain allowed targeted recordings (Fig. 2.1A, M1R; Fig. 2.1B, M3R). The two cortical areas of the IPL, area 7a and DP, were identified using the visible pattern under the transparent artificial dura (Fig. 2.1A and B). The transparent dura was removed and the natural dura was allowed to grow back.

The electrode was positioned at an angle orthogonal to the dura. The depth of the recording was quantified. The neural signal was amplified (Model 1800 Microelectrode AC Amplifier, A-M Systems, Carlsborg, WA), and then filtered using a 50/60 Hz noise eliminator Humbug (AutoMate Scientific, Berkley, CA) and a band-pass filter (300 Hz to 20 KHz). A Matlab (MathWorks, Natick, MA) based spike collection system along with

a PCMCIA-based analog-to-digital converter (NI DAQCard-6036E, National Instruments, Austin, TX) was used to collect the data. The neural activity was digitized at 40 KHz. In order to obtain an unbiased sample; activity from all neurons that could be sufficiently isolated was recorded regardless of neurons' spatial tuning, or preference for any aspect of the visually guided reaching task.

Online isolation of neurons was done using a dual-window discriminator (DIS-I, BAK Electronics, Germantown, MD) to assess neural selectivity and spatial preference during recording, along with off-line analysis for more exact times.

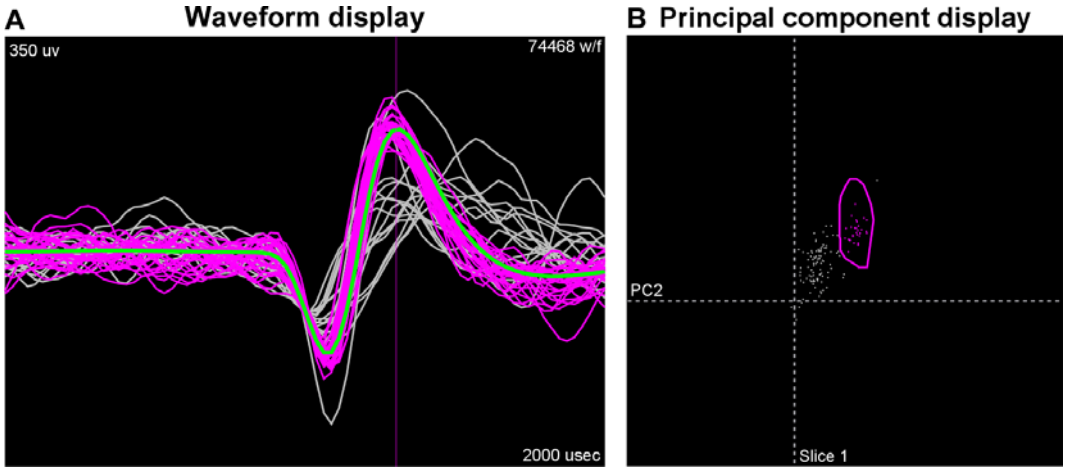


Figure 2.3: Example of a sorted neuron using Plexon. (A) Average waveform – shown in green and the selected spikes based on the principal component analysis which results in spike clustering. (B) After a threshold is set and spikes are detected, principal component analysis is used to extract spikes with similar waveforms. Spikes with similar waveforms cluster tightly.

Spike analysis

Single unit responses were recorded during all phases of the task to assess temporal and spatial aspects of neural modulation. For the off-line analysis, analog data were sorted using the Plexon software (Plexon Offline Sorter 1.39, Dallas, TX). An example of a sorted neuron is along with the principle component analysis space showing

the clustered spikes is reproduced here (Fig. 2.3). All subsequent quantitative analyses were done on the offline sorted data.

Neurons were sorted and identified based on their waveforms over the course of the experiment in conjunction with Khoros (Khoral Research, Albuquerque, NM) and customized UNIX based software. Spike rasters were synchronized to different events during each trial and the firing rate was calculated. Based on the critical events during the course of each trial different epochs of interest were defined:

Baseline epoch: The baseline epoch (Fig. 2.3, green shaded area) was defined as the time interval of 500 ms immediately before the onset of the visual stimulus (Fig. 2.4; marked by the red dotted line). During this time period only the red fixation point was on the touch screen at one of nine positions and the monkeys had maintained fixation. Since the visual effect of the fixation point was minimal, neural modulation during this epoch was due to eye

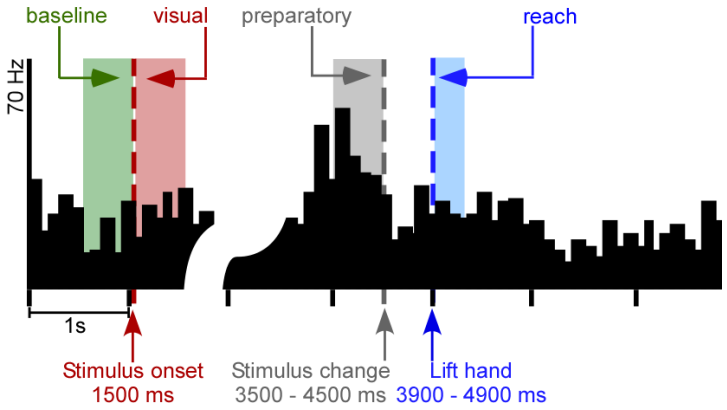


Figure 2.4: **Example of a peri-stimulus time histogram (PSTH) with synchronized events and epochs of interest**. Time in seconds is plotted along the horizontal axis. Each tick mark is positioned at one second. The firing rate of the unit in hertz (Hz) is plotted along the vertical axis. The red dotted line marks the onset of the optic flow visual stimulus which occurs at 1500 ms. Baseline epoch is the 500 ms time interval *prior* to the visual stimulus onset (1000 ms to 1500 ms; green shaded region). Visual epoch is the 500 ms time interval *after* the visual stimulus onset (1500 ms to 2000 ms; red shaded region). The gray dotted line marks the change from structured to unstructured motion of the optic flow visual stimulus, which occurs at a varied time between 2000 ms and 3000 ms. This change cues the monkeys to reach. The preparatory epoch is the 500 ms time interval *prior* to the change in visual stimulus (gray shaded region). The blue dotted line marks the time when the monkeys lift their hand off the touch sensitive panel and initiate a reach. Reach epoch is the 300 ms time interval *after* the lift hand event.

position signals.

Visual epoch: The visual epoch (Fig. 2.4, red shaded area) was defined as the 500 ms time interval immediately after the onset of the visual stimulus. Spatial tuning during this time interval provided information regarding the gain field of the unit. The gain field was defined as the eye position dependent visual response.

Preparatory epoch: To obtain the late preparatory response of the unit, the neural activity was synchronized to the change in stimulus event (Fig. 2.4; marked by a gray dotted line). This event occurred at a varied time between 2000 ms and 3000 ms after the visual stimulus onset. The change in stimulus event consisted of change in structured motion of the optic flow. The preparatory epoch was defined as the 500 ms time interval immediately before the change in stimulus event (Fig. 2.4, gray shaded area). Since the visual stimulus was constant during this time interval and the hand still steady on the starting position, any change in the neural response was likely due to the preparation of the upcoming reach movement.

Reach epoch: The reach epoch (Fig. 2.4, blue shaded area) was defined as the 300 ms time interval following the lift hand event (Fig. 2.4, marked by the blue dotted line). A 300 ms time interval instead of a 500 ms time interval was used to avoid the confounding visual stimulation caused by the hand moving into the monkeys' visual field during the later part of the reach movement. The monkeys were required to do a fast reach movement in which a maximum time interval of 500 ms was permitted to contact the touch screen.

Statistical analysis

A multi-step method was used to quantify and directly compare the spatial tuning across conditions. First, the firing rate for each of the four epochs, baseline, visual, preparatory, and reach epoch, was computed. Second, categorical regression computed the spatial and the intercept parameters which were then used to classify the units by types of interaction. Third, regressions with categorical variables denoting the different epochs or conditions explained below quantified changes in the spatial tuning.

A stepwise categorical quadratic model was used to simultaneously examine the dependency of firing rate on the condition for each epoch (condition based comparison) or on epoch during each condition (epoch based comparison). The following is the model for the change in firing rate:

$$A(x, y, E, i) = (a_x + a_{x_E})x + \left(a_y + a_{y_E}\right)y + (a_{x^2} + a_{x_E^2})x^2 + (a_{y^2} + a_{y_E^2})y^2 + c(a + a_E) + \varepsilon_i \quad \text{Eq. 2.1}$$

In case of the epoch based comparison the term $A(x, y, E, i)$ corresponds to the firing rate for the i^{th} trial. For the epoch based comparison, denoted by the term *E*, there are four categorical values, corresponding to baseline, visual, preparatory, and reach epoch. Variables $x\ and\ y$ are the horizontal and vertical locations of the fixation point corresponding to the center of the stimulus, thus marking the stimulus location. The terms a_x and a_{x^2} correspond to the linear and quadratic deviation coefficients, respectively, for the horizontal linear component. Therefore the term $(a_x + a_{x_E})x$ corresponds to the coefficient for the linear dependence on the horizontal positions of the stimulus for one of the four categories, $(a_{x^2} + a_{x_E^2})x^2$ corresponds to the coefficient for the quadratic dependence on the horizontal position. The terms a_y and a_{y^2} are the linear and quadratic

deviation coefficients the vertical linear components respectively. Terms $(a_y + a_{y_E})y$ and $(a_{y^2} + a_{y_E^2})y^2$ correspond to the coefficients of linear and quadratic components, respectively, for the vertical positions of the stimulus. Lastly, term $c(a + a_1)$ is the intercept and ε_i is the error for the i^{th} trial. Each parameter was considered but only the significant parameters ($p < 0.05$) remained in the equation. The categorical regression was implemented using GLMOD and REG procedures (SAS Institute Inc., Cary, NC).

In case of the condition based comparison, akin to the epoch based comparison, the term $A(x, y, C, i)$ corresponds to the firing rate for the i^{th} trial. C has two categorical values corresponding to EVAR and RVAR condition; pre-prism and prism condition; pre-prism and post-prism condition. The other variables follow the same convention as that in Eq. 2.1.

Epoch based comparison

The epoch based comparison was used to quantify alteration of tuning properties as the trial progressed thus quantifying and comparing the neural response temporally. For the epoch based comparison the four epochs (baseline, visual, preparatory, and reach) were compared to each other within a condition. Based on the combination of significant parameters neurons were classified in one of three following classes: (A) *Type E* – neurons that had a significant change in the overall firing rate between epochs but were not spatially tuned were classified as type E. These neurons had the same average firing rate across all nine positions. (B) *Type ExP* – neurons that significantly changed their spatial tuning between epochs were classified as type ExP. These neurons had a

multiplicative interaction between the epoch and the spatial target position. These neurons had at least one significant spatial parameter $(a_x, a_y, a_{x^2}, a_{y^2})$. (C) *Type NS* – neurons with no significant alterations in overall firing rate and spatial tuning were classified as NS. These neurons did not have any significant effects of either factor.

Neurons with significant alterations in spatial tuning (change in firing rate across the nine positions) but constant firing rate across the four epochs (only spatially tuned; P) were not found. Spatially tuned neurons with a significant change only in overall firing rate across the four epochs (additive interaction; E+P) were not found either.

Condition based comparison

The condition based comparison was used to quantify alteration of spatial tuning across two types of tasks or conditions. For the condition based comparison spatial tuning for each of the four epochs (baseline, visual, preparatory, and reach) during one condition was compared to the respective epoch in another condition. Neurons were classified in one of three following classes: (A) *Type C* – neurons that had a significant change in the overall firing rate but were not spatially tuned were classified as type C. These neurons had the same average firing rate across all nine positions however the overall firing rate altered significantly from one condition to another (e.g., EVAR versus RVAR; pre-prism versus prism; pre-prism versus post-prism). (B) *Type CxP* – neurons with significant changes in spatial tuning across conditions were classified as type CxP. These neurons had a multiplicative interaction between the condition and the spatial position, i.e. these neurons altered their firing rate across the nine positions when the two conditions were compared. These neurons had at least one significant spatial parameter

$(a_x, a_y, a_{x^2}, a_{y^2})$. (C) *Type NS* – neurons with no significant alterations in overall firing rate and spatial tuning were classified as NS. These neurons did not have any significant effects.

Neurons with constant spatial tuning and no changes in overall firing rate across the two conditions (only spatially tuned; P) were not found. Spatially tuned neurons with a significant change only in overall firing rate across the two conditions (additive interaction – no change in spatial tuning but significant change in firing rate across conditions; C+P) were not found either.

Spatial tuning

The direction of spatial tuning for each neuron was derived from the linear horizontal and vertical coefficients $(a_x, a_y, a_{x^2}, a_{y^2})$. Quadratic coefficients provide additional information regarding the shape of the spatial response fields. For neurons with only significant linear components, coefficients for *x* and *y* were used to define the angle of the spatial tuning. These resulting centers were then transformed into polar coordinates:

$$\theta = \arctan\left(\frac{a_y}{a_x}\right) \qquad \text{Eq. 2.2}$$

with the convention 0º (360º) corresponding to the position in the ipsilateral visual field along the horizontal meridian.

For neurons with mixed quadratic and linear components, spatial tuning angle was defined using the linear components and the amplitude and shape of the response field was defined by calculating the response field center (Heider et al., 2005; Quraishi et al., 2006). The spatial response fields of neurons with both horizontal and vertical significant

quadratic components along with linear components consisted of a peak, trough, or saddle depending on the sign of the quadratic component. A negative sign for both horizontal and vertical quadratic components resulted in a peak (marking the greatest firing rate) while a positive sign for both components resulted in a trough (marking the lowest firing rate). A negative sign for the horizontal component and a positive sign for the vertical component, or vise versa, resulted in a saddle shape. This in case, the greatest firing rate and/or the lowest firing rate occurred at various locations. The center of the response field was defined at the location which a maximum or minimum response occurred. The amplitude of these neurons was defined by the coordinates (X_C , Y_C) using the following equations:

$$X_C = -a_x/2a_{x^2} \quad \text{Eq. 2.3}$$

$$Y_C = -a_y/2a_{y^2} \quad \text{Eq. 2.4}$$

These resulting centers were then transformed into polar coordinates:

$$\theta = \arctan\left(\frac{Y_C}{X_C}\right) \quad \text{Eq. 2.5}$$

with the convention 0º (360º) corresponding to the position in the ipsilateral visual field along the horizontal meridian.

The spatial distribution of the population vectors was analyzed using circular statistics (Batschelet, 1981; Zar, 1984). Using the angle of the spatial tuning, the Hotelling test determined whether there was a significant mean direction of the resulting population vectors. Significance level for the *f-test* was set at $p < 0.05$. Thus, significant F-values indicate that the distribution of angles is different from a uniform distribution.

To determine the shift in spatial tuning, the resulting difference in vectors was computed between visual and preparatory ("prep") epochs ($a_{xprep} - a_{xvisual}$, $a_{yprep} -$

$a_{yvisual}; X_{Cprep} - X_{Cvisual}, Y_{Cprep} - Y_{Cvisual}$; Ch. 3). Similarly to determine the resulting shift in spatial tuning between conditions, the resulting difference in vectors was computed ($a_{xpri} - a_{xpre}, a_{ypri} - a_{ypre}; X_{Cpri} - X_{Cpre}, Y_{Cpri} - Y_{Cpre}$; difference between prism, "pri", and pre-prism, "pre", conditions; Ch. 4).

Chapter 3:
Neural representation of visually guided reaching in macaque posterior parietal cortex

Introduction

Primates interact most accurately with the environment while using visual guidance. When reaching towards an object of interest, the initiation of eye movement towards the object occurs prior to the initiation of the hand movement (Biguer et al., 1982; Gribble et al., 2002; Battaglia-Mayer et al., 2007). Thus, once the reaching target is visually identified, primates initiate an eye movement towards the target followed by the arm movement (Desmurget and Grafton, 2000).

This reaching process requires transformation of reference frame first to locate the object relative to one's body and finally to make a movement towards the object (Shadmehr and Wise, 2005). The visuomotor regions of the posterior parietal cortex (PPC) play a critical role in computing the final action based on the various heterogeneous signals such as visual, proprioceptive, and motor (Stricanne et al., 1996; Batista et al., 1999; Cohen and Andersen, 2002). In the inferior parietal lobule (IPL) this computation is thought to occur with respect to the eye position, thus following the eye-centered frame of reference (Cohen and Andersen, 2002). However, most of the reaching studies thus far focused on the properties of neurons in the parietal reach region (PRR), which is involved in planning a visually guided reach (Batista and Andersen, 2001; Scherberger and Andersen, 2007).

The main goal of the current study was to investigate the spatial and temporal relationships between the baseline (eye position), visual, preparatory (preparation of the reach), and reach signals in area 7a and dorsal prelunate (DP) of the IPL. Two types of visually guided reaching tasks, one in which the eye position varied along with the reach target (EVAR) and one in which the eye position was always centered (RVAR), were employed to investigate the influence of eye position on the reach and the preparatory response in area 7a.

The majority of previous reaching studies (Battaglia Mayer et al., 1998; Battaglia-Mayer et al., 2005; Battaglia-Mayer et al., 2007) that explored area 7a used a reaching task in which the monkeys always began each trial with their hand already in the visual field (on the screen). The reach was therefore from the center of the screen to another location on the screen. This lateral reaching movement induces an additional visual input that may influence the neural response. To correct for this issue and to study the neural response for a more natural reach, the monkeys' hand was positioned close to their torso in the current study. The monkeys were required to perform a three-dimensional (3D) reach to the touch sensitive monitor. Such a hand movement has been termed an approach (Gardner et al., 2007) or a radial (Fattori et al., 2005) reaching movement.

The first hypothesis tested temporal aspects of the neural response as the trial progressed in time from the onset of the fixation until the reward for a correct reaching movement. Since areas of the IPL receive heterogeneous spatially tuned inputs, it was hypothesized that the spatial tuning might vary as a function of task phase (baseline, visual, preparatory and reach). The second hypothesis tested whether the eye position modulates the preparatory and the reach related neural activity. It was hypothesized that

foveated versus peripheral reaching will alter the preparatory and the reach response thus showing dependency on the eye position.

Materials and methods

Behavioral task

The monkeys performed the reaching task under two conditions: the eye position varied condition (EVAR; Fig. 3.1A) and the retinal-varied condition (RVAR; Fig. 3.1B).

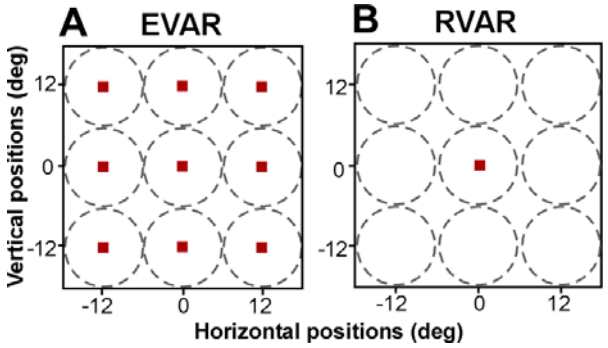


Figure 3.1: **Illustrations of the eye position varying (EVAR) and the retinal varying (RVAR) conditions**. Each square illustrates the touch sensitive monitor. The y-axis marks the vertical location of the reach targets (expanding optic flow stimulus) and the x-axis marks the horizontal locations of the reach targets in degrees. The red dots are the fixation points and the dotted circles indicate the circumference of reach targets. (A) EVAR condition: The fixation point (red dot; diagonal 0.8º) appeared at one of nine possible locations; the position of the fixation point was systematically varied. The optic flow stimulus (diameter 12º) always appeared behind the fixation point. Since this was the reach target, the endpoint hand location and the eye position were always congruent resulting in a foveal reach. (B) RVAR condition: The fixation point always appeared at the center position. The optic flow stimulus appeared at any of the possible nine locations. This resulted in a peripheral reach.

EVAR: In the EVAR condition, the monkeys preformed the visually guided reaching task described in Chapter 2 (Fig. 2.2 and 2.3). The eye position varied along with the reach target; i.e. the visual stimulus (reach target) always appeared behind the fixation point. The eye position and the endpoint hand location were therefore always in accordance resulting in a foveal reach. Thus, spatial tuning during the EVAR condition reflects variations in eye position.

RVAR: In the RVAR condition the fixation point always appeared in the center of the touch sensitive monitor. The visual stimulus (reach target) appeared in any of the possible nine positions. Therefore the retinal position of the reach target varied resulting

in a peripheral reach. Thus, spatial tuning during the RVAR condition reflects variations in retinal position.

The endpoint hand location and the eye position for the center position of the visual stimulus matched for both conditions. In both, the EVAR and the RVAR conditions the monkeys were required to reach within the 12º diameter of the visual stimuli.

Statistical analysis

A multi-step method was used to quantify and directly compare the spatial tuning across the two conditions (EVAR versus RVAR). First, the firing rate for each of the four epochs, baseline, visual, preparatory, and reach epoch (see Ch. 2, General Methods), was computed. Second, a categorical regression computed the spatial and the intercept parameters which were then used to classify the units by types of interaction. Third, regressions with categorical variables denoting the foveal (EVAR) or the peripheral reach (RVAR) quantified changes in the spatial tuning between conditions for a particular epoch.

The stepwise categorical quadratic model was used to simultaneously examine the dependency of firing rate on epoch during each condition (epoch based comparison; see Ch.2, General Methods) or on the condition for each epoch (condition based comparison; see Ch. 2, General Methods).

The resulting spatial parameters provided the basis for assessing the spatial tuning of the neurons. The amplitude and the angular tuning of the $x - vector$ and $y - vector$ (or X_C and Y_C) was then computed. The distribution of the resulting vectors was then tested using the Hotelling one-sample test to assess the population spatial tuning. Shifts in

spatial tuning were determined by computing the difference between the spatial tuning of two epochs: $(a_{xprep} - a_{xvisual}, a_{yprep} - a_{yvisual}; X_{Cprep} - X_{Cvisual}, Y_{Cprep} - Y_{Cvisual})$. Specifically, for the epoch based analysis difference vectors were computed between the preparatory and the visual epoch, as they consist of identical sensory stimulation (coherently moving optic flow, hand steady on the proximity sensor) and thus represent purely internal processing. For the condition based analysis, difference vectors were computed between EVAR and RVAR parameters separately for the preparatory and reach epochs.

The average firing rate across all nine reach positions was also directly compared between visual and preparatory epochs using paired *t-test* (for ExP type neurons). The same procedure was used for comparing RVAR and EVAR conditions during the different epochs.

Results

Behavioral data

Reach endpoint accuracy

The reach endpoint accuracy was measured by computing the distance between the reach endpoint and the center of the visual stimulus. Reach endpoints on the screen from one experiment for the EVAR and the RVAR conditions are plotted (Fig. 3.2). Reaching

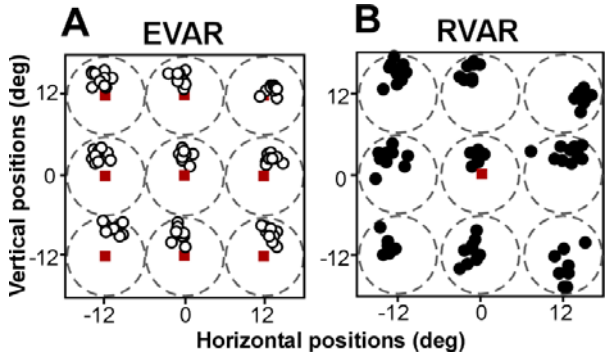


Figure 3.2: **Reach endpoints of one typical experiment during the EVAR and RVAR conditions**. (A) EVAR condition (open circles; n = 90 trials; MFR25601). (B) RVAR condition (filled circles; n = 90 trials; MFR25602). All other conventions according to Fig. 3.1. The reach accuracy was greater during the EVAR condition (foveal reaching) compared to the RVAR condition (peripheral reaching).

was more accurate, closer to the center of the visual stimulus, during the EVAR condition. A paired *t-test* comparison between the EVAR (Fig. 3.2A) and the RVAR (Fig. 3.2B) reach endpoints confirmed that accuracy was indeed greater for foveated reaches (p = 0.007). The less accurate reaching observed during the RVAR condition may be the result of peripheral reaching as the reaching distance from the fovea is larger (Henriques and Crawford, 2000; Prado et al., 2005).

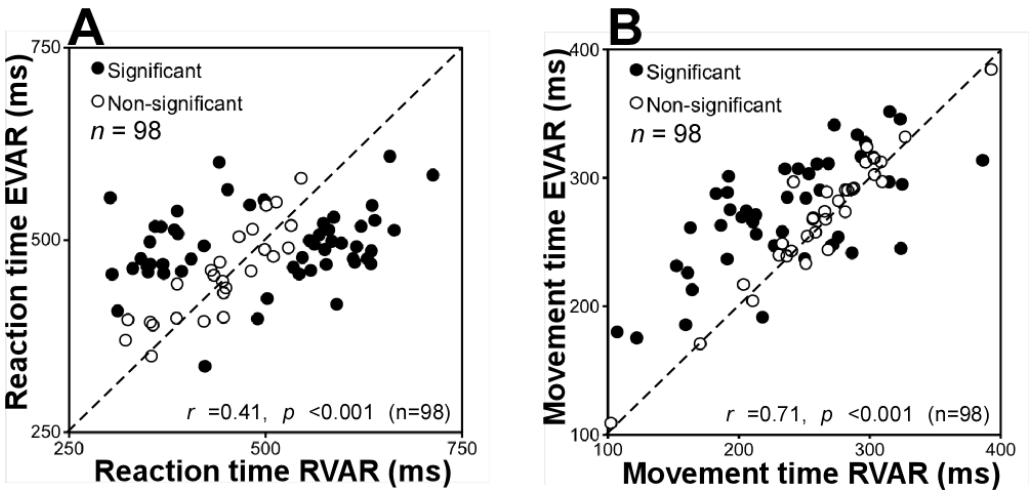


Figure 3.3: **Distribution of mean behavioral times for the RVAR and the EVAR conditions**. Filled circles represent the behavioral times that were significantly different between the RVAR and the EVAR conditions. Open circles indicate non-significant values. Student's t-test was used for the comparison. Each circle represents the mean of the behavioral times during one recording run. RT and the MVT during the RVAR condition are plotted along the horizontal axis in ms and those during the EVAR condition are plotted along the vertical axis in ms. (A) Reaction time (RT; time from stimulus change to lift hand) comparison between RVAR and EVAR conditions. No significant trend or differences were observed between the two conditions. (B) Movement time (MVT; time from lift hand to touch) comparison between RVAR and EVAR conditions. The MVT of both monkeys was significantly shorter during the RVAR condition compared to the EVAR condition (p < 0.001).

Reaction time

The reaction time latency (RT) was computed by taking the difference between the time the monkey lifted his hand off the plate and the occurrence of the change in

motion of the visual stimulus. The RT was compared for the EVAR and RVAR conditions. No significant difference in RTs was observed during a paired *t-test* comparison between the EVAR and RVAR conditions (Fig. 3.3A). Both monkeys had different mean detection times but showed the same task effects.

Movement time

The time required to touch the visual stimulus once the hand was lifted off the sensor, movement time (MVT), was computed. A paired comparison was done for MVTs during the EVAR and the RVAR conditions (Fig. 3.3B). Both monkeys reached to the visual stimulus significantly faster during the RVAR condition compared to the EVAR ($p < 0.001$). Thus, while reaching in the periphery monkeys had a shorter MVT. The mean travel time for both monkeys differed but the task effect was the same. On some days the overall MVT was longer for both monkeys and on some days the MVT was shorter but task differences were maintained. The mean reach velocity across all experiments was 1.2 m/s. This velocity is within published data for fast, ballistic reaching (Kurata and Hoshi, 2002; Churchland et al., 2006; Gardner et al., 2007).

Electrophysiological data

Extracellular single unit responses were recorded during all phases of the reach task to assess the spatial relationship between the baseline, visual, preparatory, and reach signals in areas 7a and DP. The neural response of 164 neurons (area 7a: 99; area DP: 65) was quantitatively compared to assess the temporal (comparison across epochs; see Ch. 2, General Methods) and spatial (visual stimulus position) aspects using the EVAR task. Neural activity of 119 neurons (area 7a: 65; area DP: 54) was quantitatively compared to

assess the temporal (comparison across epochs; see Ch. 2, General Methods) and spatial (visual stimulus position) aspects using the RVAR task. For a total of 98 neurons (area 7a: 53; area DP: 45) both EVAR and RVAR tasks were completed. The neural activity of these units was quantitatively compared to assess the contextual aspect of the response.

The data is presented in two ways: first, the epoch based analysis examines the temporal and spatial relationship of neural signals within EVAR and RVAR conditions. An example of response field of an area 7a neurons and a DP neuron for each condition is shown. Second, the condition based analysis directly compares the preparatory and the reach epochs between EVAR and RVAR condition. These results demonstrate the effect of the eye position on the preparatory and the reach signal in areas 7a and DP.

Single unit activity synchronized to task epochs

The neural activity was synchronized to the onset of the visual stimulus, the change in the stimulus, and the lift hand event. The epoch based analysis was used to directly compare the temporal and spatial aspect of the neural signal during the baseline (prior to the onset of the visual stimulus), visual (after the onset of the visual stimulus), preparatory (prior to the change in stimulus), and reach (after the lift hand event) epochs within each condition (EVAR and RVAR). Tuning properties during each epoch were quantified for each unit.

EVAR condition

In the EVAR condition the eye position varied along with the reach target location and thus was always in accordance with the endpoint hand position. This resulted in a foveal reach.

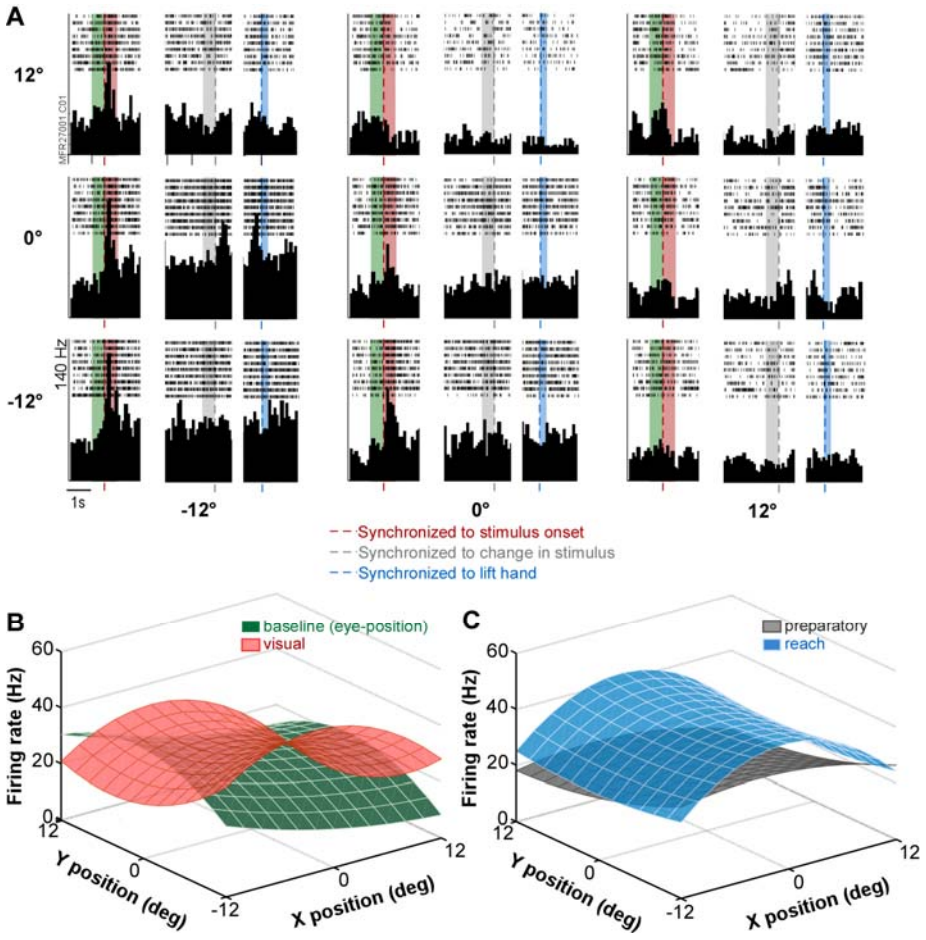


Figure 3.4: **Response of an area 7a neuron during EVAR condition.** Peri-stimulus time histograms (PSTH) of an area 7a neuron that shows modulation in the spatial tuning as the trial progresses during the EVAR condition. Red dotted line marks the onset of the expansion optic flow stimulus (visual stimulus; 1500 ms); gray dotted line marks the time the optic flow stimulus changes to a random motion (between 3500 and 4500 ms); blue dotted line marks the time the monkey initiates a reach by lifting his hand off the proximity sensory (within 400 ms after the stimulus changes its motion). The epoch identification is as follows: baseline (green shaded region), visual (red shaded region), preparatory (gray shaded region) and the reach (blue shaded region). (A) The PSTH and raster plots are arranged in a 3x3 grid. Each of the nine PSTH sets corresponds to an optic flow visual stimulus appearing at that location. Therefore, each PSTH is an average of 10 trials. Bin width = 60 ms. (B) Response fields during the baseline (green) and visual (red) epochs. Baseline response of this unit is greater for the contralateral eye positions, $A_{baseline} = -0.71x + 0.21y - 0.02x^2 - 0.08y^2 + 27.4$; whereas the gain field tuning dominates the contralateral hemifield, the vertical meridian and the lower eye positions; $A_{visual} = -0.46x - 0.76y - 0.12x^2 + 0.07y^2 + 30.5$. (C) Response fields during the preparatory (gray) and reach (blue) epochs. The preparatory response of the unit dominates lower and contralateral eye positions, $A_{preparatory} = -0.26x - 0.61y - 0.04x^2 + 0.02y^2 + 24.2$. The reach response of this unit is greatest for the lower and central contralateral eye positions and along the vertical meridian, $A_{reach} = -0.12x - 0.09y - 0.13x^2 + 0.02y^2 + 40.8$. The spatial tuning of this neuron altered along the vertical and horizontal axis significantly. The spatial tuning of this neuron was maintained for the contralateral eye positions but altered along the vertical and horizontal axes.

Area 7a neuron: The baseline response of the area 7a neuron was greater for the contralateral eye positions (Fig. 3.4A and B; green shaded region). During the visual epoch, the spatial preference of this neuron was for the visual stimuli at the lower eye position along the vertical meridian and in the contralateral eye positions (Fig. 3.4A and B; red shaded region). The preparatory response of the unit dominated the lower and contralateral eye positions (Fig. 3.4A and C; gray shaded region). The reach related response of this unit was greatest for the lower and central contralateral eye positions and along the entire vertical meridian (Fig. 3.4A and C; blue shaded region). Thus the spatial tuning of this unit was maintained for the contralateral eye positions however it changed along the vertical axis and varied slightly but significantly along the horizontal axis.

DP neuron: The baseline response of the DP neuron was weakly tuned for the lower and ipsilateral eye positions (Fig. 3.5A and B; green shaded region). At the onset of the visual stimulus the neuron had a strong transient response for all positions albeit this response was greater for varying eye positions along the horizontal meridian and for the contralateral and the ipsilateral eye positions (Fig. 3.5A and B; red shaded region). The preparatory response of this unit dominated the contralateral and the lower eye positions (Fig. 3.5A and C; gray shaded region). Once the reach was initiated, there was a drastic decrease in the response of the unit for the upper eye positions and the ipsilateral and contralateral eye positions along the horizontal meridian. The overall neural response during the reach epoch was greater for the lower positions (Fig. 3.5A and C; blue shaded region). The spatial tuning of this neuron altered dramatically as the trial progressed: the baseline preference for the lower and ipsilateral eye positions expanded to the contralateral eye positions at the onset of the visual stimulus (gain field). The tuning then

shifted towards the contralateral eye positions as the monkey prepared to reach. Finally, once the reach was initiated the neuron preferred the lower ipsilateral eye positions.

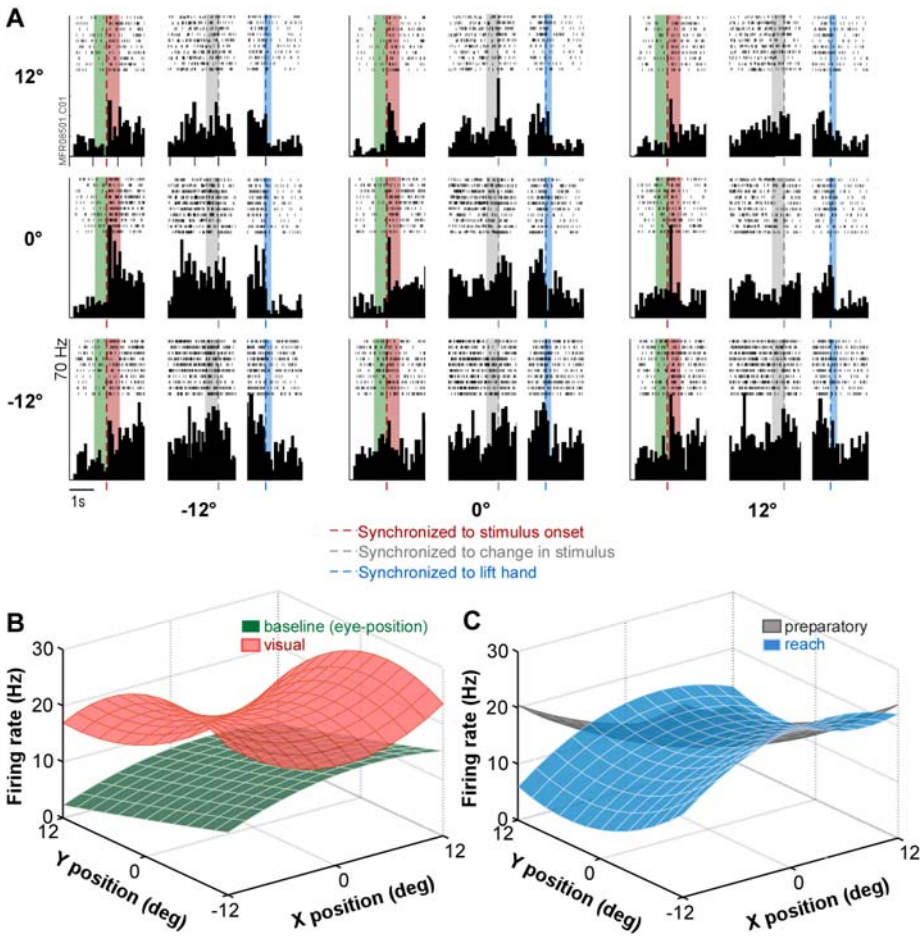


Figure 3.5: **Response of a DP neuron during EVAR condition**. PSTH of a DP neuron that shows temporal evolution of spatial tuning during the EVAR condition. All conventions same as in Fig. 3.4. (A) PSTH and raster plots for the nine stimulus locations. (B) The baseline response: weak tuning for the lower and ipsilateral eye positions, $A_{baseline} = 0.17x - 0.37y - 0.02x^2 - 0.001y^2 + 11.5$. The gain field of the unit is along the horizontal meridian, and in the contralateral and ipsilateral visual field, $A_{visual} = 0.12x - 0.39y + 0.05x^2 - 0.05y^2 + 20.1$. (C) The preparatory response of the unit is the greatest for the contralateral and lower eye positions, $A_{preparatory} = -0.44x - 0.58y + 0.02x^2 + 0.03y^2 + 14.5$. The reach response is greater for reach targets appearing in lower positions, $A_{reach} = 0.31x - 0.37y - 0.04x^2 - 0.04y^2 + 14.8$. This neuron thus shifted spatial preference from lower ipsilateral to contralateral positions and then back to lower positions.

Alteration of spatial tuning as the trial progressed was observed in 97/164 (59%; area 7a: 52/99, 52%; DP: 45/65, 69%) neurons. These were classified as the

multiplicative interactive neurons (type ExP); at least one of the four spatial parameters $(a_x, a_y, a_{x^2}, a_{y^2})$ was significant during at least two of the four epochs. For 41/97 neurons (42%), the spatial tuning modulated linearly. The angular tuning was distributed uniformly for this group of neurons. For 35/97 (36%) neurons, the spatial tuning consisted of significant linear and quadratic components. The preferred spatial tuning angle was computed using the X_C, Y_C values (see Ch. 2, General Methods) for these neurons. For the population of these mixed neurons the spatial tuning was uniformly distributed too. This suggests that areas 7a and DP represent the space in its entirety when reaching is performed to foveated targets at varying eye positions.

Spatial tuning shifts were calculated between visual and preparatory epochs. Population angular tuning of these shift vectors was non-significant. Thus there was no systematic shift in spatial preference between preparatory and visual epochs. Significant differences in firing rate between the visual and the preparatory epoch were observed in 42/97 neurons (43%). There were no overt differences in the two epochs. In both epochs the monkeys maintained fixation at one location, the visual stimulus remained constant (coherent expanding optic flow), and the hand was resting on the touch sensitive starting panel. Therefore the alteration in neural response can be attributed solely to internal processing such as attention and motor planning.

Seventeen out of 164 neurons (10%; area 7a: 12/99, 12%; DP: 5/65, 8%) were not spatially tuned but had an epoch effect, i.e. the firing rate of these neurons was uniform for all nine positions but their intercepts differed significantly between at least two epochs (type E). The intercepts between the visual and the preparatory epochs were not significantly different (p = 0.25). The activity of 50/164 neurons (30%; area 7a: 35/99,

35%; DP: 15/65, 23%) was not modulated by the chosen epochs. These neurons were also not spatially tuned and were therefore classified as not significant (type NS). As confirmed by the X^2 test, no differences were observed between area 7a and DP (p = 0.44) with respect to distribution of tuning types (ExP and E).

For the EVAR condition the spatial tuning from the visual to reach epoch thus changed in a large portion of neurons even though the reach target was always foveated. This implies that the eye position may modulate the reach movement signal or in turn that the planning and initiation of the reach movement can modulate the gain field signal.

RVAR condition

In the RVAR condition the eye position was always in the center and the visual stimuli appeared in one of nine possible locations. All reaches were peripheral except for center reach. At the center of the screen the visual stimulus appeared behind the fixation resulting in a foveal reach.

Area 7a neuron: As expected this neuron was not spatially tuned during the baseline epoch (Fig. 3.6A and D; green shaded region), as there was no spatially varying stimulation with respect to eye position during this epoch. The response of this neuron had a sharp transient increase when the visual stimulus appeared in the contralateral visual field and along the vertical meridian (Fig. 3.6A and D; red shaded region). This response decreased along the horizontal axis. The preparatory response of this unit was the greatest in the lower contralateral and center visual field. This response level decreased towards the upper ipsilateral visual field (Fig. 3.6B and E; gray shaded region). During the reach epoch the response level of the unit was greatest for the contralateral reach target locations (Fig. 3.6C and E; blue shaded region). Therefore, as the trial

progressed the spatial tuning of the neuron shifted from the contralateral visual field towards the lower contralateral visual field during the preparatory and the reach epochs.

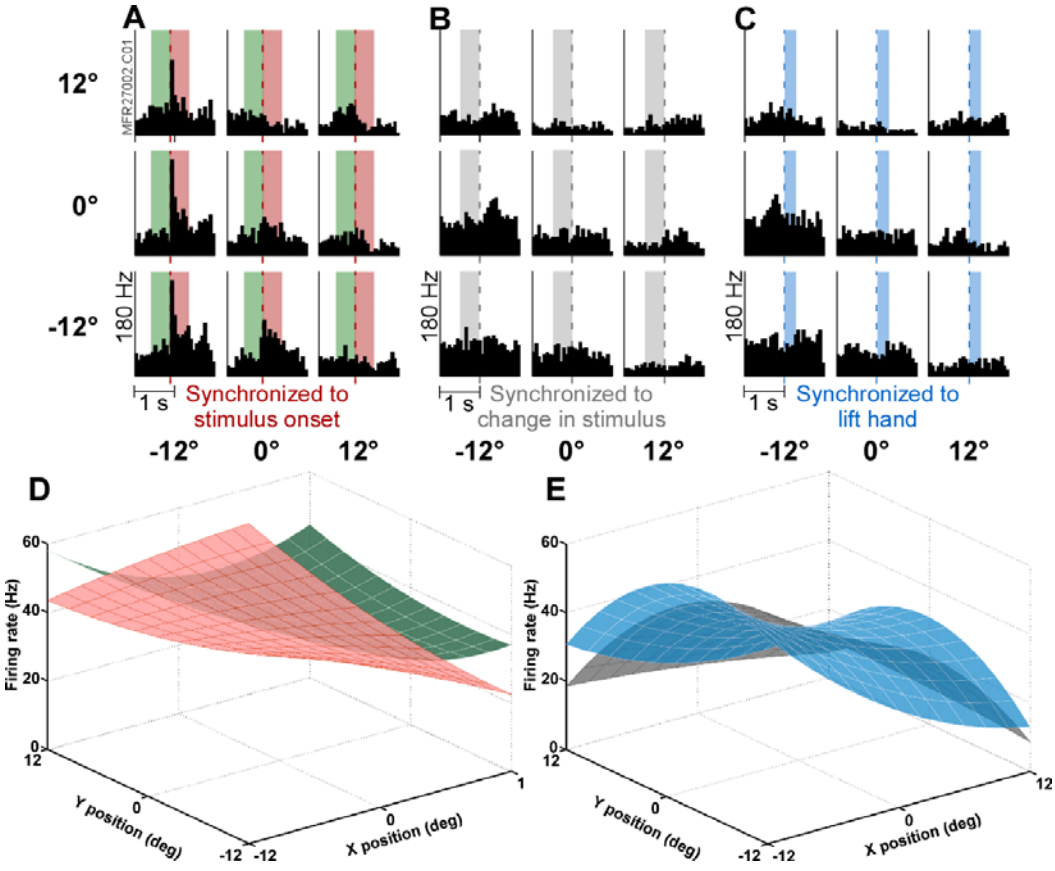


Figure 3.6: **Response of an area 7a neuron during RVAR condition**. (A - C) PSTH of an area 7a neuron that shows temporal evolution of spatial tuning during the RVAR condition. Conventions otherwise as in Fig. 3.4. (D and E) Response fields of the neuron during the four epochs. (D) The baseline response of this unit does not vary spatially, $A_{baseline} = -1.06x - 0.18y + 0.08x^2 - 0.03y^2 + 38.6$. The visual response is greatest in the contralateral visual field, $A_{visual} = -2.27x - 1.40y + 0.03x^2 - 0.01y^2 + 38.6$. (E) The preparatory response of the unit is the greatest in the lower contralateral visual field, $A_{preparatory} = -1.46x - 1.05y + 0.01x^2 + 0.08y^2 + 38.6$. The reach response is greater for reach targets appearing in contralateral locations, $A_{reach} = -1.29x - 0.56y - 0.06x^2 - 0.12y^2 + 38.6$. The spatial tuning of this neuron shifted from the contralateral visual field towards the lower contralateral visual field.

DP neuron: The baseline tuning of the DP neuron was flat as the eye position did not vary in the RVAR condition (Fig. 3.7A and D; green shaded region). At the onset of the visual stimulus the activity of the neuron increased when the stimuli appeared in the

ipsilateral visual field and along the horizontal and vertical meridian (Fig. 3.7A and D; red shaded region). During the preparatory epoch, the response of the unit was the greatest in the upper ipsilateral visual field and decreased towards the lower contralateral visual field (Fig. 3.7B and E; gray shaded region). At the initiation of the reach a sharp decrease in the activity of the neuron was observed for all but the lower visual field and center position (Fig. 3.7C and E; blue shaded region). The peak of the reach field of this neuron was thus in the lower ipsilateral visual field; the reach response was the least in the upper contralateral visual field. The spatial tuning of this neuron therefore shifted from the center to the upper ipsilateral visual field followed by a shift towards the lower ipsilateral visual field and lower center position as the trial progressed in time.

Alteration of spatial tuning as the trial progressed was observed in 54/119 (45%; area 7a: 29/65, 45%; DP: 25/54, 46%) units during the RVAR condition, which were classified as multiplicative interactive neurons (type ExP). For 16/54 neurons (30%), the spatial tuning modulated linearly, for which the distribution of angles was uniform. For 18/54 (33%) neurons significant spatial modulation was observed along linear and quadratic components. For these neurons the spatial tuning was also uniformly distributed. This suggests that areas 7a and DP represent the space in its entirety when the visual stimuli (reaching targets) were presented in varying retinotopic locations.

Analogous to the EVAR condition spatial, shifts between visual and preparatory epoch were distributed uniformly for the RVAR condition, however, the paired analysis revealed significant differences in firing rate between the visual and the preparatory epoch in 28/54 ExP neurons (52%).

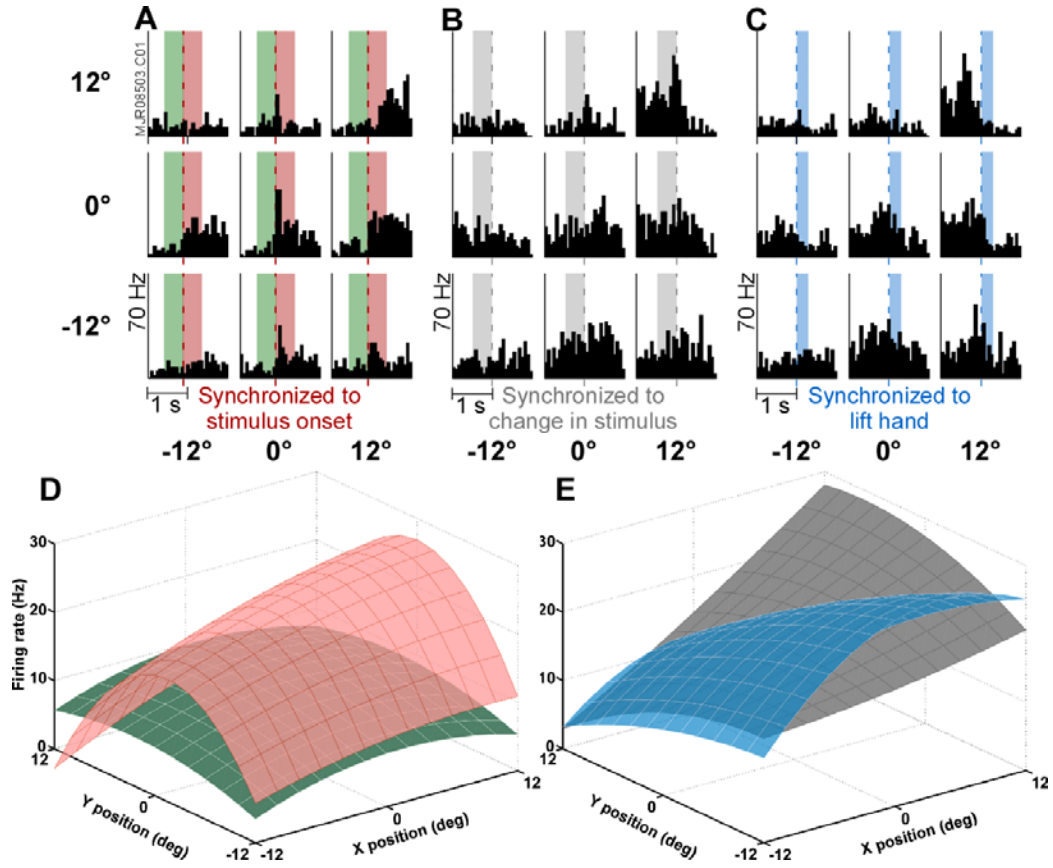


Figure 3.7: **Response of a DP neuron during RVAR condition**. (A – C) PSTH of a DP neuron that shows temporal evolution of spatial tuning during the RVAR condition. Conventions otherwise as in Fig. 3.4. (D) The baseline response of this unit does not vary significantly for across the nine stimulus locations, $A_{baseline} = 0.08x - 0.09y - 0.02x^2 - 0.02y^2 + 11.4$. The visual response is greatest in the ipsilateral visual field and along the horizontal meridian, $A_{visual} = 0.39x - 0.19y - 0.01x^2 - 0.11y^2 + 23.8$. (E) The preparatory response of the unit is the greatest in the upper ipsilateral visual field, $A_{preparatory} = 0.64x - 0.10y + 0.01x^2 + 0.02y^2 + 19$. The reach response is greater lower ipsilateral reach target locations, $A_{reach} = 0.26x - 0.65y - 0.06x^2 - 0.01y^2 + 21.3$. The spatial tuning shifted from the center to the upper ipsilateral visual field and then towards the lower ipsilateral visual field and lower center position.

Twenty-one out of 119 neurons (18%; area 7a: 11/65, 17%; DP: 10/54, 19%) had an epoch effect but were not spatially tuned. The intercept values for the visual epoch were significantly greater than for the preparatory epoch (p = 0.006). The activity of 44/119 neurons, NS neurons, (37%; area 7a: 25/65, 38%; DP: 19/54, 35%) was not modulated by the chosen epochs. These neurons were also not spatially tuned. As

confirmed by the X^2 test, no differences in distribution of the E and ExP types were observed between area 7a and DP (p = 0.88).

The regression analysis provided a robust quantitative measure of the differential effects of the four epochs within the EVAR and the RVAR conditions. For a majority of the neurons (Fig. 3.8A, EVAR, 114/164, 70%; Fig. 3.8B, RVAR, 75/119, 63%) the spatial tuning and/or the overall firing rate altered as the trial progressed temporally. A majority of these alterations were in the form of spatial changes as opposed to gain changes. The changes in spatial response fields implies that inputs from areas using different frames of reference modulate these 7a and DP neurons, as the monkeys identify the spatial location of the visual stimulus, prepare to reach it, and finally execute the motor behavior.

In order to test the effect of eye position, the preparatory and the reach epoch during the EVAR condition were compared directly with the respective epoch during the RVAR condition.

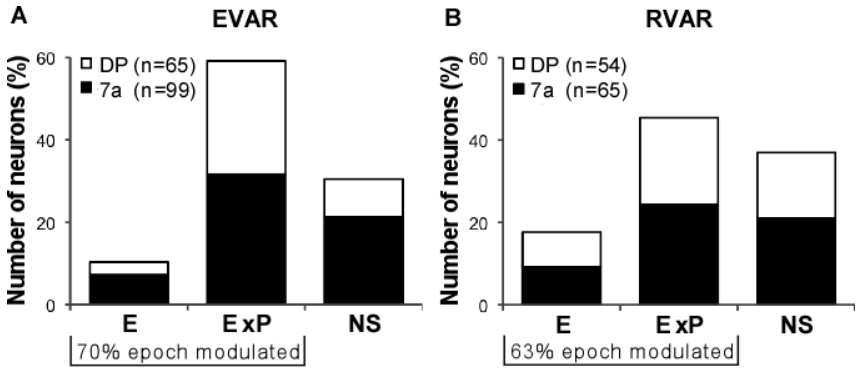


Figure 3.8: **Population distribution of epoch based comparison**. Epoch based analysis was used to compare the fours epochs of interest: baseline, visual, preparatory, and reach. Proportions of interaction types between epoch (E) and position (P) are plotted separately for each area (7a, filled bars; DP, open bars). (A) Proportions of interaction types during the EVAR condition. (B) Proportions of interaction types during the RVAR condition. Type E neurons had a single effect of epoch (change in mean firing rate) but were not spatially tuned. Type ExP neurons had a multiplicative interaction between epoch and position; these neurons had different spatial tuning between epochs. NS cells had no effect of either factor. The spatial tuning of a majority of neurons altered as the trial progressed during both EVAR and RVAR conditions.

Comparison of single unit activity between EVAR and RVAR conditions

In both the EVAR and the RVAR condition the visual stimulus location was identical; therefore the reach endpoint locations were also identical. However the reach targets were foveated in the EVAR condition resulting in a foveal reach whereas the reach targets were in the periphery in the RVAR condition resulting in a peripheral reach. The eye position varied congruently with reach target during the EVAR condition. During the RVAR condition the eye position was always held constant in the center of the touch screen monitor. The center target during the RVAR condition remained foveated thus being a 'control' for the EVAR versus RVAR comparison of attentional or set effects. A categorical regression analysis was used to directly compare the neural response for the preparatory and the reach epochs between the EVAR and the RVAR condition (EVAR versus RVAR). Two factors were included in this comparison: the condition (C) and the nine visual stimulus positions (P).

Baseline and visual epochs

The center position for both the EVAR and the RVAR condition served as a control as the reach to this location was foveated. The eye position and the visual stimulation were constant across the two conditions. Thus the neural response for the baseline (monkey fixating a fixation point) and the visual (onset of the visual stimulus) epoch should not vary for the center position. Upon direct comparison it was observed that this was indeed the case. Firing rates between the two conditions did not differ significantly for the baseline ($p = 0.9$) and the visual ($p = 0.36$) epoch. Comparison of visual responses of 7a neurons under different eye positions and retinotopic stimulus

positions have been studied previously (Read and Siegel, 1997) and will not be considered further.

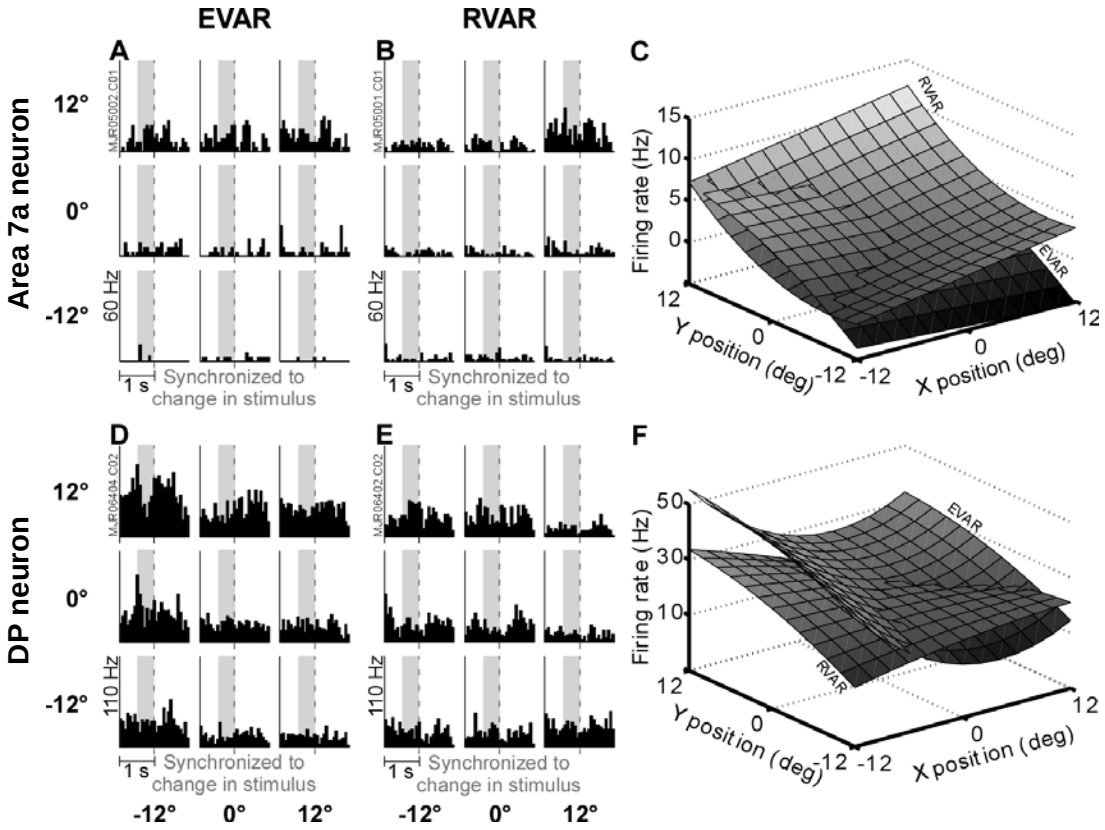


Figure 3.9: **Preparatory response during EVAR and RVAR conditions**. Condition based analysis comparing the preparatory response during the EVAR and RVAR conditions. Conventions otherwise as in Fig. 3.4. (A) PSTH showing the response of a typical area 7a neuron during the preparatory epoch under the EVAR condition. (B) PSTH showing the response of a typical area 7a neuron during the preparatory epoch under the RVAR condition. (C) Response fields of the neuron in A and B during the EVAR and RVAR conditions. Spatial tuning was in the upper visual field during the EVAR condition; $A_{EVAR} = -0.07x + 0.45y + 0.003xy - 0.01y^2 + 2.53$. The neuron prefers the upper ipsilateral visual field during the RVAR condition; $A_{RVAR} = 0.19x + 0.33y + 0.02xy - 0.02y^2 + 2.53$. (D) PSTH showing the response of a typical DP neuron during the preparatory epoch under the EVAR condition. (E) PSTH showing the response of a typical DP during the preparatory epoch under the RVAR condition. (F) Spatial tuning dominated the contralateral upper visual field – EVAR; $A_{EVAR} = -0.91x + 0.79y - 0.004xy - 0.12x^2 + 21$. Neural response was lowest in the upper ipsilateral visual field – RVAR; $A_{RVAR} = -0.46x + 0.06y - 0.07xy - 0.01x^2 + 21$. The differential spatial tuning properties of area 7a and DP neurons during the preparatory epoch imply that different cortical networks are recruited for foveal and peripheral reaching.

Preparatory epoch

During the preparatory epoch, the monkey maintained fixation at the structured optic flow visual stimulus. The hand was stationary at the starting location. Therefore there was no overt motor behavior or other sensory stimulation. Alteration in spatial tuning properties during this epoch can thus be attributed only to internal processing.

The activity of an area 7a neuron during the preparatory epoch was different under EVAR (Fig. 3.9A and C) and RVAR (Fig. 3.9B and C) conditions. This neuron preferred the upper eye positions EVAR condition. Under the RVAR condition, this neuron responded mostly to the stimulus in the ipsilateral upper visual field. Spatial tuning properties of a DP neuron differentially altered depending upon the condition. For this example neuron the preparatory response field dominated the contralateral upper eye positions under the EVAR condition (Fig. 3.9D and F). During the RVAR condition (Fig. 3.9E and F) the neural response was the lowest in the contralateral lower and the ipsilateral upper visual fields. Activity was greater along the diagonal drawn between contralateral upper and ipsilateral lower visual field. In both example neurons, the differences in spatial tuning properties imply that different cortical networks may be recruited to execute peripheral versus foveal reaching behaviors.

Such a differential condition and position (CxP) effect was observed in 45/98 neurons (46%; area 7a: 21/53, 40%; DP: 24/45, 53%). Analogous to the example area 7a and DP neurons this group of neurons showed a change in spatial tuning even though the monkey reached to identical reach target locations. The CxP neurons had at least one significant spatial parameter $(a_x, a_y, a_{x^2}, a_{y^2})$. Linear modulation across the vertical and/or horizontal axis was observed in 16/45 (36%) neurons. Quadratic modulation in

addition to linear modulation was observed in 18/45 (40%) neurons. The spatial tuning of neurons with significant linear coefficients and significant linear and quadratic coefficients was uniform, that is, these spatial tuning angles collective showed a distributed representation of space. The spatial shifts between EVAR and RVAR were also uniformly distributed. The firing rate of 29/98 neurons (30%; area 7a: 16/53, 30%; DP: 13/45, 29%) differed under the two conditions, however, these neurons were not spatially tuned (type C). The intercept values did not differ significantly between conditions for this group of neurons (p = 0.74). Neither the condition nor the spatial factor had an effect on the neural response of 24/98 neurons (24%; area 7a: 16/53, 30%; DP: 13/45, 29%). A X^2 test confirmed that the two areas, area 7a and DP, were not significantly different (p = 0.53) with respect to the distribution of C and CxP type neurons.

Reach epoch

The reach epoch was defined as the 300 ms time interval after the monkey initiated the reach (lifted his hand off the touch sensor). The neural activity during this period is essentially the response to initiation of the reaching movement. The reach target location was identical in the two conditions however in EVAR condition the monkey reached to foveated visual stimuli whereas in RVAR the monkey reached to visual stimuli in the periphery.

The spatial tuning of the area 7a neuron during the reach epoch was almost opposite along the horizontal axis for the EVAR (Fig. 3.10A and C) and the RVAR (Fig. 3.10B and C) conditions. During the EVAR condition the reach response of this neuron was greater for upper contralateral eye position. In the RVAR condition, response during

the reach epoch was the greatest in the upper ipsilateral visual field and decreased towards the lower visual field. This differential response pattern for EVAR and RVAR conditions can be attributed to the difference in eye positions and retinotopic stimulation, thus implying that both factors modulate the reach response of the neurons.

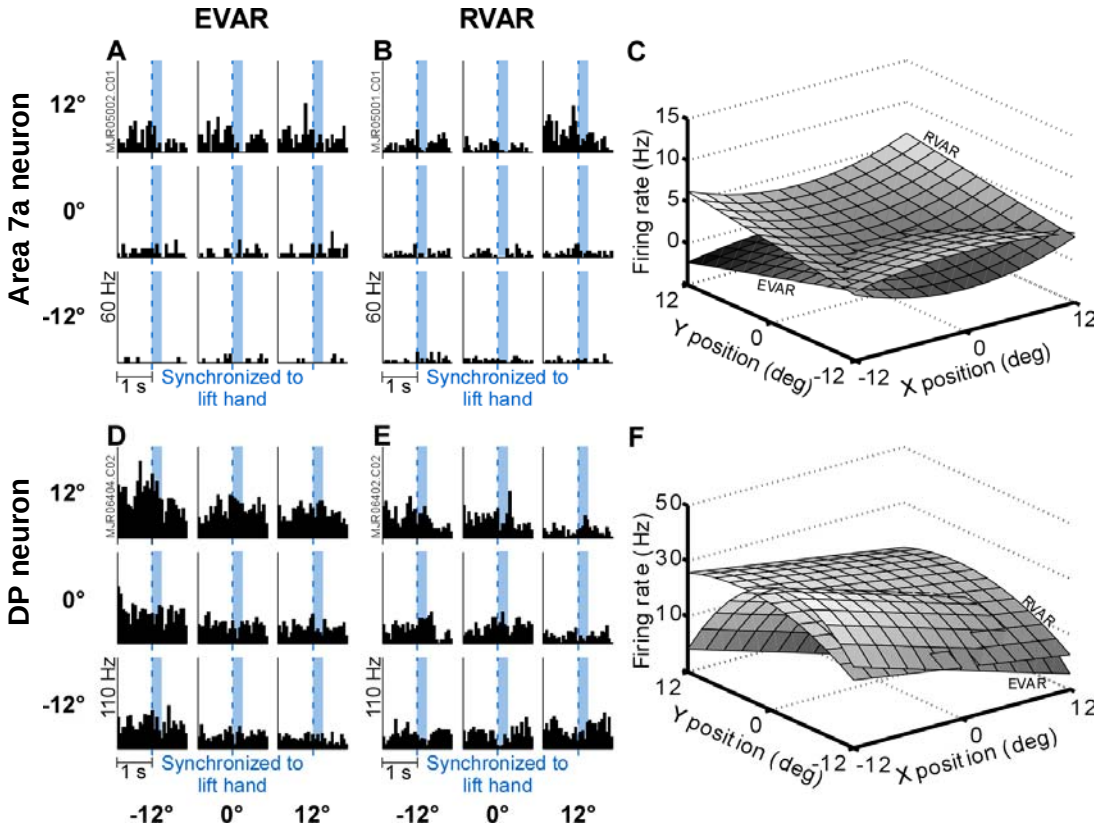


Figure 3.10: **Reach response during EVAR and RVAR conditions**. Condition based analysis comparing the reach response during the EVAR and RVAR conditions. Conventions otherwise as in Fig. 3.4. (A) PSTH showing the reach response of a typical area 7a neuron during the EVAR condition. (B) PSTH showing the reach response of a typical area 7a neuron during the RVAR condition. (C) Response fields during EVAR and RVAR. EVAR: Spatial tuning dominates the upper contralateral visual field; $A_{EVAR} = -0.24y - 0.01x^2 + 1.78$. RVAR: Here the neurons prefers the upper ipsilateral visual field; $A_{RVAR} = 0.14y + 0.02x^2 + 1.78$. (D) PSTH showing the reach response of a typical DP neuron during EVAR condition. (E) PSTH showing the reach response of a typical DP during the RVAR condition. (F) Response fields of DP neuron during EVAR and RVAR. EVAR: Neural response is greatest in the upper contralateral upper visual field and decreases towards the lower ipsilateral visual field; $A_{EVAR} = -0.98x - 0.88y - 0.18y^2 + 22.4$. RVAR: Neural response dominates the upper, contralateral, and center locations of the reach target; $A_{RVAR} = -0.49x + 0.47y - 0.06y^2 + 22.4$. Differential response during the reach epoch between the EVAR and the RVAR condition implies that eye position affects the reach response in area 7a and DP.

The reach response differed across the two conditions in a DP neuron. In the EVAR condition (Fig. 3.10D and F) the reach response of the unit was greatest for the upper contralateral eye position and decreases towards the lower ipsilateral eye position. In the RVAR condition (Fig. 3.10E and F) the reach response dominated the upper and contralateral visual field. Analogous to the area 7a neuron, this difference in spatial properties between the two conditions implies that the eye position and retinotopic stimulation modulate the reach response.

Identical reach targets resulted in different spatial tuning depending on whether the reach was foveated or in the periphery in 53/98 (54%; area 7a: 27/53, 51%; DP: 26/45, 58%) neurons (CxP). Only linear modulation was observed in 17/53 (32%) neurons whereas a combination of quadratic and linear modulation was observed in 20/53 (38%) neurons. Uniform spatial distributions were observed for both groups of neurons with significant spatial parameters. The spatial shifts between EVAR and RVAR conditions were also distributed uniformly. Twenty-six out of 98 (27%; area 7a: 15/53, 28%; DP: 8/45, 18%) neurons showed a change in firing rate across the two conditions but these neurons were not spatially tuned (type C). For this type, the intercept values between EVAR and RVAR conditions were not significantly different (p = 0.96). Nineteen out of 98 (19%; area 7a: 11/53, 21%; DP: 8/45, 18%) neurons did not show a spatial or a condition effect and were thus classified as non-significant. A X^2 test confirmed that distribution of C and CxP types did not differ significantly (p = 0.74) between areas 7a and DP.

Analogous to the temporal comparisons, the regression analysis provided a robust quantitative measure of the differential effects of the two conditions for each epoch. For a majority of the neurons (Fig. 3.11A, preparatory, 74/98, 76%; Fig. 3.11B, reach, 79/98, 81%) the spatial tuning and/or the overall firing rate altered across the two conditions.

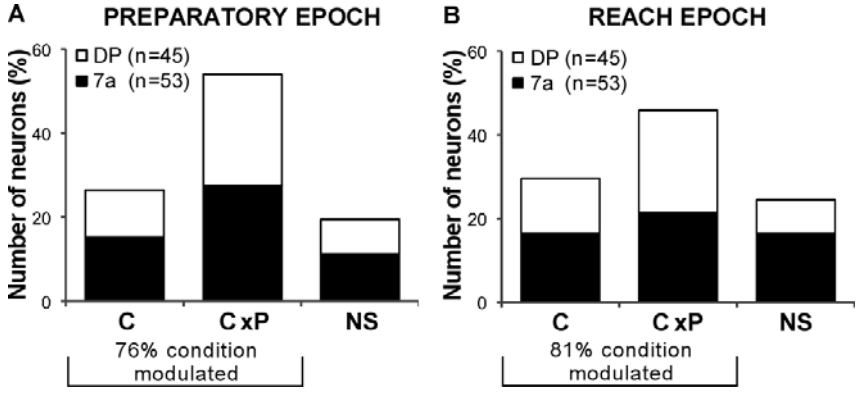


Figure 3.11: **Population distribution of condition based comparison**. Comparison based analysis was used to compare the neural response under the EVAR and the RVAR conditions. Proportions of interaction types between condition (C) and position (P) are plotted separately for each area (7a, filled bars; DP, open bars). (A) Proportions of interaction types during the preparatory. (B) Proportions of interaction types during the reach epoch. Type C neurons had a single effect of condition (change in mean firing rate) but were not spatially tuned. Type CxP neurons had a multiplicative interaction between condition and position; these neurons had different spatial tuning between epochs. NS cells had no effect of either factor. Majority of the neurons in area 7a and DP showed a condition effect.

Since no statistical differences were found between areas 7a and DP the data for the two areas are combined in the subsequent chapter.

Summary

Primates generally use visually guided reaching in order to accurately reach to objects in their external space. Visually guided reaching requires interplay of visual and motor signals. It is thus important to examine the neural response before the initiation of the reaching behavior. The main goal of the current study was to investigate whether these two areas are involved in the sensorimotor transformation, which involves several

phases. The neural response during the onset of the visual stimulus, preparation to the reaching behavior, and the reaching behavior was considered. The spatial and temporal relationship between the visual, preparatory and reach signals was quantitatively investigated. The eye position effect on the preparatory and the reach signals was also examined. Monkeys were required to perform two variations of visually guided reaching tasks. In one task, EVAR, the eye position varied in accordance with the locations of the reach target (nine possible locations) resulting in a foveal reach. In another task, RVAR, the eye position remained centered while the monkey reached to targets appearing in nine different locations resulting in a peripheral reach. Extracellular single unit recordings were used to investigate the neural properties of areas 7a and DP. It was observed that in a large number of neurons the spatial tuning alters as the reaching tasks progress temporally i.e. the visual, preparatory and the reach spatial tuning significantly differed as the trial progressed. The eye position modulated the reach signal thus implying that areas 7a and DP follow the eye-centered coordinate system and that the sensorimotor transformation occurs in these two areas using the eye-centered frame of reference.

Discussion

This section will discuss the behavioral data and caveats of the current study. The electrophysiology data will be discussed in the General Discussion (Chapter 5).

Behavioral data

Visually guided or goal-directed reaching movements are conducted using an eye-centered or retinal reference frame (Henriques et al., 1998; Batista et al., 1999; Vetter et al., 1999). The initial location of a visual stimulus for goal-directed movement is encoded

in eye-centered coordinates in the PPC (Goldberg and Bruce, 1990). This stimulus location then needs to be transferred into another coordinate system, for example, the hand-centered coordinate system in order to complete the goal-directed movement successfully. Therefore the accuracy of reach endpoint is affected by neural accuracy of visuomotor calibration. If the spatial calibration of a peripheral reach target is less accurate than that of a foveal target the error would be reflected in the reach endpoint location. Initial motor programming may consist of an error for peripheral target (Prablanc et al., 1986). In situations where the foveal information is present, the foveal information may allow online improvement in accuracy (via proprioceptive input), which does not occur in presence of peripheral information (Prablanc et al., 1986). The RTs are slightly slower for the RVAR condition as the peripheral targets are more difficult to detect than foveal targets (Prablanc et al., 1986). Slower detection times for peripheral targets were observed in a primate attentional study (Quraishi et al., 2007). The significant difference in MVT between EVAR and RVAR conditions suggests that distinct computations occur during foveal and peripheral reaching (Moran and Schwartz, 1999; Snyder et al., 2006). These behavioral and psychophysical differences between foveal (EVAR) and peripheral (RVAR) reaching imply that different networks may be recruited for accurate execution of foveal and peripheral reaches (Prado et al., 2005; Clavagnier et al., 2007). Reaching in the periphery requires a more extensive network (Clavagnier et al., 2007) suggesting that motor programming occurs over a bigger time interval when computing a motor plan to reach to a peripheral target.

Caveats

Since the kinematics of the three dimensional arm movements were not monitored, the reach trajectory could not be accounted for. It could be that the reach trajectory during the foveal and peripheral reach was different. Secondly, the monkeys were allowed to reach anywhere on the reach target which had a diameter of 12º. The larger reaching differences may have resulted in differential reach responses during foveal and peripheral reaching conditions. However this is unlikely as the receptive field sizes of area 7a and DP neurons are large (Motter and Mountcastle, 1981; Andersen et al., 1990) and the reach endpoints were accurately placed close to the center of the target (within 2º of visual angle) as shown by the behavioral data of the current study.

Chapter 4:
Spatial effects of shifting prisms on neuronal properties of posterior parietal cortex

Introduction

Primates depend upon an adaptive sensorimotor control in order to successfully interact with their environment. Behavioral adaptation and neural plasticity are intertwined with each other and necessary for an accurate interaction with the changing demands with the environment. Plasticity of neural representations occurs when there is a change in sensory input (Kaas et al., 1990; Allard et al., 1991; Gilbert, 1996a, b; Crist et al., 2001; Li et al., 2004; Polley et al., 2006).

Distortion of the visual field by spatial displacement results in a discrepancy between the perceived location of the target and the actual location of the target. Thus, when trying to reach to the target, there is a mismatch between the visual input (resulting in a change in sensory input) and the motor output. There are a number of studies that have explored behavioral plasticity in human and non-human primates as a result of distortion of the visual field using shifting and inverting prisms (Healy et al., 1973; Kitazawa and Yin, 2002; Berberovic and Mattingley, 2003; Marotta et al., 2005). It is known for decades that reaching errors decrease over a period of time (Healy et al., 1973; Flook and McGonigle, 1977; Kitazawa and Yin, 2002; Richter et al., 2002; Berberovic and Mattingley, 2003) as a result of long term prism adaptation. These reaching errors were corrected only in presence of visual feedback; tactile and proprioceptive cues alone did not result in a corrected reach (Healy et al., 1973). Similarly, human subjects showed

adaptation to reaching with reversing prisms (left-right reversal) only when visual feedback of the reach was present (Marotta et al., 2005). The timely occurrence of the visual feedback is also important. Prism adaptation did not occur if the visual feedback was delayed by over 500 ms (Kitazawa and Yin, 2002). The reaching errors after the prism was removed (after-effects of prism adaptation) also remained if the visual feedback was delayed. The after-effects of the prism adaptation decreased over time i.e., monkeys tested within 10 ms of prism adaption showed larger reaching errors (half the distortion angle) compared to those tested after 24 hours (Yin and Kitazawa, 2001).

Very few experiments have been conducted to study the neural plasticity as a result of alteration of sensory input. Merely deviating the position of the eyes with prisms as the monkey fixated did not affect the gain fields of parietal neurons (Andersen et al., 1985). Sugita (1996) investigated the long-term adaptation of V1 neurons to inverting prisms; after adaptation a small percentage of cells responded to the ipsilateral visual field as well as the standard contralateral field. Kurata and Hoshi (2002) examined the effects of shifting prisms on single unit activity in the ventral premotor (PMv) cortex. Neurons in the PMv altered their spatial tuning when the monkey initiated reaching. There has been no systematic electrophysiological study of prism adaptation in primate parietal cortex. Because the neurons of PPC represent an important intermediate step between sensory input and motor output, these neurons should be ideally suited to reflect plastic changes due to prism adaptation.

The hypothesis tested is whether visual gain field tuning and the reach field tuning of the cells in areas 7a and DP alters as the perceived visual field is displaced using shifting prisms. The current study showed that the reach field tuning of the neurons

altered as a result of the prismatic distortion. However, the change in spatial tuning as a result of the prism shift was not predictable. For a given prism shift in a population of neurons, the units responded with a varied shift in spatial tuning resulting in a distributed representation of space.

Materials and methods

Behavioral task

The monkeys performed the visually guided foveal reaching task (described in Ch. 2 and referred to as the EVAR condition in Ch. 3). Measurements were made under three conditions: pre-prism, visual distortion (prism), and recovery (post-prism). Each condition consisted of 90 (10 for each of the nine positions) correct trials.

Pre-prism condition: In the pre-prism condition, the monkeys preformed the visually guided foveal reaching task with the prism holder in place but without the prism inserted.

Prism condition: The visually guided foveal reaching task was used in the prism condition along with a 12° Fresnel prism (Fresnel Prism & Lens Co., LLC, Eden Prairie, MN). The prism shifted the visual field horizontally or vertically by 12º, resulting in shifts in four directions: upward, downward, contralateral, and ipsilateral. The shifts were in reference to the recording chamber placed over the right hemisphere. The fixation point and the visual stimulus (reach target) were perceived to be shifted resulting in a mismatch between the eye position (perceived reach target position) and the actual reach target position. The monkeys were required to reach to the actual location of the reach target. If the monkeys reached outside the reach target (e.g. perceived location), it was

considered an incorrect reach and the trial was aborted. Visual feedback was only available when the monkeys' hand was close to the reach endpoint. The reach endpoint location was corrected over trials; trained monkeys corrected the reach within five to nine trials. The exact prismatic distortion was measured with a laser beam for all nine positions and was confirmed to be uniform (12º).

Post-prism condition: After the monkeys successfully completed the prism condition, the prism was removed. Both monkeys were required to perform the visually guided reaching task to test the behavioral recovery and the spatial tuning of the unit. Analogous to the prism condition, the monkeys adapted to the lack of a prism and reached to the actual location within five to nine trials. It was not always possible to obtain the full set of the three runs. The completion of the post-prism condition was dependent on the stability of the recording and the performance and motivation of the monkeys. Thus some recordings consisted only of the pre-prism and prism conditions or in some cases an incomplete post-prism condition.

Statistical analysis

A multi-step method was used to quantify and directly compare the spatial tuning across two conditions (pre-prism vs. prism or pre-prism vs. post-prism). First, the firing rate for each of the four epochs, baseline, visual, preparatory, and reach epoch (see Ch. 2, General Methods) was computed. Second, categorical regressions computed the spatial and the intercept parameters which were then used to classify the units by types of interaction. Third, regressions with categorical variables denoting the presence or absence of the prism distortion quantified changes in the spatial tuning.

A stepwise categorical quadratic model was used to simultaneously examine the dependency of firing rate on epoch during each condition (epoch based comparison; see Ch. 2, General Methods) or on the condition for each epoch (condition based comparison; see Ch. 2, General Methods).

In order to test for changes in spatial tuning for a given prism shift spatial tuning of the neurons was computed based on the amplitude and the angular tuning during the pre-prism, prism, and the post-prism conditions. The population vectors were tested using the Hotelling one-sample test to determine the mean spatial tuning. Shifts in spatial tuning were determined by computing the difference between the spatial tuning of neurons during pre-prism and prism conditions: ($a_{xpri} - a_{xpre}$, $a_{ypri} - a_{ypre}$; $X_{Cpri} - X_{Cpre}$, $Y_{Cpri} - Y_{Cpre}$; difference between prism, "pri", and pre-prism, "pre", conditions).

Results

Behavioral data

Reach endpoint accuracy

The highly trained monkeys reached accurately to all locations during the pre-prism condition. In the prism condition, as expected the monkeys initially "misreached" to the perceived, shifted target locations. After sufficient training with the prism condition, the monkeys quickly adapted and reached to the actual location within five to nine trials. During the post-prism condition, after the prism had been removed, the initial reach endpoint was misplaced in the opposite direction relative to the prism shift. This overshoot was corrected also within a few trials.

The reach endpoint accuracy during the pre-prism, the prism, and the post-prism conditions was measured by computing the distance between the reach endpoint and the center of the visual stimulus. Reach endpoints on the screen from one experiment for all three conditions are plotted (Fig. 4.1A). Here the 12º prism was used to shift the visual field upwards. Reaching was most accurate during the pre-prism condition (black circles) for all 90 trials. The initial reach endpoints during the prism condition (red circles) were shifted upwards (due to a 12° upward prism shift), but the adaptation was fast after which

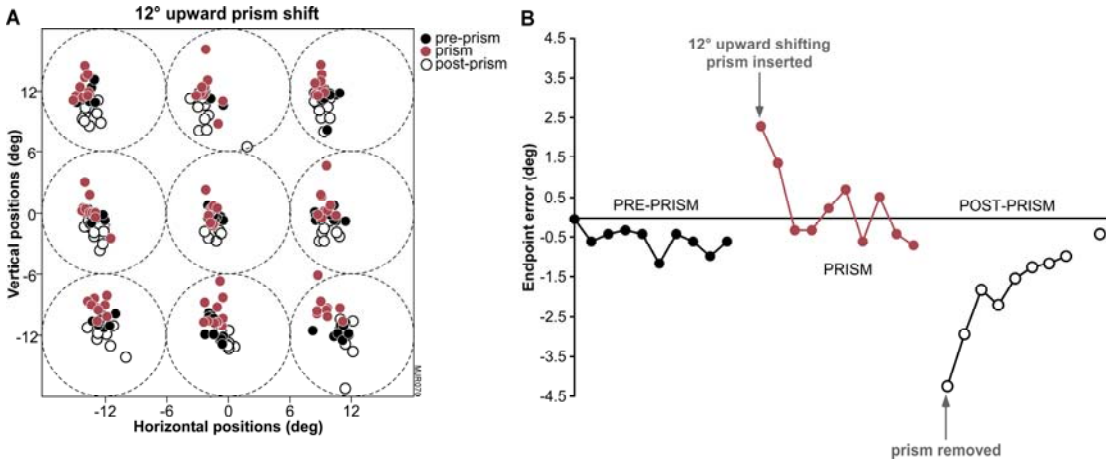


Figure 4.1: **Reach endpoint accuracy and rapid adaptation to prisms**. Reach endpoint accuracy and error for the pre-prism condition (black circles), prism condition (red circles), and post-prism condition (open circles). Each dot in A and B is one reach endpoint of the monkey during one experiment on one day. (A) Reach endpoints of one experiment during the three conditions (90 trials in each condition). The square illustrates the touch sensitive monitor with a 36°x36° of touch surface. Each dotted circle is a possible position of the visual stimulus. Each black circle is a reach endpoint during the pre-prism condition. Each red circle is a reach endpoint during the prism condition. Each open circle is a reach endpoint during the post-prism condition. Endpoint accuracy is the greatest during the pre-prism condition. In presence of the 12° upward shifting prism, the monkey makes an erroneous reach which he corrects immediately. Once the prism is removed, the initial reaches are erroneous in the opposite of the prism shift but progressive improvement in reaching shows behavioral adaptation. (B) Endpoint error when the monkey reached to the visual stimulus appearing in the upper right corner. The horizontal axis shows the progression of number of trials. The vertical axis shows the reach errors in degrees. Initial reach errors during the prism and the post-prism conditions do not equal the magnitude of the prismatic distortion. Rapid adaptation takes place during prism and post-prism.

the monkey reached accurately. Once the prism was removed (post-prism condition – open circles), the initial reach endpoints were overshot in the opposite direction of the prismatic distortion. Again the accuracy was restored within nine trials.

The following are combinations of paired *t-test* comparisons of reaching errors for one recording session. A paired *t-test* comparison between pre-prism and prism conditions ($p = 0.27$), pre-prism and post-prism conditions ($p = 0.22$) and prism and post-prism conditions ($p = 0.38$) revealed that the reaching errors were not significantly different. These comparisons were done on all trials in the respective two conditions. Because the monkeys adapted rapidly to the insertion and the removal of the prism, the reaching accuracies during both the prism and the post-prism conditions did not differ significantly from the pre-prism condition. However a paired *t-test* comparison between the first nine trials of the pre-prism and the prism condition confirmed that the reach errors were greater for the prism condition ($p = 0.002$). A paired *t-test* comparison between the pre-prism and the post-prism condition (first nine trials of each) confirmed that reaching error was larger for the post-prism condition ($p = 0.02$). Lastly, paired *t-test* comparison between prism and post-prism condition revealed that the reaching errors for the first nine trials were not significantly different ($p = 0.06$). This was expected as the monkey reached erroneously in both the prism and the post-prism conditions and only the absolute value of the reach errors were considered. During the prism condition the monkey initially reaches to the shifted location of the reach target (perceived location) whereas during the post-prism condition the monkey initially overshoots the reach. The significance in reach error for the first few trials (for the paired comparison between pre-prism and prism or post-prism conditions) but the lack of this significance when all trials

are considered confirms the claim that the monkeys adapt quickly to the prismatic distortion.

Quantification of the erroneous reach endpoints showed that the maximum error of reaching did not equal the amount of prism shift; rather it was one fourth to half the angle of distortion (Fig. 4.1B; reach to the upper position in the ipsilateral visual field). The reach error varied from day to day but was maintained at one fourth to half the angle of distortion at the initial presentation of the prism. These behavioral data are in agreement with the findings of human (Cressman and Henriques, 2009) and non-human primate (Kurata and Hoshi, 2002) studies with reaching under visually distorted conditions.

Reaction time

Reaction time (RT) latency to detect the change in stimulus was compared for the pre-prism and the prism conditions for 108 recordings. RT was computed by subtracting the time of the change in stimulus from the time the monkey lifted his hand off the sensor. The overall RT latency was shorter for M1R (black circles; Fig. 4.2A) as compared to M3R (red circles; Fig 4.2A). The RT latency of M3R was significantly greater during the prism condition for 29/64 (45%) experiments. RT latency of M1R did not show a specific trend. The mean RTs differed between the two monkeys but were consistent within each monkey for the two conditions (pre-prism, n = 9493 trials: M1R 461±147 ms, M3R 333±117 ms; prism, n = 10097 trials: M1R 462±165 ms, M3R 355±120 ms; stdev). The prism condition was behaviorally more demanding than the pre-prism condition resulting in slightly greater RT latencies during the prism condition.

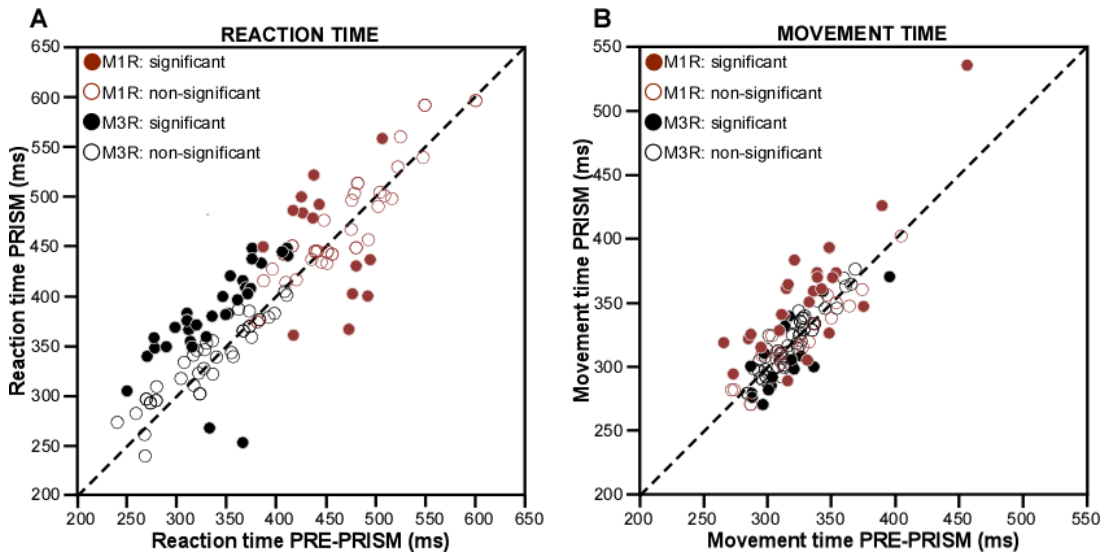


Figure 4.2: **Distribution of mean behavioral times for the pre-prism and the prism conditions**. Reaction time (RT; time from stimulus change to lift hand) and movement time (MVT; time from lift hand to touch) comparison between the pre-prism and the prism condition of M1R (red filled circles – significant; red open circles - non-significant) and M3R (black filled circles – significant; black open circles – non-significant). Student's t-test was used for the comparison. RT and the MVT during the pre-prism condition are plotted along the horizontal axis in ms and those during the prism condition are plotted along the vertical axis in ms. (A) RT comparison between the pre-prism and prism condition does not show a specific trend. The RT latency of M3R was significantly greater for 45% of the experiments. The RT latency of M3R does not show such a trend. (B) The MVT of both the monkey is independent of the condition.

Movement time

Movement time (MVT), which is time required for the monkey to reach to the touch screen, was compared for the pre-prism and the prism conditions. MVT was computed by subtracting the time at which the monkey lifted his hand off the sensor from the time his hand contacted the touch screen. MVT was not predictable depending on the condition (Fig. 4.2B). The mean MVTs for both monkeys were above 300 ms during both conditions (pre-prism, n = 9493 trials: M1R 328±69 ms, M3R 317±59 ms; prism, n = 10097 trials: M1R 340±76 ms, M3R 316±58 ms; stdev). The similarity in movement

times suggests that the fast, ballistic reaching behavior was maintained during the pre-prism and the prism conditions.

Electrophysiological data

Single unit responses were recorded during all phases of the task to assess temporal and spatial aspects of neural modulation during the pre-prism condition, prism condition, and the post-prism condition. The neural response of 166 (area 7a: 114; area DP: 52) neurons was quantitatively compared during the pre-prism and the prism condition. Out of 166 neurons, 105 (area 7a: 77; area DP: 28) neurons were compared for pre-prism and post-prism conditions.

The data is presented in three ways: First, the epoch based analysis is used to examine the temporal and spatial relationship of neural signals within the pre-prism, prism, and post-prism conditions. Neural response of three different neurons is shown for the three conditions. Second, the condition based analysis is used to directly compare the neural response for each epoch (baseline, visual, preparatory, reach) between the pre-prism and prism conditions. Shifts in spatial tuning are quantified to determine if there is a correlation between the prismatic distortion and the resulting shift in spatial tuning. Third, the condition based analysis is used to directly compare the spatial tuning for each epoch between the pre-prism and the post-prism conditions.

The regression model for each epoch is included in the legend of the example neurons' figures. Because no significant differences were observed between areas 7a and DP in the previous experiment (see Results in Ch.3), data for the two areas were combined.

Single unit activity synchronized to task epochs

In the first analysis, temporal and spatial relationship of neural signals was examined using the epoch based comparison. The neural activity was synchronized to the onset of the visual stimulus, the change in the stimulus, and the lift hand event. The four epochs of interest were: baseline (prior to the onset of the visual stimulus), visual (after the onset of the visual stimulus), preparatory (prior to the change in stimulus), and reach (after the lift hand event) epoch. Tuning properties during each epoch were plotted for each neuron. Categorical regression analysis was used to directly compare these tuning properties during the baseline, visual, preparatory, and reach epochs within each condition.

Once the Fresnel prism was introduced and the visual field was shifted, the overall firing rate of the neuron could change substantially (i.e., increases or decreases with respect to the firing rate during the pre-prism condition). If in this situation the scaled PSTHs were shown for the same neuron, the temporal effect during each condition would be diluted and not very clear. Therefore, three different example neurons are used to show the spatial and temporal relationship of neural signals within each condition (pre-prism, prism, and post-prism).

Pre-prism condition

An example area 7a neuron showed modulation in the spatial tuning as the task progressed in time (Fig. 4.3). The activity of the unit is shown in the peri-stimulus time histograms (PSTH) in a three by three grid (Fig. 4.3A). Each of the nine PSTH

corresponds to an optic flow stimulus location on the touch screen and the resultant eye position. Thus each PSTH is an average of ten trials.

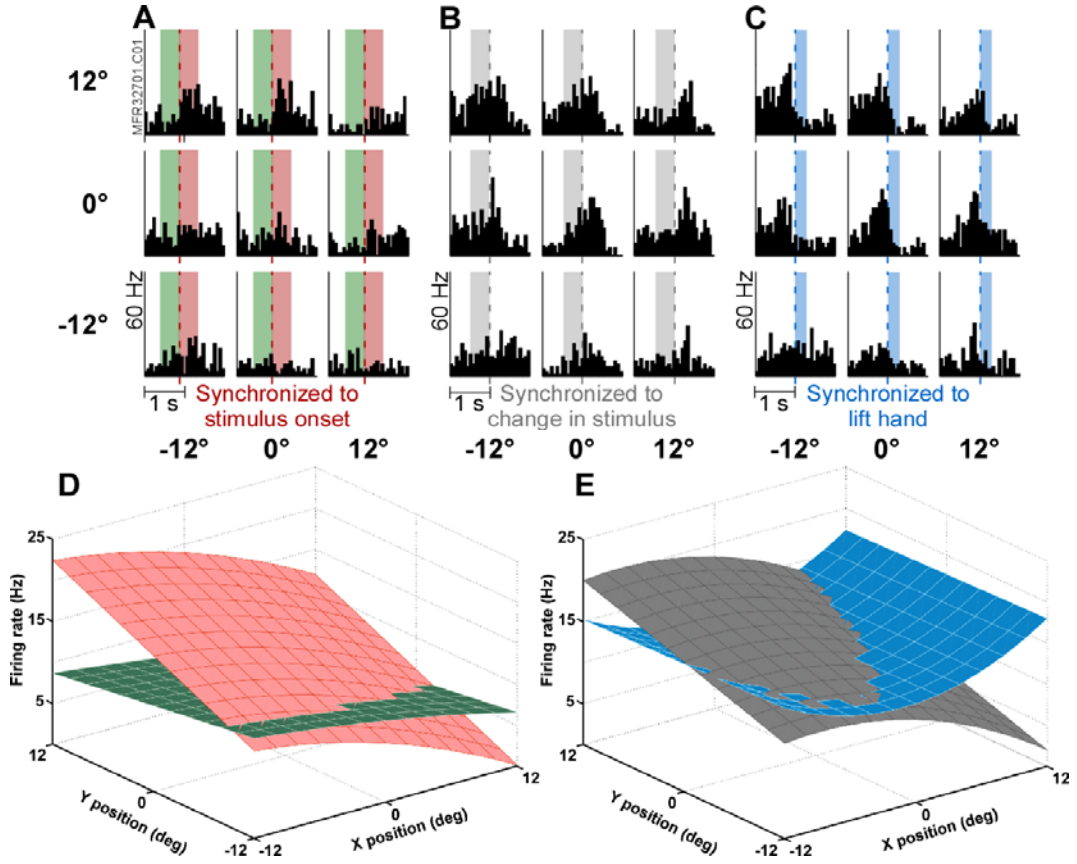


Figure 4.3: **A neuron's response during the pre-prism condition**. (A – C) Peri-stimulus time histograms (PSTH) for a cell that shows modulation in the spatial tuning as the trial progresses during the pre-prism block. Red dotted line marks the onset of the expansion optic flow stimulus (visual stimulus; 1500 ms); gray dotted line marks the time the optic flow stimulus changes to a random motion (between 3500 and 4500 ms); blue dotted line marks the time the monkey initiates a reach by lifting his hand off the touch sensor. The epoch identification is as follows: baseline (green shaded region), visual (red shaded region), preparatory (gray shaded region) and the reach (blue shaded region). The PSTH are arranged in a 3x3 grid. Each of the nine PSTH corresponds to an optic flow visual stimulus appearing at that location. Therefore, each PSTH is an average of 10 trials. Bin width = 60 ms. (D and E) Response fields of the area 7a neuron during the four epochs. (D) Baseline (green) spatial tuning shows preference for the lower contralateral eye positions, $A_{baseline} = -0.23x - 0.15y + 8.22$; whereas the gain field (red) tuning at stimulus onset dominates the contralateral eye positions, $A_{visual} = -0.44x + 0.49y + 13.1$. (E) The preparatory (gray) response of the unit dominates the horizontal meridian and the upper contralateral eye positions, $A_{preparatory} = -0.40x + 0.35y + 14.3$. The reach (blue) response of this unit decreases at the initiation of the reaching behavior, $A_{reach} = 0.09x - 0.03y + 11.7$. The response of this neuron shows an overall change in spatial tuning and neural activity.

This neuron had a minimal baseline response (Fig. 4.3A and D; green shaded region) mostly for lower contralateral eye positions. An increase in the firing rate was observed at the onset of the optic flow stimulus when it appeared in the upper contralateral and center position and in the lower contralateral position. The overall firing rate during the visual epoch (Fig. 4.3A and D; red shaded region) was greater for contralateral eye positions. Therefore, this neuron showed a contralateral gain field preference. During the preparatory epoch (Fig. 4.3B and E; gray shaded region), the neuron showed a spatial preference for stimuli appearing in the contralateral and center upper positions, and along the contralateral horizontal meridian. This change in spatial tuning from the visual epoch implies that transformation occurs as there is a shift from sensory input to an intermediate level before the monkey reaches. An overall sharp decrease in the firing rate of the unit was observed during the reach epoch (Fig. 4.3C and E; blue shaded region) in all but the lower contralateral position. The firing rate of the neuron decreased significantly at the initiation of a reach. Change in spatial tuning and overall firing rate were observed as the trial progressed. This implies that the initial spatial eye position tuning during baseline and visual epochs was modulated by the preparation and initiation of the motor behavior.

Alteration of spatial tuning as the trial progressed was evident in 94/166 (57%) neurons. The tuning curves of these neurons had at least one of four spatial parameters $(a_x, a_y, a_{x^2}, a_{y^2})$ with a significant coefficient. These neurons were therefore classified as multiplicative (ExP; Fig. 4.6); where factor E has four categorical variables (baseline, visual, preparatory, reach) and factor P corresponds to the nine positions of the visual stimuli. The angular tuning for the type ExP neuron population was distributed

uniformly. Fourteen out of 166 (8%) neurons were not spatially tuned but alteration in the firing rate was observed as the trial progressed temporally (type E; Fig. 4.6). Therefore, the change in epoch effect was observed in a majority of the neurons (type ExP and type E combined: 108/166; 65%). No change in response fields and firing rate was observed in 58/166 (35%) neurons; these neurons were classified as non-significant (Fig. 4.6).

Prism condition

The pre-prism condition was followed by the prism condition during which a 12° Fresnel prism was inserted in front of the monkey. The direction of shift was roughly chosen depending upon the gain field tuning of the unit. The spatial tuning was quantified and directly compared using categorical regression across the baseline, visual, preparatory, and reach epochs.

Another example neuron (from DP) showed a modulation in the spatial tuning as the task progressed in time with a 12° upward shift (Fig. 4.4). The baseline response increased towards the contralateral eye positions and those along the horizontal meridian (Fig. 4.4A and D; green shaded region). A transient increase in firing rate was observed at the onset of the stimuli for the upper eye positions resulting in an upper gain field tuning. Following this transient increase in the firing rate, decrease in activity was observed for stimuli appearing in all locations; however this decrease was greater for the upper eye positions (Fig. 4.4A and D; red shaded region). During the preparatory epoch (Fig. 4.4B and D; gray shaded region), the firing rate was the greatest along the horizontal meridian. Thus the spatial tuning of the neuron moved from the upper eye positions during the visual epoch (upper gain field) to center positions along the horizontal meridian during the preparatory epoch, and even further downward towards

the lower positions of the reach endpoints (Fig. 4.4C and D; blue shaded region). Again, this suggests that as the trial progressed, there was an increased modulation of the sensory signals by the motor aspects of the task.

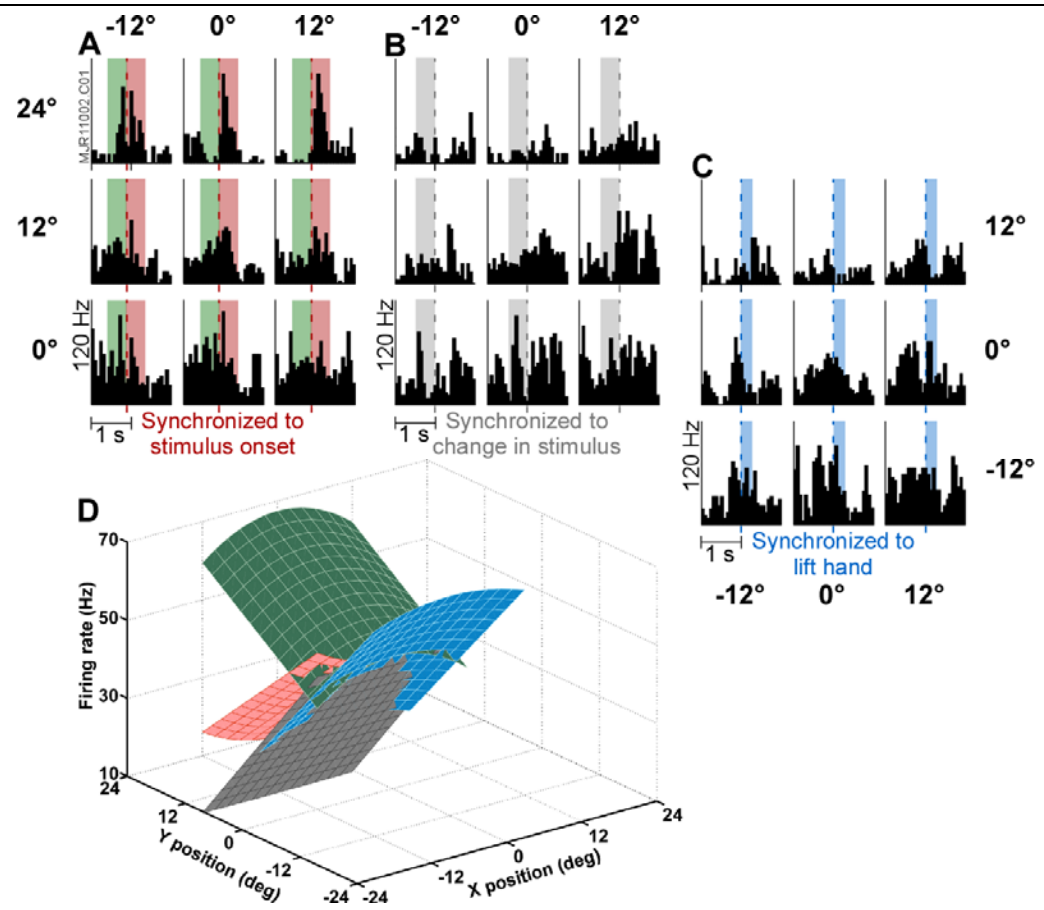


Figure 4.4: **A neuron's response during the prism condition**. (A – C) PSTH for a cell showing modulation in the spatial tuning as the trial progresses during the prism block (12° upward shift). This figure follows the same conventions as Fig. 4.3. Panel A and B are positioned such that the 0° eye position along the vertical axis matches the 0° hand position along the vertical axis. (D) Response fields of the DP neuron during all four epochs. The baseline (green) activity increases towards the eye positions along the horizontal meridian, $A_{baseline} = 0.98y - 0.11y^2 + 43.9$; while the gain field (red) dominates the upper eye positions, $A_{visual} = -1.42y + 0.06y^2 + 43.9$. (B) The preparatory (gray) response is greatest for the eye positions along the horizontal meridian, $A_{preparatory} = -2.03y + 0.03y^2 + 43.9$. (C) The reach (blue) response is greatest for the lower eye positions, $A_{reach} = -1.87y - 0.10y^2 + 43.9$. The spatial tuning of this neuron altered with temporal progression of the trial.

Alteration of spatial tuning was evident in 96/166 (58%) neurons during the prism condition and these were classified as multiplicative neurons (ExP; Fig. 4.6). In these neurons at least one of four spatial parameters were observed to be significant. The angular tuning of these neurons was uniformly distributed. A pure epoch effect on the firing rate (type E; Fig. 4.6) was observed for 11/166 (7%) neurons; these neurons were not spatially tuned. Thus, the epoch effect was observed for a majority of the neurons (type ExP and E together: 107/166; 64%). A total of 59/166 (35%) neurons did not have a significant effect of the epoch; these neurons were not spatially tuned and did not alter their firing rate as the trial progressed (NS; Fig. 4.6).

Post-prism condition

Following the prism condition, the Fresnel prism was removed and the monkey was required to perform the reaching task for the post-prism condition. The post-prism condition was conducted only when the isolation of a neuron remained stable. The spatial tuning of these neurons was quantified for the baseline, visual, preparatory, and reach epochs.

Another area 7a neurons showed modulation in the spatial tuning as the task progressed in time (Fig. 4.5). The baseline response (Fig. 4.5A and D; green shaded region) of this neuron was the lowest when the eye was positioned in the upper contralateral and the center locations. This response increased towards the ipsilateral and contralateral lower eye positions. The firing rate of the unit was the greatest when the optic flow stimulus appeared in the lower ipsilateral positions (Fig. 4.5A and E; red shaded region). This rate decreased progressively towards the upper contralateral corner position resulting in a lower ipsilateral gain field. During the preparatory epoch (Fig.

4.5B and E; gray shaded region), the firing rate was greatest for the lower contralateral eye position. During the reach epoch (Fig. 4.5C and E; blue shaded region), the firing rate was the greatest for ipsilateral positions and decreased progressively towards the lower contralateral corner. The response field therefore dominated the ipsilateral positions. The spatial tuning of this neuron thus started in the lower quadrant in the ipsilateral eye

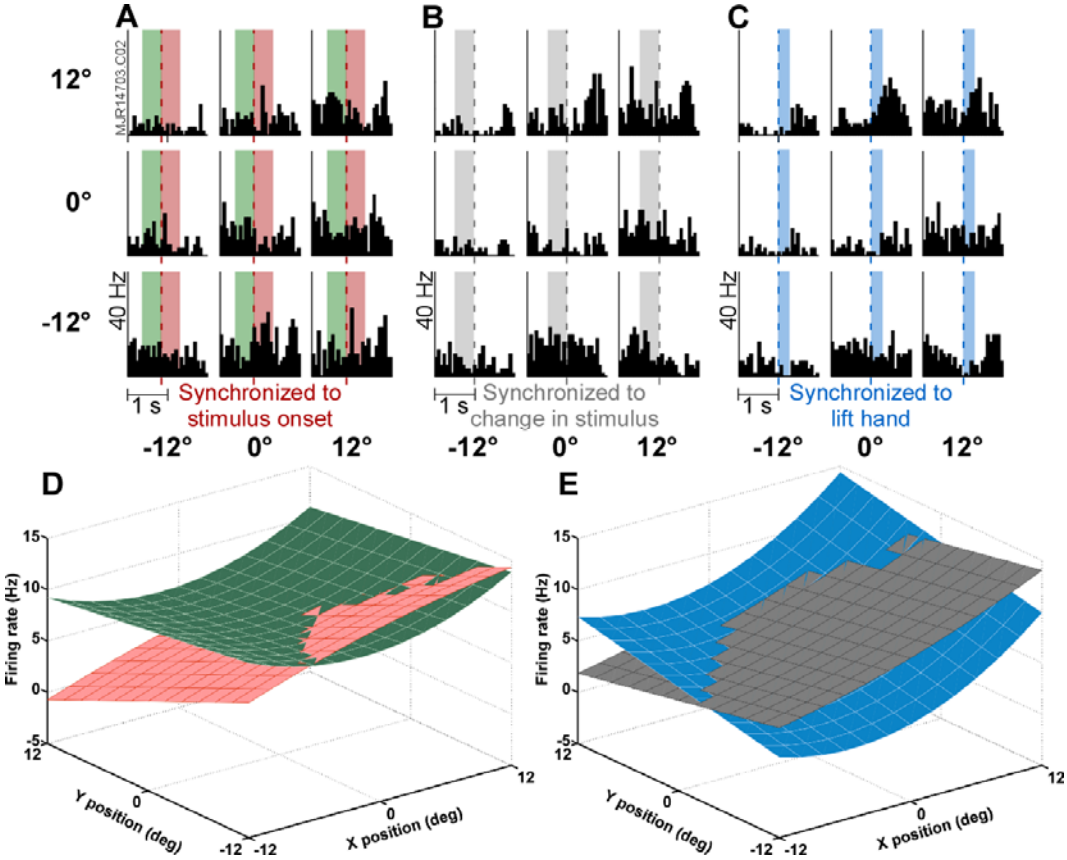


Figure 4.5: **A neuron's response during the post-prism condition**. (A – C) PSTH for a cell showing modulation in the spatial tuning as the trial progresses during the post-prism block. This figure follows the same conventions as Fig. 4.3. (D and E) Response fields of the area 7a neuron during the four epochs. (D) The baseline response (green) of the unit is the greatest for ipsilateral and lower contralateral eye positions, $A_{baseline} = 0.08x - 0.12y + 8.22$. The gain field (red) of the unit dominates the lower eye positions, $A_{visual} = 0.26x - 0.37y + 7.51$. (E) The preparatory response (gray) of the unit is the greatest for lower center and ipsilateral eye positions, $A_{preparatory} = 0.35x - 0.16y + 7.07$. The reach (blue) tuning of the unit dominates the ipsilateral positions. The reach response of the unit decreases towards the center position and the upper contralateral position, $A_{reach} = 0.29x + 0.19y + 4.78$. The spatial tuning of this neuron altered with respect to different temporal events.

positions at the onset of the visual stimulus, then shifted to the lower contralateral eye positions during the preparatory epoch and finally shifted to the upper ipsilateral positions as the monkey initiated the reach.

Alteration of spatial tuning as the trial progressed was evident in 52/105 (50%) neurons classified as ExP (Fig. 4.6). The population spatial tuning for these neurons showed a uniformly distributed representation of space. In 7/105 (7%) neurons a change in overall firing rate (intercept) was observed although these neurons were not spatially tuned (type E; Fig. 4.6). Thus the epoch effect was observed for a majority of the neurons (type ExP and E neurons combined: 59/105; 57%). The non-significant group of neurons consisted of 29/105 (28%) neurons. These neurons neither had altered firing rate, nor were they spatially tuned (NS; Fig. 4.6).

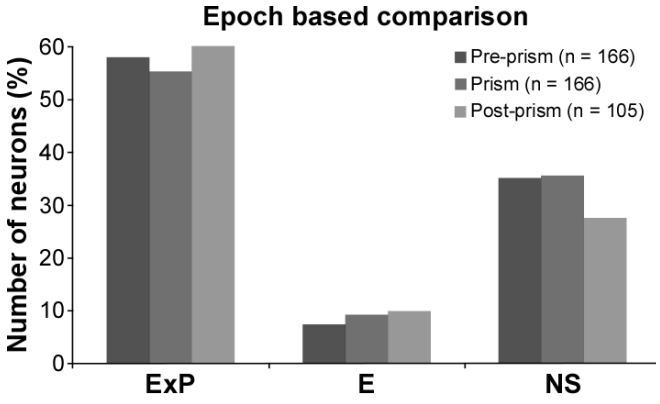


Figure 4.6: **Population distribution of epoch based comparison**. Proportions of interaction types between epoch (E) and position (P) during the pre-prism, prism, and post-prism conditions. Type ExP neurons had a multiplicative interaction between epoch and position; these neurons had different spatial tuning between epochs. Type E neurons had a single effect of epoch; these neurons were not spatially tuned but had an alteration in mean firing rate. NS cells had no effect of either factor. Majority of the neurons altered their spatial tuning over time during all three conditions.

Summary

In the majority of neurons (Fig. 4.6; type ExP and E cells combined: pre-prism, 65%; prism, 64%; post-prism, 57%) the tuning properties modulated as the trial progressed. Quantified spatial tunings for all the epochs separately for pre-prism, prism,

and post-prism conditions showed that the spatial tuning for the baseline, visual, preparatory, and reach epoch were different for more than half of the neurons tested. The change in spatial tuning confirmed that there was a shift in cortical representation of space as the behavior progressed from perception of a sensory stimulus to the initiation of the motor response. The lack of spatial specificity observed (uniform angular tuning of type ExP neurons) in areas 7a and DP implies that there is an equally distributed representation of space in these two areas.

Comparison of single unit activity between pre-prism and prism conditions

In the second type of analysis, condition based comparison was performed to examine cortical plasticity as a result of prismatic distortion. The neural activity during each epoch (baseline, visual, preparatory, and reach) in the pre-prism condition was quantified and directly compared to the respective epoch in the prism condition using categorical regression. The Fresnel prism was used to induce a 12º shift along the horizontal or vertical axis. The direction of the induced distortion was based approximately on the gain field tuning during the initial condition (pre-prism). This resulted in four shifts: contralateral (n = 15), ipsilateral (n = 44), upward (n = 70), and downward (n = 37). These four shifts were used to examine the spatial modulation and the spatial representation of the neural signals for the different epochs.

Each unit was tested for only one prism shift. Each block of 90 trials was completed in approximately 40 minutes, depending on the monkeys' performance. Thus the completion of the entire set of three blocks (pre-prism, prism, and post-prism) required about two hours. Monkeys were required to reach to the actual physical location

of the visual stimulus and not the perceived location. Thus the actual reach target locations under both conditions were identical; however the perceived target location and therefore the eye-positions were shifted depending on the prism shift during the prism condition. Therefore any change in the reach response of a neuron can be attributed to the shifted or altered eye-position.

Condition based comparison was used to compare each epoch (e.g. baseline, visual, preparatory, and reach) during the pre-prism condition to the respective epoch during the prism condition.

Baseline epoch

During the baseline epoch the monkey is fixating a red square (with a 0.8° diagonal) in one of nine possible locations. An area 7a neuron showed alteration of spatial tuning once the prism induced a 12° downward shift (Fig. 4.7). The baseline response of this neuron had a weak preference for the eye positions in the center and the lower positions along the vertical meridian during the pre-prism condition (Fig. 4.7A, green shaded region; Fig. 4.7C, light green shaded region). The neuron was tuned to contralateral eye-positions during the prism condition (Fig. 4.7B, green shaded area; Fig. 4.7C, dark green shaded region). Slight alteration of spatial tuning during the baseline epoch was expected because of a physical shift in eye position resulting from the prismatic distortion.

Change in spatial tuning was observed in 95/166 (57%) neurons. Because there was an interaction between the condition (C; pre-prism vs. prism) and the position (P; nine positions) these neurons were classified as neurons with multiplicative interaction

(CxP; Fig. 4.10). For the response field of these neurons, at least one of the four spatial parameters $(a_x,\ a_y,\ a_{x^2},\ a_{y^2})$ reached the level of significance.

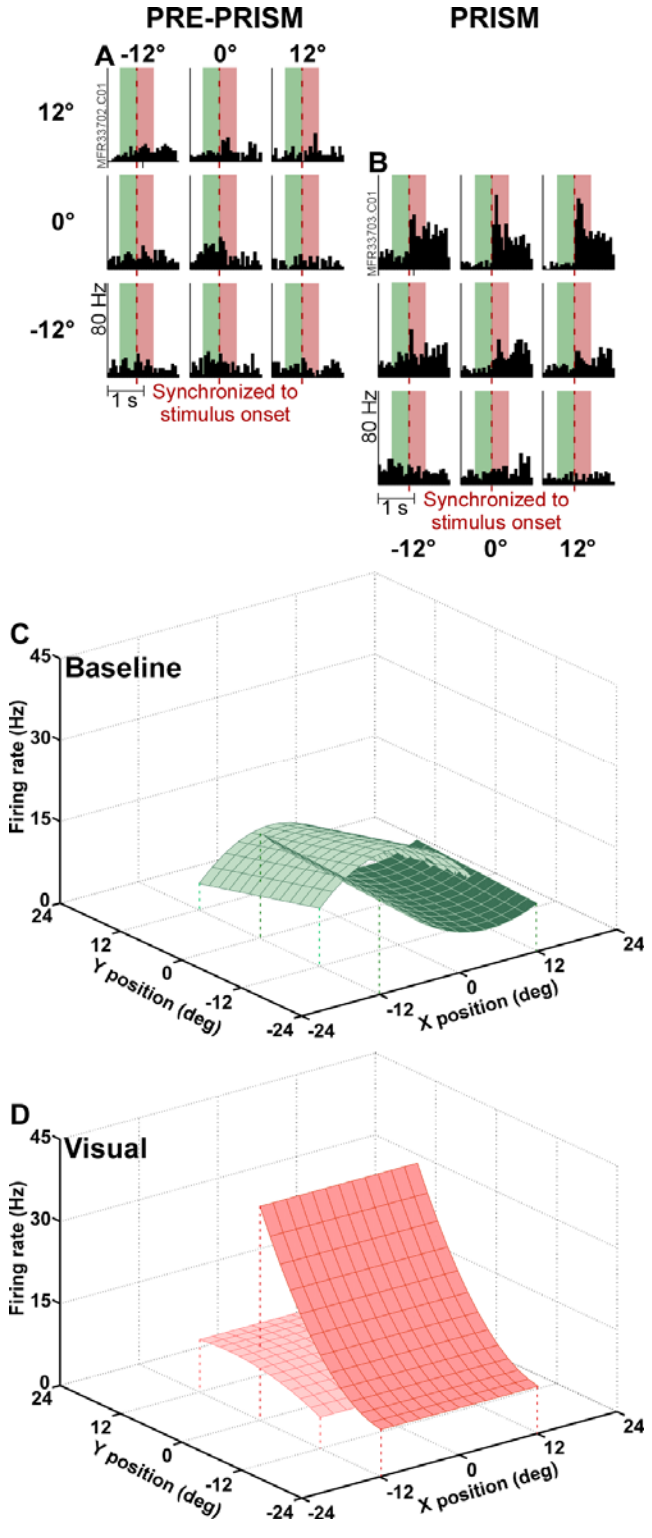


Figure 4.7: **Response of a neuron during baseline and visual epochs of the pre-prism and prism conditions**. Neural response of a unit during the pre-prism and prism (12° downward shift) conditions for the baseline, visual epochs. This figure follows the same conventions as Fig. 4.3. Panel B is positioned such that the 0° eye position along the vertical axis matches the 0° eye position (along the vertical axis) during the pre-prism condition. (A) PSTH during the pre-prism condition. (B) PSTH during the prism condition. (C) Baseline epoch during pre-prism condition (light green): $A_{pre-prism} = -0.13x - 0.24y - 0.06x^2 + 14.8$. Baseline epoch during prism condition (dark green): $A_{prism} = -0.39x + 0.06y - 0.04x^2 + 8.79$. (D) Visual epoch during pre-prism condition (light red): $A_{pre-prism} = 0.16y - 0.01y^2 + 9.5$. Visual epoch during prism condition (dark red): $A_{prism} = 2.41y - 0.05y^2 + 39.1$.

Upon comparing the spatial tuning for baseline and visual epochs with and without prism, it was observed that the presentation of the prism alters the spatial tuning of this neuron.

Table 4.1 lists the distribution of CxP type neurons with significant linear and quadratic coefficients based on the prism shift (up, down, ipsilateral, and contralateral).

	Up (n = 70)	Down (n = 37)	Ipsilateral (n = 44)	Contralateral (n = 15)
Total CxP type neurons	49 (70%)	18 (49%)	23 (52%)	5 (33%)
Linear modulation only	31	9	9	1
Linear and quadratic modulation	10	3	14	1
Quadratic modulation only	8	6	0	3

Table 4.1: Distribution of CxP type neurons during the baseline epoch. Neurons were classified as type CxP if their tuning properties showed a multiplicative interaction effect between the condition (C; pre-prism and prism) and the position (P, nine positions). This table lists the number of neurons for which the linear, quadratic, or both components were observed to be significant (type CxP) during the baseline epoch. Neurons tested with different prism shifts are listed separately. Due to a large difference in the number of neurons in each sample pool, no conclusive trend can be confirmed.

Only condition effect (type C; Fig. 4.10) was observed in 38/166 (23%) neurons. These neurons were not spatially tuned but the overall firing rate was significantly different during the two conditions. That is, the firing rate of these neurons was uniform for all nine positions but this rate altered once prisms were inserted. Thus the condition effect (prism effect) was observed in a majority of neurons (type CxP and C combined: 134/166, 80%). Neither a condition effect nor a spatial effect was observed in 33/166 (20%) neurons (NS; Fig. 4.10).

Visual epoch

The visual epoch was defined as the 500 ms time interval immediately after the onset of the expanding optic flow stimulus. The monkey's hand was placed at the starting

point on the touch sensor while his eye was positioned on the fixation point and the visual stimulus. During the visual epoch of pre-prism condition (Fig. 4.7A, red shaded region; Fig. 4.7D, light red shaded region), the unit showed a weak gain field tuning in for the center and upper eye positions. However in presence of the prism shifting the target stimuli downward, the overall firing and the spatial tuning of the unit changed dramatically. The firing rate of the unit was the greatest for stimuli appearing along the horizontal meridian (what used to be the three upper positions during pre-prism condition, now matched to center eye positions and perceived location of the stimuli – Fig. 4.7B, red shaded region; Fig. 4.7D, dark red shaded region). The unit thus had a spatial tuning that peaked along the horizontal meridian and decreased along the vertical axis (downward) in presence of the prism.

	Up (n = 70)	Down (n = 37)	Ipsilateral (n = 44)	Contralateral (n = 15)
Total CxP type neurons	40 (57%)	14 (38%)	22 (50%)	6 (40%)
Linear modulation only	17	8	4	4
Linear and quadratic modulation	12	4	9	1
Quadratic modulation only	11	2	9	1

Table 4.2: Distribution of CxP type neurons during the visual epoch. Neurons were classified as type CxP if their tuning properties showed a multiplicative interaction effect between the condition (C; pre-prism and prism) and the position (P, nine positions). This table lists the number of neurons for which the linear, quadratic, or both components were observed to be significant (type CxP) during the visual epoch. Neurons tested with different prism shifts are listed separately. Due to a large difference in the number of neurons in each sample pool, no conclusive trend can be confirmed.

Spatial tuning of 82/166 (49%) neurons altered during the visual epoch and were thus classified as type CxP (Fig. 4.10). At least one of the four spatial parameters

$(a_x, a_y, a_{x^2}, a_{y^2})$ reached significance. Table 4.2 lists the distribution of CxP type neurons with significant linear and quadratic spatial tuning based on the type of prism shift (up, down, ipsilateral, and contralateral).

Only the condition effect (change in firing rate but no spatial tuning; type C; Fig. 4.10) was observed in 48/166 (29%) neurons during the visual epoch. These neurons were either not spatially tuned or had gain fields that extended beyond the display size and thus could not be properly mapped. Nonetheless, they significantly changed their overall firing rate between pre-prism and prism condition. Therefore a majority of neurons (type CxP and C combined: 130/166, 78%) were affected by the prismatic distortion. These results were expected because the physical eye position is altered with respect to the prism shift. Since the eye position modulates the visual response, tuning properties of a majority of neurons in area 7a and DP changed during the visual epoch. The rest of the 36/166 (22%) neurons did not show any effect and were thus classified as not significant (NS; Fig. 4.10).

Preparatory epoch

The time interval 500 ms prior to the change in visual stimulus was considered the preparatory epoch. During this epoch the monkey was fixating the visual stimulus and the hand was resting on the touch sensor. Thus overt behavior during the preparatory epoch was identical to the visual epoch. Changes in spatial tuning between the pre-prism and prism condition would imply that during this late preparatory phase the system recruits different neural circuits. Modulation in spatial tuning under the two conditions during this time interval may also suggest that differential mechanisms affect spatial tuning once the sensory input is perturbed.

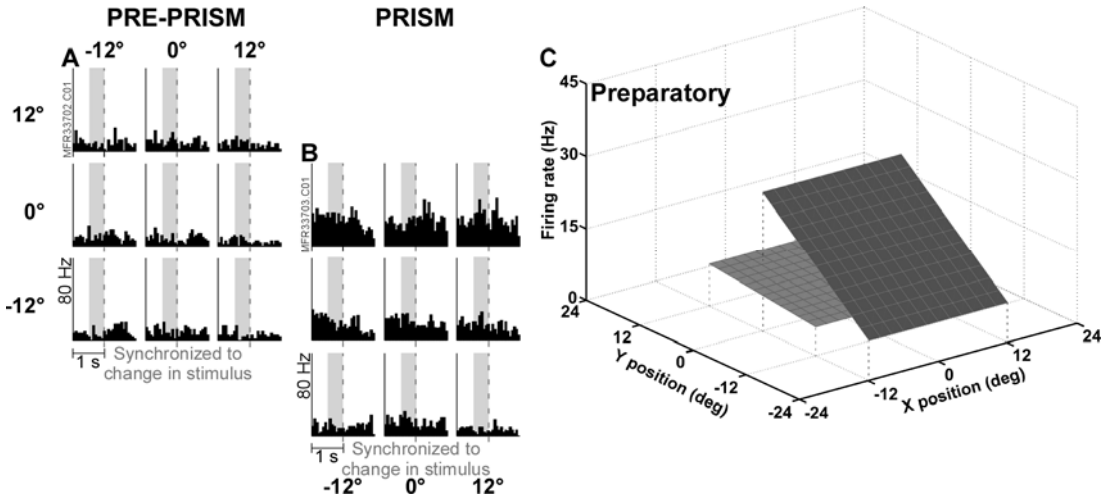


Figure 4.8: **Response of a neuron during preparatory epoch of the pre-prism and prism conditions**. Neural response of the same neuron shown in Fig. 4.7 during the pre-prism and prism (12° downward shift) conditions for the preparatory epoch. This figure follows the same conventions as Fig. 4.7. (A) PSTH during the pre-prism condition. (B) PSTH during the prism condition. (C) Preparatory epoch during pre-prism condition (light gray): $A_{pre-prism} = 0.12y + 7.36$. Preparatory epoch during prism condition (dark gray): $A_{prism} = 0.86y + 28.9$. Comparison of the spatial tuning responses during the preparatory epoch with and without prism indicated that visual perturbation led to alteration in the spatial tuning of this neuron.

For the preparatory epoch during the pre-prism condition (Fig. 4.8A, gray shaded region; Fig. 4.8C, light gray shaded region), this unit was not spatially tuned and overall firing rate was low. However, during the prism condition the unit had an overall increase in firing rate and had a strong spatial tuning for the eye positions along the horizontal meridian (matched locations for the eye positions – Fig. 4.8B, gray shaded region; Fig. 4.8C, dark gray shaded region) which decreased linearly along the vertical axis.

Modulation in spatial tuning during the preparatory epoch was observed in 88/166 (53%) neurons. These neurons had at least one significant spatial parameter $(a_x, a_y, a_{x^2}, a_{y^2})$ and were classified as type CxP (Fig. 4.10). Table 4.3 lists the distribution of CxP type neurons with significant linear and quadratic spatial tuning based on the type of prism shift (up, down, ipsilateral, and contralateral).

	Up (n = 70)	Down (n = 37)	Ipsilateral (n = 44)	Contralateral (n = 15)
Total CxP type neurons	43 (61%)	18 (49%)	22 (50%)	5 (33%)
Linear modulation only	26	6	7	2
Linear and quadratic modulation	9	5	11	1
Quadratic modulation only	8	1	4	2

Table 4.3: Distribution of CxP type neurons during the preparatory epoch. Neurons were classified as type CxP if their tuning properties showed a multiplicative interaction effect between the condition (C; pre-prism and prism) and the position (P, nine positions). This table lists the number of neurons for which the linear, quadratic, or both components were observed to be significant (type CxP) during the preparatory epoch. Neurons tested with different prism shifts are listed separately. Due to a large difference in the number of neurons in each sample pool, no conclusive trend can be confirmed.

About one third of neurons were classified as type C (57/166; 34%; Fig. 4.10). These neurons were not spatially tuned but changed their overall firing rate upon the insertion of a prism. The prism effect was thus observed in a majority of the neurons (145/166, 87%; type CxP and C combined). The rest of the neurons (21/166; 13%) were not affected by the prism and were therefore classified as not significant (NS; Fig. 4.10).

Reach epoch

Although the prismatic distortion resulted in a perceptual shift of the visual field, the monkeys were required to reach to the actual physical location of the visual stimulus. This resulted in adjusted reaches during the prism conditions; i.e., reaches were not made directly to the perceived location of the visual stimulus but away from it. Since the physical reach endpoints were similar between the two conditions (pre-prism and prism), spatial tuning during the reach epoch should remain unaltered. Differences in spatial tuning during the reach epoch under the two conditions would imply that the reach signal

is dependent on the physical eye position. The physical eye position is altered due to the prismatic distortion; thus modulating the reach response.

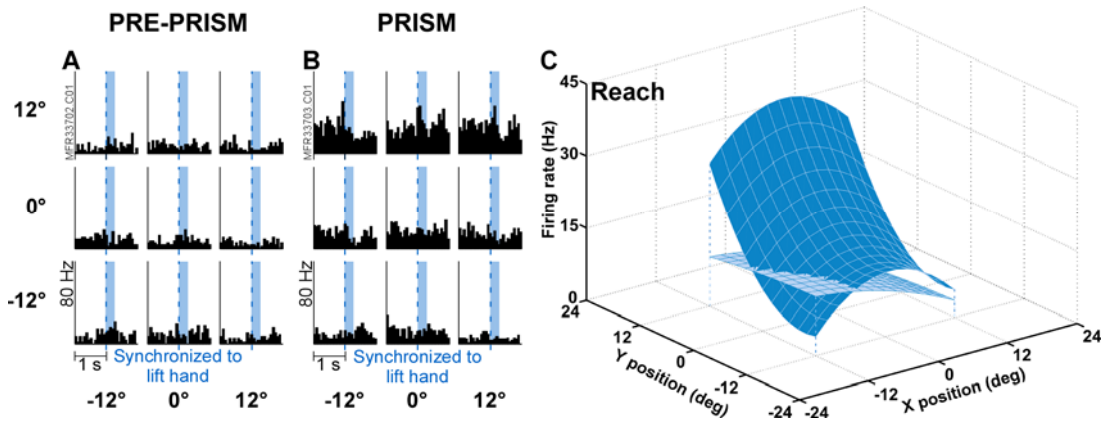


Figure 4.9: **Response of a neuron during reach epoch of the pre-prism and prism conditions**. Neural response of the same neuron shown in Fig. 4.7 during the pre-prism and prism (12° downward shift) conditions for the preparatory epoch. This figure follows the same conventions as Fig. 4.7. (A) PSTH during the pre-prism condition. (B) PSTH during the prism condition. (C) Reach epoch during the pre-prism condition (light blue): $A_{pre-prism} = -0.36x - 0.08y - 0.01x^2 - 0.002y^2 + 8.93$. Reach epoch during the prism condition (dark blue): $A_{prism} = 0.08x - 1.07y - 0.06x^2 - 0.06y^2 + 18$.

The example area 7a neuron was not spatially tuned during the reach epoch under the pre-prism condition (Fig. 4.9A, blue shaded region; Fig. 4.9C, light blue shaded region). Upon inserting the prism, the neuron responded with an increase in firing rate for reaches made to reach targets in the upper and central positions (Fig. 4.9B, blue shaded region; Fig. 4.9, dark blue shaded region). Although the reach end positions were similar for the pre-prism and the prism conditions, the spatial tuning of the neuron was significantly different during the reach epoch under the two conditions. The neural activity was greater for the upper positions of the reach endpoint under the prism condition, whereas the neuron was not spatially tuned for the reach epoch during the pre-prism condition. The alteration of the response field along with the change in the eye

position confirms that the reaching behavior and the eye position are related and that the reach signal is eye position dependent.

Spatial tuning modulation in presence of the Fresnel prism was observed in 99/166 (60%) neurons during the reach epoch. These neurons showed a multiplicative interaction between condition and reach target position and were classified as CxP (Fig. 4.10). Spatial modulation of the tuning of a majority of the neurons implies that the reach signal in the IPL is eye position dependent. Table 4.4 lists the distribution of CxP type neurons with significant linear and quadratic spatial tuning based on the type of prism shift (up, down, ipsilateral, and contralateral).

	Up (n = 70)	Down (n = 37)	Ipsilateral (n = 44)	Contralateral (n = 15)
Total CxP type neurons	45 (64%)	18 (49%)	28 (64%)	8 (53%)
Linear modulation only	22	6	12	2
Linear and quadratic modulation	15	7	9	3
Quadratic modulation only	8	5	7	3

Table 4.4: Distribution of CxP type neurons during the reach epoch. Neurons were classified as type CxP if their tuning properties showed a multiplicative interaction effect between the condition (C; pre-prism and prism) and the position (P, nine positions). This table lists the number of neurons for which the linear, quadratic, or both components were observed to be significant (type CxP) during the reach epoch. Neurons tested with different prism shifts are listed separately. Due to a large difference in the number of neurons in each sample pool, no conclusive trend can be confirmed.

Some neurons (35/166; 21%) were classified as type C (Fig. 4.10) neurons. These neurons were not spatially tuned but had an alteration in overall firing rate upon the insertion of a prism. The tuning properties of a total of 134/166 (81%) neurons (type CxP and C combined) were affected by the prismatic distortion. The reach location of for the

pre-prism and the prism condition was identical however the eye position was physically shifted due to the prismatic distortion. The modulation of spatial tuning of a majority of neurons during the reach epoch confirms the claim that reach signal is dependent on the eye position. The rest of the neurons (32/166; 19%) were not affected by the prism and were therefore classified as not significant (NS; Fig. 4.10).

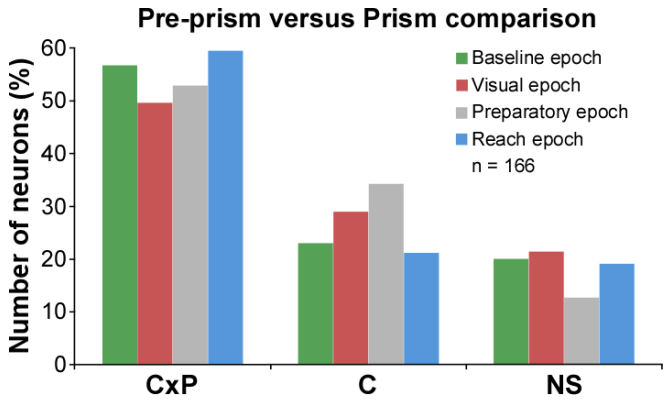


Figure 4.10: **Population distribution of pre-prism vs. prism comparison**. Condition based analysis was used to compare pre-prism and prism conditions separately for the four epochs: baseline (green), visual (red), preparatory (gray), and reach (blue). Proportions of interaction types between condition (C) and position (P) are plotted. Type CxP neurons had a multiplicative interaction between condition and position; these neurons had different spatial tuning between the two conditions. Type C neurons had a single effect of condition; these neurons were not spatially tuned but had an alteration in mean firing rate upon introducing the Fresnel prism. NS cells had no effect of either factor. Majority of the neuron altered their tuning properties once the prism was inserted.

Summary

Based on rigorous quantitative direct comparison between pre-prism and prism conditions multiplicative interactive (CxP) neurons were observed for all epochs. The spatial tuning of these neurons altered once the prism was inserted. Furthermore type C neurons, which were not spatially tuned but had a condition based change in overall firing rate, were observed for all epochs. Therefore a majority of neurons (Fig. 4.10; type CxP and C cells combined: baseline, 80%; visual, 78%; preparatory, 87%; reach, 81%) were affected by inducing a prism shift. This implies that the prismatic distortion induced dramatic changes in the firing pattern of these neurons.

Modulation of spatial tuning due to displacement of the perceived visual field

The change in tuning due to the prism displacement was assessed for each of the four epochs (baseline, visual, preparatory, and reach) separately. The spatial tuning for all significant neurons during each of the four epochs was distributed uniformly during the pre-prism condition. The preferred axis (horizontal or vertical) was maintained by all neurons even in presence of the prism but the magnitude along the axis changed (Fig. 4.9; area 7a neuron).

Baseline epoch: During the baseline epoch under the pre-prism condition (Fig. 4.11A; green shaded region) the neuron was weakly tuned to the upper and lower eye positions along the vertical meridian and in the contralateral direction. With a 12º upward prism shift (Fig. 4.11B; green shaded region) the spatial tuning altered along both the vertical and the horizontal axis. The firing rate decreased for the upper eye positions (positions that were originally preferred) and also for the ipsilateral eye positions. This is a surprising finding as the prism only manipulated the visual perception along the vertical axis but the spatial tuning alteration occurred along the horizontal axis (Fig. 4.11C).

Visual epoch: A similar shift in spatial tuning was observed during the visual epoch (Fig. 4.11A compared to Fig. 4.11B; red shaded regions). Response to the onset of the visual stimulus was greatest along the vertical meridian and decreased for the ipsilateral and contralateral eye positions during the pre-prism condition (Fig. 4.11A; red shaded region). In presence of the prism the firing rate was greatest for stimuli appearing along the horizontal meridian (Fig. 4.11B; red shaded region) and was maintained toward the contralateral positions. This response decreased for the upper and the ipsilateral eye positions. The spatial tuning altered along the vertical *and* horizontal axis (Fig. 4.11C).

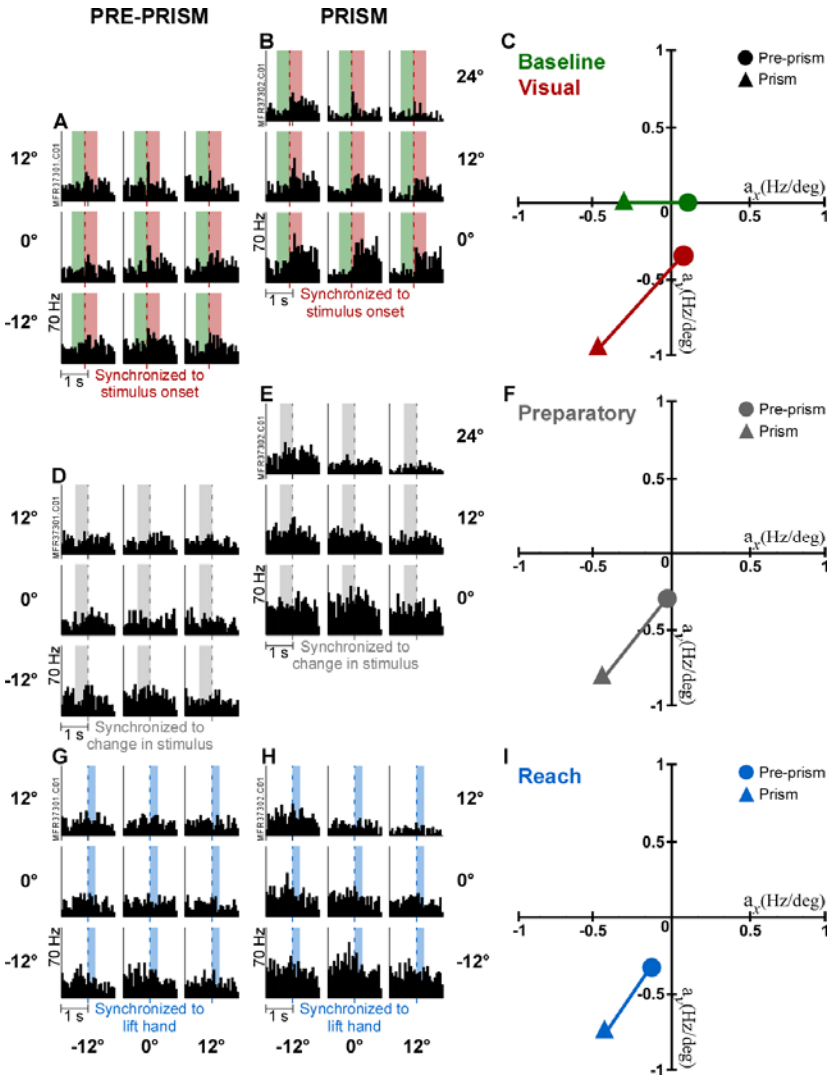


Figure 4.11: **Response of a neuron during pre-prism and prism conditions**. Neural response of a unit during the pre-prism and prism (12° upward shift) condition for the baseline, visual, preparatory, and the reach epochs. This figure follows the same conventions as Fig. 4.7. (A) Baseline epoch during pre-prism condition: $A_{pre-prism} = 0.09x + 0.03y^2 + 15.5$. Visual epoch during pre-prism condition: $A_{pre-prism} = 0.08x - 0.34y - 0.02x^2 + 21.3$. (B) Baseline epoch during prism condition: $A_{prism} = -0.32x - 0.01y^2 + 13.5$. Visual epoch during prism condition: $A_{prism} = -0.46x - 0.94y - 0.006x^2 + 33.5$. (C) The linear components derived from regression analysis for the pre-prism (circle) and prism (triangle) conditions during the baseline (green) and visual (red) epochs. (D) Preparatory epoch during pre-prism condition: $A_{pre-prism} = -0.02x - 0.31y - 0.02x^2 + 16.8$. (E) Preparatory epoch during prism condition: $A_{prism} = -0.44x - 0.81y - 0.02x^2 + 32.3$. (F) Linear components during the preparatory (gray) epoch. Conventions same as panel C. (G) Reach epoch during the pre-prism condition: $A_{pre-prism} = -0.12x - 0.33y + 16.8$. (H) Reach epoch during the prism condition: $A_{prism} = -0.42x - 0.74y + 21.2$. (I) Linear components during the reach (blue) epoch. Conventions as per panel C. Even though the visual field was displaced along the vertical axis, a change in tuning along the horizontal axis was observed for all four epochs.

Preparatory epoch: During the pre-prism condition, the neuron was weakly tuned and preferred the lower positions (Fig. 4.11D; gray shaded region). With the prisms the neuron was more strongly tuned for the contralateral positions and positions along the horizontal meridian (Fig. 4.11E; gray shaded region). Similar to the visual epoch, the spatial tuning altered along an axis that was not manipulated (Fig. 4.11F).

Reach epoch: The reach response of this neuron dominated the contralateral and the lower reach endpoint location along the vertical meridian during the pre-prism condition (Fig. 4.11G; blue shaded region). With the prism shift the response was greatest for the lower contralateral endpoint location (Fig. 4.11H; blue shaded region). Thus, the prism attenuated the neural response along the preferred axes, which was not the axes that was manipulated (Fig. 4.11I). This was very surprising and indicated that more than just the eye position influenced the neural response during reaching.

Shifts in spatial tuning: Shifts in spatial tuning did not necessarily follow the shift induced by the prism. Instead the modulation in spatial tuning occurred in various directions with respect to the prism shift, which are categorized as follows:

Orthogonal: The prism distortion was along the horizontal axis and the spatial tuning altered along the vertical axis or vice versa.

Ipsilateral: Spatial tuning altered in the same direction as the prism shift, i.e., the prism was used to shift the visual field to the right and the spatial tuning altered towards the right.

Contralateral: Spatial tuning altered in the opposite direction to the prism shift, i.e., the prism was used to shift the visual field to the right and the spatial tuning altered towards the left.

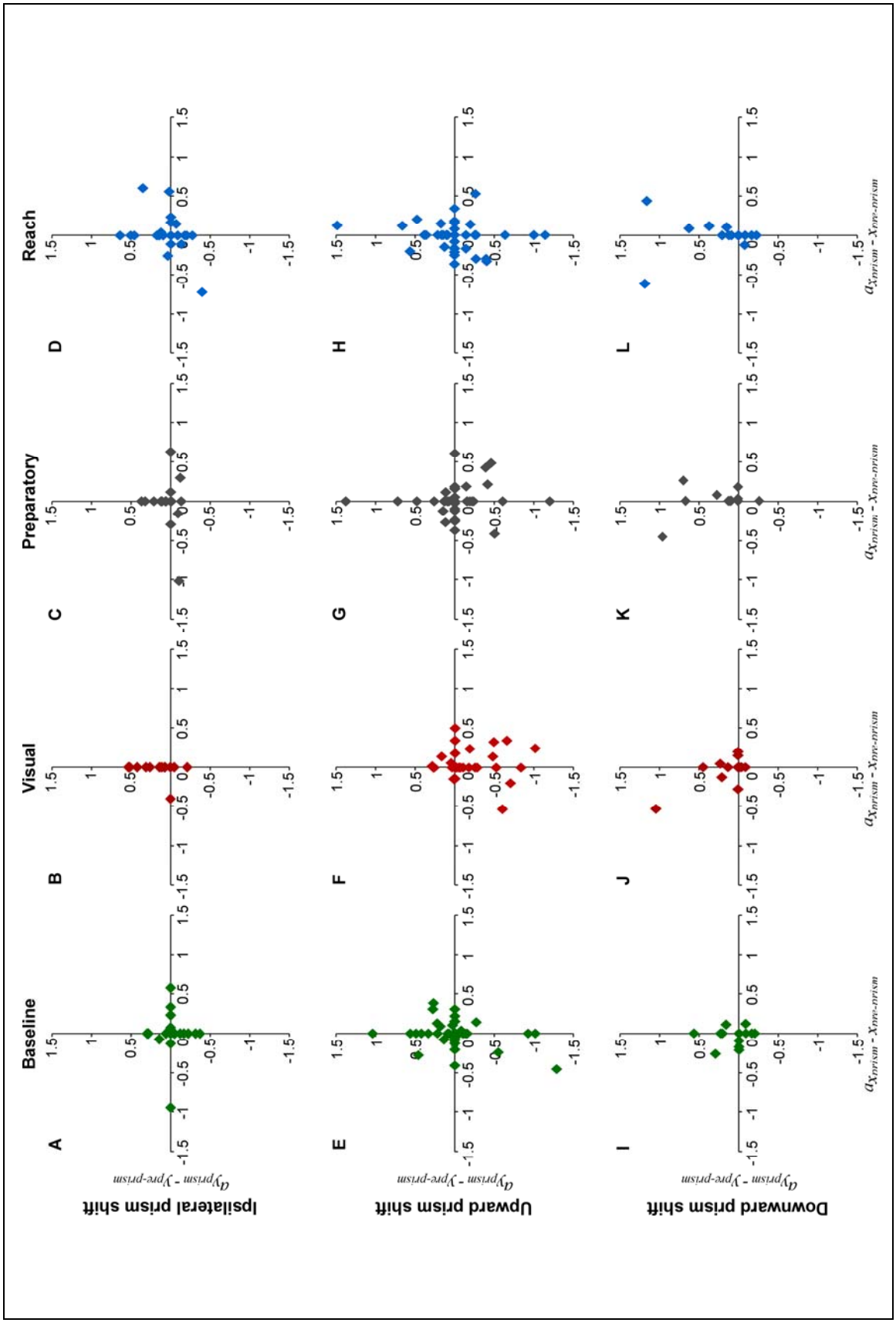
For a neuron to compensate for the prism distortion, the expected change in spatial tuning would be in the direction contralateral to the prism distortion. However, the changes in spatial tuning due to the prismatic distortion did not follow the expected changes in the majority of neurons (Fig. 4.12).

Ipsilateral prism shift (Fig. 4.12A – D): When the Fresnel prism was used to displace the visual field ipsilaterally, the resulting changes in spatial tuning were observed in all four directions for the neural population. Such a uniform distribution was observed during the baseline (Fig. 4.12A), preparatory (Fig. 4.12C), and the reach (Fig. 4.12D) epoch.

Upward prism shift (Fig. 12E – H): An upward prism shift modulated the spatial tuning of the neurons along both the horizontal and the vertical axis during the baseline (Fig. 4.12E), visual (Fig. 4.12F), preparatory (Fig. 4.12G), and reach (Fig. 4.12H) epoch.

Downward prism shift (Fig. 4.12I – L): Inducing a downward prism shift altered the spatial tuning of the population of neurons in all four directions. Such a change in spatial tuning was observed for all four epochs: baseline (Fig. 4.12I), visual (Fig. 4.12J), preparatory (Fig. 4.12K), and reach (Fig. 4.12L).

Figure 4.12: **Population overview of spatial tuning modulation**. Modulation of spatial tuning following ipsilateral (A – D), upward (E – H), and downward prism shift during the four epochs (baseline – green; visual – red; preparatory – gray; reach – blue). Each colored diamond represents one neuron's difference in linear coefficients. X-axis plots the difference between the horizontal components of the center of the spatial tuning fields during the prism and the pre-prism conditions ($a_{X_{prism} - X_{pre-prism}}$). Y-axis plots the difference between the vertical components of the center of the spatial tuning fields during the prism and the pre-prism conditions ($a_{Y_{prism} - Y_{pre-prism}}$). (A) Ipsilateral prism shift, baseline epoch; (B) Ipsilateral prism shift, visual epoch; (C) Ipsilateral prism shift, preparatory epoch; (D) Ipsilateral prism shift, reach epoch; (E) Upward prism shift, baseline epoch; (F) Upward prism shift, visual epoch; (G) Upward prism shift, preparatory epoch; (H) Upward prism shift, reach epoch; (I) Downward prism shift, baseline epoch; (J) Downward prism shift, visual epoch; (K) Downward prism shift, preparatory epoch; (L) Downward prism shift, reach epoch. Modulation of spatial tuning occurred in all directions for all epochs and was independent of the type of prism shift.


Baseline
Visual
Preparatory
Reach
A
B
C
D
E
F
G
H
I
J
K
L
Ipsilateral prism shift
Upward prism shift
Downward prism shift
a_{Yprism} - $Y_{pre\text{-}prism}$
a_{Xprism} - $X_{pre\text{-}prism}$

Contralateral prism shift: The sample pool tested for the contralateral prism shift was very small (n = 15) and therefore not enough for conclusion of results.

The above data show that modulation of spatial tuning was not dependent on the type of prism shift. All prism shifts (ipsilateral, upward, and downward) resulted in changes in spatial tuning in all four directions. Similar results were observed for the contralateral prism shift. Data for this type of distortion is not shown due to a very small sample pool. Table 4.5 is a summary of distribution of type CxP neurons with modulation in spatial in various directions.

	Baseline (n = 95)	Visual (n = 82)	Preparatory (n = 88)	Reach (n = 99)
Orthogonal	26 (27%)	19 (23%)	24 (27%)	25 (25%)
Ipsilateral	23 (24%)	14 (17%)	12 (14%)	5 (5%)
Contralateral	12 (13%)	8 (10%)	14 (16%)	18 (18%)
Orthogonal and Ipsilateral	10 (11%)	8 (10%)	8 (9%)	17 (17%)
Orthogonal + Contralateral	4 (4%)	10 (12%)	9 (10%)	11 (11%)

Table 4.5: Distribution of CxP type neurons with spatial tuning shifts in various directions. If the neurons were simply correcting for the prism shift, the spatial tuning would alter only in the direction opposite to the prism shift in order to compensate for the distortion. According to this hypothesis, only 13% (baseline), 10% (visual), 16% (preparatory), and 18% (reach) of the neurons changed their spatial tuning as predicted. In majority of the neurons however the spatial tuning altered such that the prism shift was not compensated for as predicted. Additionally spatial tuning for some neurons altered along the axis that was not manipulated (orthogonal alterations). Since no specific differences between the four prism shifts (ipsilateral, upward, downward, and contralateral) were found, all distortion types were combined.

All cells for all epochs maintained their original tuning axis. For example, a cell tuned along the horizontal axis modulated its spatial tuning along this axis regardless of the prism shift. Thus, the preferred axis of tuning was maintained even after the prism

was introduced. These data imply that there was no correlation between prism shift and the resulting shift in spatial tuning.

The Hotelling test was used to assess whether the vertical or the horizontal prism shift altered spatial tuning of the neural population in a particular direction. The results of these tests confirmed that neither vertical (V) nor horizontal (H) prism shift altered the spatial tuning in any particular direction for the baseline (V: $p = 0.89$; H: $p = 0.65$), visual (V: $p = 0.67$), preparatory (V: $p = 0.60$; H: $p = 0.18$), and reach (V: $p = 0.76$; H: $p = 0.87$) epoch. Only during the visual epoch did the horizontal prism shift alter the spatial tuning of the neurons predominantly along the vertical axis resulting in a significantly non-uniform distribution of tuning shifts (H: $p = 0.03$). However, this might be because a majority of the neurons had a spatial tuning along this axis during the pre-prism condition as mentioned above. These results indicate that for a given shift in the perceived visual field, areas 7a and DP neurons responded with changes in spatial tuning in varied directions, that is, the shifts in spatial tuning were uniform. This also suggests that the neurons might compensate for the prism shifts by expanding their spatial tuning.

Comparison of single unit activity between pre-prism and post-prism conditions

For cells that remained isolated, the monkeys were required to perform the visually guided reach task after the prism was removed (post-prism condition). The neural response for all epochs during the pre-prism condition was quantitatively compared to the respective epochs during the post-prism condition. The linear coefficients were used to quantify the angular shift.

Tuning properties remain altered (pre-prism tuning properties ≠ post-prism tuning properties)

Upon removing the prism, a majority of the neurons did not regain their original tuning properties completely; spatial tuning alterations were observed in 58/105 (55%; baseline), 59/105 (56%; visual), 58/105 (55%; preparatory), 60/105 (57%; reach) neurons (type CxP) and firing rate remained affected in 29/105, (28%; baseline), 31/105 (30%; visual), 31/105 (30%; preparatory), 24/105 (23%; reach). Either the spatial tuning or the firing rate or both did not return to the original level after the prism was removed, as illustrated by an example neuron from DP (Fig. 4.13). The baseline response of the neuron for the lower ipsilateral eye position during the post-prism condition (Fig. 4.13A; darker green) was considerably greater than that during the pre-prism condition (Fig. 4.13 A; light green). The tuning properties during the visual epoch under the pre-prism condition (Fig. 4.13B; light red) and the post-prism condition (Fig. 4.13B; dark red) were significantly different. The overall firing rate during the visual epoch was greater for the post-prism condition compared to the pre-prism condition along the horizontal meridian and the lower eye positions. The opposite was true for the upper eye positions. The firing rate during this epoch decreased once the prism was removed, however, it did not return to the pre-prism level. During the post-prism condition the preparatory response was the greatest for the visual stimuli appearing in the lower visual field (Fig. 4.13C; dark gray). The preparatory response during the pre-prism condition however was the greatest for the contralateral eye positions (Fig. 4.13C; light gray). Thus during the preparatory epoch the tuning properties were not regained. During the reach epoch, the firing rate differed for the lower three positions during the pre-prism (Fig. 4.13D; light blue) and the post-prism condition (Fig. 4.13D; dark blue).

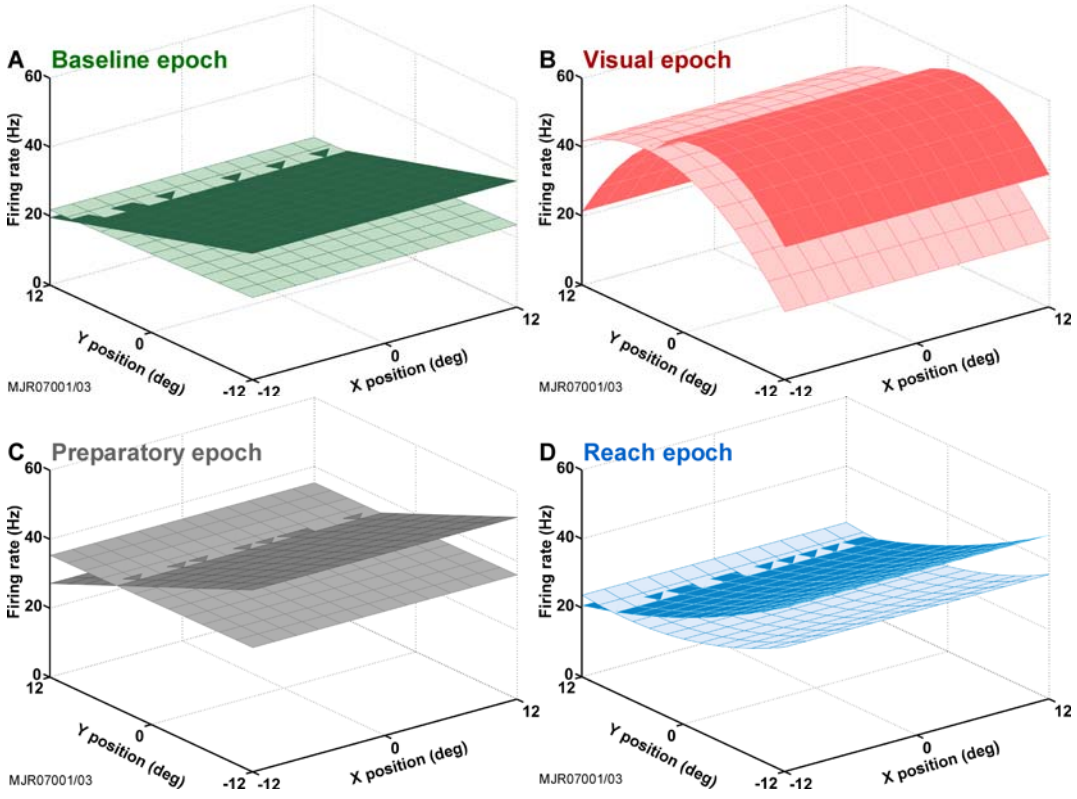


Figure 4.13: **Different tuning properties of a neuron during pre-prism and post-prism conditions**. Neural response of a unit during the pre-prism and post-prism condition for the baseline, visual, preparatory, and the reach epochs. The prism was used to induce a 12° upward shift. Response fields with lighter shading corresponds to the pre-prism condition. Response fields with darker shading corresponds to the post-prism condition. (A) Baseline epoch during pre-prism condition: $A_{pre-prism} = -0.09y + 22.8$. Baseline epoch during post-prism condition: $A_{post-prism} = -0.71y + 28$. (B) Visual epoch during pre-prism condition: $A_{pre-prism} = 0.92y - 0.11y^2 + 46.1$. Visual epoch during post-prism condition: $A_{post-prism} = -0.71y - 0.18y^2 + 55.4$. (C) Preparatory epoch during pre-prism condition: $A_{pre-prism} = -0.03y + 35.7$. Preparatory epoch during post-prism condition: $A_{post-prism} = -1.07y + 40$. (D) Reach epoch during the pre-prism condition: $A_{pre-prism} = -0.52y + 0.04y^2 + 24.7$. Reach epoch during the post-prism condition: $A_{post-prism} = -1.12y + 0.02y^2 + 30.8$. Upon comparing the spatial tuning for each of the four epochs during the pre-prism and the post-prism conditions, it was observed that this neuron does not regain its original tuning properties.

Population results

Alteration of spatial tuning of 58/105 (55%; baseline), 59/105 (56%; visual), 58/105 (55%; preparatory), 60/105 (57%; reach) neurons was observed. For these

neurons at least one of the four spatial parameters $(a_x, a_y, a_{x^2}, a_{y^2})$ reached the level of significance. These neurons were therefore classified as type CxP (Fig, 4.14). Some of these neurons did not have different mean firing rates between the pre-prism and post-prism conditions: 30/58 (52%, baseline); 31/59 (53%, visual); 29/58 (50%, preparatory); 35/60 (58%, reach). Another group of neurons (baseline: 29/105, 28%; visual: 31/105, 30%; preparatory: 31/105, 30%; reach: 24/105, 23%) were not spatially tuned but had significantly different overall firing rates between the pre-prism and the post-prim conditions and were classified as type C (Fig. 4.14). The rest of the neurons during each of the four epochs (baseline: 18/105, 17%; visual: 15/105, 14%; preparatory: 16/105, 14%; reach: 21/105, 20%) regained their spatial tuning and firing rates completely. Thus the tuning properties of these neurons were not significantly different between the pre-prism and the post-prism conditions (NS; Fig. 4.14).

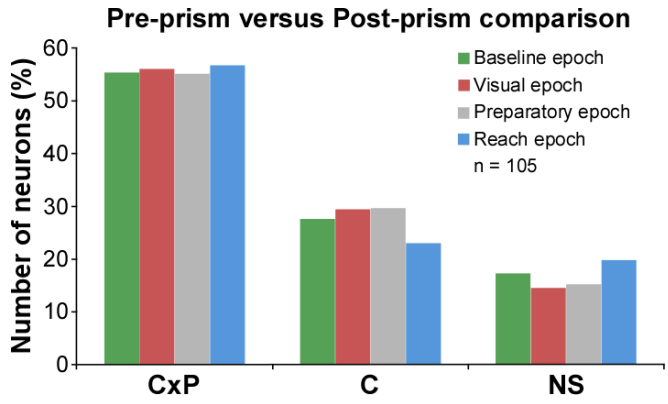


Figure 4.14: **Population distribution of pre-prism vs. post-prism comparison**. Condition based analysis was used to compare pre-prism and post-prism conditions separately for the four epochs: baseline (green), visual (red), preparatory (gray), and reach (blue). Proportions of interaction types between condition (C) and position (P) are plotted. Type CxP neurons had a multiplicative interaction between condition and position; these neurons had different spatial tuning between the two conditions. Type C neurons had a single effect of condition; these neurons were not spatially tuned but had an alteration in mean firing rate upon introducing the Fresnel prism. NS cells had no effect of either factor. Majority of the neurons had different tuning properties between the two conditions

Taken together, a majority of the neurons did not regain their original tuning properties (Fig. 4.14; type CxP and C units combined: baseline, 83%; visual, 86%;

preparatory, 85%; reach, 80%). These data imply that distortion of the sensory input induces changes in neural properties that may linger even after the distortion is removed.

Summary

The inferior parietal lobule (IPL) of macaques combines multimodal signals: sensory (e.g., visual, proprioceptive) and motor (e.g., efference copy). The goal of the current study was to test the plasticity of the cortical representation of space. Two male rhesus macaques were required to perform a visually guided reaching task with and without prisms. Fresnel prisms were used to induce a 12º visual shift in one of four directions (contralateral, ipsilateral, upward, or downward). This resulted in a mismatch between the eye position and the reach endpoint hand location; however the monkeys were expected to adapt and reach to the physical location of the stimuli. Behaviorally, the monkeys adapted very quickly to the prismatic distortion and reached accurately within a few trials. Changes in spatial tuning for the baseline, visual, preparatory, and reach responses of the neurons in area 7a and DP were measured. Alteration of spatial tuning of more than half of the neural population was observed implying that cortical plasticity occurred as a result of prismatic distortions. Surprisingly, the spatial tuning did not always alter in a compensatory manner. For a neuron to compensate for the prism shift, the spatial tuning of a neuron would be expected to shift in the direction opposite to the prismatic distortion. However, the spatial tuning of a majority of the neurons altered in the same direction to the prism shift or orthogonal to it. Thus, the resulting change in spatial tuning was not dependent on the type of the prism shift; however the original axis of tuning was maintained. The alteration of spatial tuning of neural responses during all

four epochs was observed suggesting that the neurons in area 7a and DP transform the sensory information into the motor information following an eye-centered coordinate system. Upon testing the neurons after removing prisms it was observed that the tuning properties were not regained for a majority of the neurons. This indicates that prism distortion may result in long-term cortical plasticity.

Discussion

Analogous to Chapter 3 this section will discuss the behavioral data and caveats of the current study. Electrophysiology data will be discussed in the General Discussion (Chapter 5).

Behavioral data

Human and non-human primates adapt to prismatic distortion once they receive visual feedback. A rapid (within five to nine trials) improvement in reach accuracy occurred over repeated trials in the current study. While the monkeys did not receive any visual feedback during the reach, feedback was available at the end of the reach, i.e., immediately before the hand touched the screen. These data confirm the findings of previous human (Sugita, 1996; Berberovic and Mattingley, 2003; Marotta et al., 2005) and non-human primate studies (Healy et al., 1973; Sugita, 1996; Kurata and Hoshi, 1999; Kitazawa and Yin, 2002; Kurata and Hoshi, 2002; Kurata, 2007) that visual feedback results in rapid prismatic adaption. A model describing a simple linear dynamical system shows that the sensorimotor calibration occurs on a trial-by-trial basis (Cheng and Sabes, 2007). This model states that sensory feedback signals drive

adaptation. Adaptation is therefore dependent on the visually perceived error between perceived target position and the position of the feedback at the reach endpoint. By receiving visual feedback at the end of every trial, the reach is perceptually calibrated. Human subjects corrected the reaching accuracy by more than 20% on each trial. This shows that the nervous system has the capabilities to adapt to perceptual shifts and therefore altered sensory stimuli rapidly.

The RT was not significantly affected by the presence of the prisms. Similarly, the MVT did not vary with the prism, which was also observed by Kurata (2007). The lack of difference in the RT and MVT and the increased accuracy of reaching as the trials progressed suggest that plasticity of neural representation occurs very swiftly as the monkeys adapt to the prismatic distortion. Moreover, the constant MVTs indicate that the monkeys did not decrease their movement speed due to the distortion. A possibility that there was a change in movement trajectories cannot be excluded and would have to be studied separately. Hence the neural plasticity that is observed is a pure result of sensorimotor adaptation. The cortical remapping of the extra-personal space likely occurs in order to correct the mismatch between the visual and proprioceptive feedback at the end of the reach.

Caveats

Long term versus short term exposure to prisms

It is expected that short-term prism exposure, as used in the current study, yields very different results compared to long-term exposure, where subjects are exposed continuously to the prism for days or weeks (Rossetti et al., 1998; Richter et al., 2002;

Rode et al., 2003). Long term exposure to prisms would certainly result in different neural effects. It is expected that with long term prism exposure, the spatial tuning would remain altered even after the prism was removed. Behaviorally, the monkeys would probably not show a rapid improvement in reaching during the post-prism condition after a single long-term prism exposure. Since both monkeys were "over-trained" for the prism condition due to repeated exposures, the adaptation to the prism condition was very rapid. Due to the rapid behavioral adaptation, spatial tuning shifts during the brief adaptation period could not be quantified. One way to rectify this issue would be to conduct electrophysiological recordings while a naïve monkey performs the prism adaptation task.

As areas 7a and DP neurons are coarsely spatially tuned both for eye position and retinotopy, a larger prism shift (greater than 12º) might result in more drastic shifts in spatial tuning.

Other possible manipulations

Once a prism is placed in front of the monkeys and they begin interacting with the environment while they look through the prism, the neural system begins to alter. It is likely that different neural circuits are recruited and synaptic connections are altered. Even though extracellular single unit recording focuses on one or two neurons at a time, the prismatic distortion affects the central nervous system globally. This may result in mass modulation of tuning properties. Using four different prism shifts (upward, downward, contralateral, and ipsilateral) constantly over a period of multiple years may result in drastic changes in spatial tuning of the neurons. Thus, systematic changes in

spatial tuning might have been diluted by the variety of prism directions. One way to avoid this problem is to train one monkey on one prism shift therefore introducing the system to only one type of distortion. Testing the spatial tuning shifts in this situation will increase our understanding about whether the neurons' tuning properties alter systematically or in a distributed pattern. Other methods of measuring cortical activity might also offer more insight for example by using intrinsic optical imaging (or any method that may allow the study of a population of neurons at once) while one or all four prism shifts are used. This would enable to directly compare the modulation of spatial tuning of a large population of neurons under different prismatic distortions.

Chapter 5:
General Discussion

Overview

In order to test the influence of eye position on the reach response of the neurons in areas 7a and DP and to understand the dynamics of sensorimotor transformation, monkeys were trained to perform a visually guided reaching task under five conditions (Chapter 3: EVAR, RVAR; Chapter 4: pre-prism, prism, post-prism), and neural responses were recorded from single neurons in areas 7a and DP of the posterior parietal cortex.

In the EVAR condition the trial began with an onset of the fixation point in one of nine possible locations. An expanding optic flow visual stimulus then appeared behind the fixation point. Once the stimulus lost its coherency, the monkeys were required to reach to the stimulus. This resulted in a foveal reach. During the RVAR condition, the fixation point always appeared in the center of the screen while the stimulus appeared in one of the nine possible locations. This resulted in eight peripheral reaches and one foveal reach (center position). The reaching accuracy was significantly greater for the foveal reach compared to the peripheral reach. The lower reach accuracy during the RVAR condition can be attributed to gaze dependent errors when pointing to peripheral targets (Henriques and Crawford, 2000). The RT between the two conditions was not significantly different however the MVT was significantly faster for the RVAR condition compared to the EVAR. This significant behavioral difference indicates that distinct computations occur during foveal and peripheral reaching (Moran and Schwartz, 1999;

Snyder et al., 2006). It is also possible that different neural circuitries are used for foveal and peripheral reaching (Prado et al., 2005; Clavagnier et al., 2007).

The EVAR (foveal reaching task) condition was further used to test the effect of prisms to visually distort the reach display. The pre-prism condition was identical to the EVAR condition used previously. Following the pre-prism condition, which established a baseline performance without distortion, a 12º Fresnel prism was placed in front of the monkeys such that it covered both eyes and monkeys again performed the foveal reaching task. The Fresnel prism was used to displace the visual field contralateral or ipsilateral to the recording chamber, upward, or downward. The prism condition was then followed by the post-prism condition in which the prism was simply removed and the monkey was required to repeat the foveal reaching task. For all three conditions, pre-prism, prism, and post-prism, the monkeys performed the foveal reaching task. Upon inserting the prism, the monkeys initially reached to the displaced (perceived) location of the visual stimulus. However this reaching error was corrected within the first five to nine trials. These results are in agreement with prior prism studies (Healy et al., 1973; Sugita, 1996; Kurata and Hoshi, 1999; Kitazawa and Yin, 2002; Kurata and Hoshi, 2002; Kurata, 2007). Once the prism was removed, the monkeys "misreached" in the direction opposite to the prism shift. Again, the error in reaching was corrected within five to nine trials. Computational evidence based on a human error-corrective learning study suggests that primates correct a reaching error simply based on sensory feedback by about 20% for each trial (Cheng and Sabes, 2007). This explains the rapid adaptation to prismatic distortion. Both RT and MVT were not different with and without prisms. This finding is in agreement with previous prism studies (Kurata and Hoshi, 2002; Kurata, 2007).

Survey of studies investigating goal directed movements shows that the PPC is involved in integrating the sensory information regarding the object of interest and planning the motor movement to reach to the object (Andersen et al., 1997; Snyder et al., 2006; Rozzi et al., 2008). This integration involves identifying the spatial location of the object and the location of the limb that will be used to reach the target. Neurons in the IPL receive afferent information regarding the upper limb movement and spatial location of the body. Specifically area 7a of the IPL has been shown to be involved in reaching under visual guidance (Hyvarinen and Poranen, 1974; Mountcastle et al., 1975; Blum, 1985; MacKay, 1992; Battaglia-Mayer et al., 2005; Battaglia-Mayer et al., 2007).

The reaching paradigm used in the current experiments investigated multiple signals in areas 7a and DP of the IPL. Single unit recordings were conducted while monkeys performed variations of the visually guided reaching task. Neural response synchronization was then used to study the neural response during four epochs of interest: baseline, visual, preparatory, and reach.

The current study shows that spatially tuned neurons were observed in both area 7a and DP. Eye position, visual, and reach signals have already been shown in area 7a (Hyvarinen and Poranen, 1974; Mountcastle et al., 1975; Blum, 1985; MacKay, 1992; Battaglia-Mayer et al., 2005; Battaglia-Mayer et al., 2007). Eye position and visual signals have been shown in DP (Li et al., 1989; Siegel et al., 2003; Raffi and Siegel, 2007). The current study demonstrates that area DP also had reach related tuning, a surprising new finding.

Furthermore, the spatial tuning was modulated as the trial progressed in time. This could indicate that a reference frame transformation was occurring as the sensory

(visuospatial) information was being used to plan and execute a reach movement (motor behavior). Differential responses during the preparatory and reach phases were observed between the EVAR (foveal reach) and RVAR (peripheral reach) conditions. This implies that foveal and peripheral reaching involve different computations. Likewise, distinct neural networks are in use during foveal and peripheral reaching. Using the Fresnel prism further supported the notion that eye position modulates the preparatory and the reach response in area 7a and DP suggesting that these two areas function predominantly using an eye-centered reference frame. Furthermore, alterations in spatial tuning properties were observed when the pre-prism and the prism conditions were compared. This indicates that cortical plasticity occurs along with behavioral plasticity.

In summary, this thesis shows the following: First, the alteration of spatial tuning of the neurons in area 7a and DP is demonstrated as the trial progresses. Thus an evolution of spatial tuning is observed during the visual, preparatory, and reach epoch. Second, reach response observed in DP is discussed. Third, differential reach related properties of neurons during foveal and peripheral reaching are addressed. Fourth, the eye position modulation of the neural response during the reach epoch is verified implying that reaching occurs in eye-centered coordinates in areas 7a and DP. Fifth, cortical plasticity as a result of gross displacement of visual field is confirmed. This modulation of spatial tuning is observed as a result of perceptually displacing the visual field using Fresnel prisms.

Based on the anatomical connections of DP discussed in the Introduction of this thesis, there is reason to hypothesize the DP neurons respond differentially to reaching in extrapersonal space. In addition to having reciprocal connections with area 7a, DP

receives projections from V6A (Andersen et al., 1990) an area that is involved in reach movement planning (Fattori et al., 2005). Neurons in area V6A and 7a (Battaglia-Mayer et al., 2007) are spatially tuned to the direction of the arm movement. However, there have been no studies that have investigated the reach related properties in DP. The behavioral paradigms in the current experiments were designed to investigate the spatial tuning of the neurons in DP during the reaching phase of the task. Based on the results (presented in the Results section and discussed in greater detail below), DP neurons respond to preparation and initiation of the reaching behavior. A majority of the neurons altered their spatial tuning during this preparation and initiation phase in presence of the prism. This implies that when the eye position and the endpoint hand location were mismatched, the reach related neural activity altered. Thus the neural response was dependent on the eye position.

It is known for decades that area 7a neurons respond to arm movements directed towards specific spatial locations in the extrapersonal space. However either the spatial locations of the reach targets were not systematically varied, or the reach paradigm used required the monkeys to place their hand on the screen at the beginning of the trial (Battaglia-Mayer et al., 2005; Battaglia-Mayer et al., 2007). Thus, the hand was constantly in the visual field and may have confounded the neural response during the reach phase as the arm also moved during that phase. To correct for these issues, we used a radial reaching movement described in the subsequent section. Briefly, a radial reaching movement is where the arm is initially placed at the waist level, proximal to the torso. The reach cues are placed in front of the monkeys, therefore, this results in a three-dimensional reach into the extrapersonal space. Due to such a paradigm, the hand did not

enter the visual field until it was directly in from of the reach target. Since neural activity only 300 ms after the initiation of the reach was analyzed, the presence of the hand inside the visual field was not an issue. A majority of the neurons altered their spatial tuning during the preparation and the initiation of the reaching behavior. Furthermore, a majority of the neurons altered their response fields once the eye position was displaced using visual perturbation. This indicates that not only do the neurons in area 7a respond to reaching but that this activity is manipulated by the position of the eyes.

There have been no studies in the past that have used a reaching paradigm similar to the one used here to investigate the effect of eye position and retinal stimulation when the spatial locations of the two were varied systematically. The EVAR and the RVAR conditions were used to investigate the influence of eye position and retinal stimulation respectively, over the reach response of neurons in DP and area 7a. A majority of the neurons were observed to have differential preparatory and reach responses when the neural activity during EVAR and RVAR condition was directly compared. This indicates that both, the eye position and the retinal stimulation affect the reach related neural activity in DP and area 7a.

That the reach response of the neurons is solely dependent on the eye position while reaching to foveated targets has not been previously investigated. Furthermore, cortical plasticity as a result of gross perturbation has not been explored in the past. In order to do this, the visual field was displaced using a 12º Fresnel prism, which in turn resulted in a perceptual shift. Due to this perceptual shift, the position of the eye was displaced by 12º. This resulted in a mismatch between the eye position and the hand position. For a majority of the neurons, the spatial tuning for all four epochs (baseline,

visual, preparatory, and reach) altered as a result of the perceptual shift. This indicates that cortical plasticity occurs in DP and area 7a. The altered response fields specifically during the preparatory and reach phases of the task indicate that the shift in eye position resulted in the change in neural activity. However, upon close inspection it was observed that this change was not simply a result of the displaced eye position. The spatial tuning changes occurred in various directions for each eye position displacement (up, down, ipsilateral, and contralateral). This effect is also discussed in greater detail below. This implies that signals other than eye position manipulate the neural response in DP and area 7a. Attentional modulation has been shown in area 7a (Bushnell et al., 1981; Raffi and Siegel, 2005; Quraishi et al., 2007) and DP (Raffi and Siegel, 2005), indicating that spatial tuning changes in various direction may result due to changes in attentional demands. Therefore, eye position is not the only factor that influences reach related neural responses in DP and area 7a.

Why use a radial reaching movement?

Most reaching paradigms require the monkeys to begin each trial with their hand placed on the screen (Battaglia-Mayer et al., 2005; Battaglia-Mayer et al., 2007). Area 7a and other parietal areas in general respond to visual stimulation (Read and Siegel, 1997). Thus, the hand being constantly in the visual field may influence the neural response during reaching movements in those studies. Thus any modulation of neural response may have been the result of change in visual stimulus due to the hand movement in addition to the reach related response (Battaglia-Mayer et al., 2007).

To completely avoid this confound, a radial reaching movement was used in the current studies. The monkeys were required to do a reach task during which the hand was not seen. The monkeys began each trial with their hand positioned close to their torso where the hand was not visible at the beginning of the trial (refer to Ch. 2 for a detailed description of the reaching task). The reaching hand was visible only when it was very close to the touch screen monitor and overlapping the visual stimulus. All the time intervals used to quantify the neural responses were prior to the time the hand entered the visual field. Such a radial reaching task resembles the natural reaching movement and puts a higher demand on the visuomotor integration (MacKay, 1992; Fattori et al., 2005; Gardner et al., 2007).

The visual stimuli were presented at systematically varied locations on the screen. The reaches were either foveal or peripheral (Chapter 3). With foveal reaching, the eye position varied with the location of the stimulus, whereas during peripheral reaching eye position was kept constant on the center. These two conditions allowed the quantification of neural response of reaching dependency on the eye position. Cortical plasticity was tested using Fresnel prisms, which displaced the perceived visual field (Chapter 4). This perceptual displacement resulted in a mismatch of eye position and endpoint hand location. In order for a successful completion of the reach movement, a behavioral remapping of the reach movement was necessary. Using Fresnel prisms it was possible to confirm the dependency of the reach signal on the eye-position and to measure the cortical plasticity.

Evolution of the neural signal during foveal reaching

In the EVAR condition (Chapter 3) the expanding optic flow stimulus always appeared behind the fixation point. Thus the eye-position and the endpoint hand location were always congruent resulting in a foveal reach. The fixation point location (i.e., eye position), and therefore the visual stimulus and reach location, varied systematically.

Baseline and visual response

Neural response during baseline fixation and after stimulus onset varied with eye position during the EVAR condition. These results are in line with previous studies that have demonstrated eye position signals in area 7a (Read and Siegel, 1997; Siegel and Read, 1997; Siegel et al., 2003; Battaglia-Mayer et al., 2007) and DP (Li et al., 1989; Read and Siegel, 1997; Siegel and Read, 1997; Siegel et al., 2003). The neural response to the onset of the expanding optic flow visual stimulus was observed in about half of the neurons sampled as shown in earlier studies for area 7a (Mountcastle et al., 1987b; Read and Siegel, 1997; Siegel and Read, 1997; Merchant et al., 2001; Youakim et al., 2001; Battaglia-Mayer et al., 2007). Neurons in DP responded similarly to the optic flow stimulus (Youakim et al., 2001; Raffi and Siegel, 2007). The anatomical connections between DP and V3A (Zeki et al., 2003; Peterhans et al., 2005), and DP and MST (Celebrini and Newsome, 1994; Graziano et al., 1994; Britten and Van Wezel, 2002) explain the motion selective neurons observed in DP in the current study. Optic flow sensitivity in area 7a can be explained by reciprocal connections with DP and MST (Andersen et al., 1990).

Preparatory response

Forty-three percent of the neurons altered their tuning properties during the preparatory epoch when tested using the EVAR condition. There were no overt changes in attention or sensory stimulation during this epoch; the onset of the stimulus had occurred several seconds before this interval and was thus constant; there was no change in the motor behavior as the hand was held constant at the starting or resting position. A variation of the neural response during this phase of the visually guided reaching task can therefore be attributed to the alteration in internal or cognitive state.

Reach planning modulation of neural response occurs in the PRR of the SPL (Snyder et al., 2000; Andersen and Buneo, 2002; Andersen and Cui, 2009) and in the PMd of the prefrontal cortex (Boussaoud and Wise, 1993; Hoshi and Tanji, 2000, 2006). Based on feedforward and feedback projections to areas 7a and DP, it is probable that the preparatory response reflects aspects of reach planning that arise in various areas of parietal and frontal cortex (Andersen, 1997; Snyder et al., 2000; Scherberger et al., 2005). Neurons in area 7a were responsive during the memory phase of a delayed reaching task (Snyder et al., 1997). It is likely that this response was a result of covert motor planning. Considering the above observations it is likely that areas 7a and DP are involved in a larger neural circuitry involved in producing or programming an accurate reach via transforming the visuospatial (sensory) information into a motor plan resulting in the completion of the motor goal (Scherberger and Andersen, 2007).

Reach response

Initiation of the reach movement altered the neural response in areas 7a and DP with the EVAR condition which is in agreement with previous area 7a reaching studies (MacKay, 1992; Battaglia-Mayer et al., 2007). The reach epoch was defined as the time interval of 300 ms immediately following the initiation of the reach movement marked by the lifting of the hand off the touch sensitive sensor.

During the reach epoch overt changes in sensory stimulation (stimulus change), and the motor behavior (e.g., efference copy) as the monkeys initiated the reach movement contributed to the neural response. In addition to these inputs, proprioceptive input also contributed to the neural response as primates can accurately localize limbs in their extrapersonal space even in the absence of visual and tactile inputs (Kalaska, 1988; Prud'homme and Kalaska, 1994; Scheidt et al., 2005). Neural modulation resulting from proprioceptive manipulations can be attributed to projections from somatosensory or proprioception related areas such as area 5 (Ferraina et al., 1997; Ferraina et al., 2001; Breveglieri et al., 2006) to area 7a.

Direct input from prefrontal motor areas (Cavada and Goldman-Rakic, 1989a; Tanne et al., 1995) and indirect input from motor areas via area 7b (Gardner et al., 2007), the PRR, and AIP (Pandya and Seltzer, 1982; Andersen et al., 1990; Felleman and Van Essen, 1991) likely contribute to the motor response of the area 7a neurons. Reach related ractivity in DP can be attributed to strong reciprocal connections between DP and area 7a (Andersen et al, 1990).

Evolution of the neural signal during peripheral reaching

In the RVAR condition (Chapter 3) the monkeys were required to maintain fixation in the center of the screen throughout the task. The expanding optic flow visual stimulus appeared in the periphery. The monkeys reached to the stimulus while maintain fixation in the center of the screen, thus performing a peripheral reaching movement (except for the center stimulus).

Baseline and visual response

The baseline response was not modulated during the RVAR task, as there was no stimulus present and eye position remained constant on the center. Spatially tuned neural responses to the onset of the visual stimulus were observed in the neurons sampled thus showing that neurons in area 7a and DP responded to the retinal location of the stimuli. These results agree with the visual responses of area 7a neurons observed in previous studies (Mountcastle et al., 1987a; Read and Siegel, 1997; Siegel and Read, 1997; Merchant et al., 2001; Heider et al., 2005; Battaglia-Mayer et al., 2007). Projection from early visual cortical areas representing peripheral visual field to DP (Neal et al., 1988; Baizer et al., 1991; Ungerleider et al., 2008) explain the coarse spatial tuning of the neurons in area 7a and DP which collectively show a distributed representation of space.

Preparatory response

In the RVAR condition, 52% of the neurons altered their firing rate during the 500 ms time interval immediately prior to the cue to reach (change in visual stimulus). In

this condition the stimulus remained in the periphery throughout the task, while the monkey prepared the upcoming reach movement.

It is therefore likely that attention was covertly shifted from the locus of fixation to the reach target location in the periphery as soon as the stimulus appeared and maintained on the reach target. A shift in spatial locus of attention altered the neural response properties in areas 7a and DP (Bushnell et al., 1981; Mountcastle et al., 1981; Bender and Youakim, 2001; Raffi and Siegel, 2005; Quraishi et al., 2007).

Analogous to the EVAR condition, it is likely that motor planning contributed to the preparatory signal during the RVAR condition. Both areas 7a and DP are reciprocally connected to other cortical areas where reach planning responses have been demonstrated (Boussaoud and Wise, 1993; Hoshi and Tanji, 2000; Snyder et al., 2000; Andersen and Buneo, 2002; Hoshi and Tanji, 2006; Andersen and Cui, 2009). It has to be assumed that the monkeys continued to plan and prepare the reaching movement until they were cued to reach. This is also the phase of the trial where intermediate reference frames between eye-centered and body-centered (Chang and Snyder, 2010) are used to plan the reach movement, thus integrating multiple signals for sensorimotor tranformation (Scherberger and Andersen, 2007).

Reach response

Upon the initiation of the reaching movement, alteration in tuning properties of the neurons in areas 7a and DP was observed while the monkeys reached in the periphery. These results are in agreement with previous area 7a reaching studies (Battaglia-Mayer et al., 2005; Battaglia-Mayer et al., 2007).

Analogous to the neural response for the EVAR condition during the reach epoch, the neural response under the RVAR condition involved proprioceptive input along with motor behavior related activity. This proprioceptive input also modulated the neural response. However just as areas 7a and DP are connected to other somatosensory cortical areas, these areas of the IPL also receive strong feedback projections from various prefrontal areas that are involved in reaching behaviors (Cavada and Goldman-Rakic, 1989a; Tanne et al., 1995; Gregoriou et al., 2005). The reciprocal connections combine multiple inputs over time as the trial progresses and thus contribute to transforming the visual signal into a motor behavior.

Reach related response in DP

The epoch based analysis showed that a majority of neurons in DP altered their spatial tuning as the trial progressed (EVAR, 77%; RVAR, 65%). This indicates that reach related activity was observed in DP, which is a novel and unexpected finding. Previous reaching studies (MacKay, 1992; Rushworth et al., 1997b; Battaglia-Mayer et al., 2007) and the current study have demonstrated that area 7a neurons respond to reaching movements of the upper limb. Area 7a receives projections from other areas that are involved in the reach circuitry (Cavada and Goldman-Rakic, 1989b; Tanne et al., 1995; Rozzi et al., 2006; Rozzi et al., 2008). These projections are reciprocal and therefore result in multiple inputs being modulated and combined in an ongoing process that compares visual and motor information (Beurze et al., 2007). This combined signal then propagates backwards to DP via the strong reciprocal connections between DP and area 7a (Cavada and Goldman-Rakic, 1989a; Andersen et al., 1990; Stepniewska et al.,

2005). DP also receives modulatory feedback from other frontal and parietal areas (Lewis and Van Essen, 2000). Therefore, the reach related response observed in DP can be explained via these feedback anatomical connections. Although DP is considered to be lower in hierarchy compared to area 7a (Andersen et al., 1990; Felleman and Van Essen, 1991), the tuning properties of neurons in DP during preparation and initiation of the reach resembled those of area 7a neurons under both EVAR and RVAR conditions. Both areas 7a and DP have been known to receive visual input (Cavada and Goldman-Rakic, 1989a; Andersen et al., 1990; Lewis and Van Essen, 2000) and therefore respond to visual stimulation (Blum, 1985; Read and Siegel, 1997; Siegel and Read, 1997; Siegel et al., 2003; Heider et al., 2005; Battaglia-Mayer et al., 2007).

Differential neural response for foveal and peripheral reach

A comparison between the preparatory epoch during foveal reach (EVAR) and peripheral reach (RVAR) showed that 76% of the neurons had different tuning properties. During the reach epoch, the EVAR versus RVAR comparison showed that 81% of the neurons responded differentially. These results suggest that preparation and initiation of the reach movement occurs via different neural circuitries or via different computations within the circuitry when reaching to foveal and peripheral targets.

Reaching to targets in the periphery increases the difficulty, as the oculomotor signal is no longer available to guide and therefore influence the eye-hand accuracy. This may result in increased activation or recruiting more regions of the brain involved in planning and execution of the reaching behavior. In a human functional imaging study,

distinct regions of the parietal lobe and the PMd were active while reaching to peripheral versus foveal targets (Prado et al., 2005). Foveal reaching resulted in activation of the medial intraparietal sulcus and the caudal PMd region. In addition to these areas the parieto-occipital junction and a larger portion of the PMd responded during peripheral reaching. It is thus likely that area 7a and DP receive modulatory input from different cortical areas during foveal and peripheral reaching. Therefore, the two reaching conditions yielded different neural responses.

Neurons in various reach related areas are known to receive multimodal inputs, specifically, eye and hand related signals (Boussaoud and Bremmer, 1999; Snyder et al., 2000; Battaglia-Mayer et al., 2001; Kurata and Hoshi, 2002; Battaglia-Mayer et al., 2007). These signals are integrated to execute complex behaviors such as reaching to specific locations. The observance of maintained eye position signal in the PMd during the reaching phase of the visually guided reaching task suggests that the eye-position signal influences the reaching behavior (Boussaoud and Bremmer, 1999; Batista et al., 2007). During the peripheral reaching the eye position is not congruent with the endpoint location of the hand. It is likely that foveal and peripheral reaching involve different computations in order to complete the reach movement successfully resulting in distinct neural responses.

Quantitative methods have shown that successful reaching can be achieved by encoding the distance between the gaze fixation and hand position based on eye and hand gain fields in the PRR (Chang et al., 2009). This is based on the observation that both eye and hand position signals are present in the PRR (Andersen et al., 1998; Batista et al., 1999; Cohen and Andersen, 2000; Buneo et al., 2002; Marzocchi et al., 2008). Area 7a is

also known to have to both eye and hand position signals (Mountcastle et al., 1975; MacKay, 1992; Read and Siegel, 1997; Siegel et al., 2003; Battaglia-Mayer et al., 2007). Current results show that DP neurons also respond during the reach behavior implying that in addition to eye position signals (Li et al., 1989; Siegel et al., 2003), DP contains hand position signals. Considering the eye and hand position inputs observed in area 7a and DP, it is likely that the reach movement is planned and executed using similar encoding methods as used in the PRR. The distance between the hand and gaze fixation is different during the peripheral and foveal reach confirming that the two types of reaching behaviors are executed using distinct computations.

Modulation of visual, preparatory, and reach responses due to prismatic distortion

The Fresnel prism shifted the visual field by 12º and thus displaced the eye position. This created a mismatch between perceived and actual reach target locations. Neural responses during the pre-prism condition were compared with those during the prism condition for the four epochs (baseline, visual, preparatory, and reach) separately.

Baseline response

The spatial tuning of 59% of the units during the baseline epoch changed with the 12º Fresnel prism. This confirms the observations from previous studies showing the presence of eye position signal in area 7a (Andersen et al., 1990; Bremmer et al., 1997; Battaglia-Mayer et al., 2000; Bender and Youakim, 2001; Battaglia-Mayer et al., 2005; Battaglia-Mayer et al., 2007). The change in the spatial tuning of the baseline response

was expected as the eye position is physically altered because of the prismatic displacement of the visual field.

Visual response

Inserting the Fresnel prism resulted in an alteration of spatial tuning of 52% of the neurons. Since the visual stimulus always appeared centered behind the fixation point, the only behavioral difference was the eye position. Although the physical appearance and the retinal location of the visual stimuli were constant in both the conditions, the gain field was clearly altered. These data confirm the presence of gain fields in area 7a and DP (Mountcastle et al., 1987b; Read and Siegel, 1997; Siegel and Read, 1997; Battaglia-Mayer et al., 2007). The change in gain field indicated that cortical remapping of the visual space occurred and further confirms that this change was modulated by the eye position signal.

Preparatory response

The spatial tuning of 54% of the neurons changed when comparing the preparatory response of the neurons during the pre-prism and the prism condition. As in the visual response, the only difference between the pre-prism and the prism condition was the spatial position of the reach stimulus and thus the angle of the eyes. Therefore this is suggestive that the eye angle modulates the preparatory signal in area 7a and DP. Moreover, the change in the preparatory response fields with visual field displacement implies that there was a remapping of cortical representation of space. During the preparatory epoch the monkey was planning a reach towards the actual position especially after adapting (five to nine trials) to prism condition. Thus, he did not reach to

where his eye position was but to where the actual position of the target was. As the monkey behaviorally processed visual information and "planned" a motor response, the cortex processed the transition between the visual processing and the motor execution. Due to the shift in eye position, the neurons in the area 7a and DP remapped the cortical representation of space thus changing the neural activity in the preparatory epoch. The presence of a reach planning related activity or preparatory activity in the PPC has been demonstrated by human (Koch et al., 2008) and non-human (Battaglia-Mayer et al., 2000; Battaglia-Mayer et al., 2007) primate studies.

Reach response

Comparison between the pre-prism and the prism condition showed that 61% of the neurons altered their reach spatial tuning. The monkeys were required to reach to the actual location of the visual stimulus and not the perceived location. Therefore the reach movement during the pre-prism condition was similar to the prism condition. The current behavioral results show that the MVT of both the monkeys did not vary between pre-prism and prism condition indicating that the reach speed was maintained by both monkeys despite the visual distortion. If the reach signal and the eye position signal were independent, alteration in the spatial response fields ("reach field") would not have been observed. However, a majority of the cells showed an alteration in their reach fields thus confirming that the reach signal is dependent on the eye position. Another study has shown that the reach activity in the PPC follows the eye-centered coordinate system (Buneo and Andersen, 2006). The eye position signal is maintained in PMd even towards the end of the reaching behavior suggesting that this signal influences the reach related neural response (Boussaoud and Bremmer, 1999). This further explains the altered reach

responses observed in presence of prisms. Differential neural responses while reaching with and without prisms suggest that different computations occur (Chang et al., 2009). Even though the perceived eye and hand positions were congruent during the prism condition, there was actually a physical mismatch between the two. Therefore, the eye-hand distance during the pre-prism and prism conditions was not equal. This difference affected the 'compound gain field'. Such a distinct 'compound gain field' effect explains the differential neural response. The observed influence of eye position on the motor response suggests that integration of multiple signals occurs in areas 7a and DP leading to sensorimotor transformation.

Effect of prismatic distortion on behavioral adaptation and changes in spatial tuning resulting in cortical plasticity

Behavioral adaptation

Adaptation can occur either as a result of a perceptual shift of visual input, i.e. reaching to the stimuli in a "perceptually corrected" field, or as a shift in motor output. In the first case, the hand movement is maintained, while the visual perception is changed; in the latter, the hand movement is shifted to match the visual perception (Welch et al., 1974; Redding et al., 1985; Clower et al., 1996). The current behavioral data shows that the RT was affected slightly whereas the MVT remained unaffected during the prism condition. This suggests that adaptation occurred via reaching to "perceptually corrected" field, where the motor output is not shifted. However, a majority of the cells alter their reach fields. This may be the result of the altered eye position, thus strengthening the claim that neurons in area 7a and DP follow an eye-centered coordinate system.

The proprioceptive input is also important during prism adaptation. For an accurate reach, it is necessary that there is a correspondence between the visual and proprioceptive representation of the hand. When this correspondence is mismatched, an erroneous reach occurs. Upon receiving visual information regarding the endpoint location of the hand and detecting the mismatched proprioceptive location of the hand, the monkeys adapted by shifting the perceived hand position proprioceptively (Wilkinson, 1971; Redding et al., 1985; Redding and Wallace, 1988). This results in elimination and therefore a compensation of the visual and proprioceptive mismatch over the first five to nine trials. This further explains the adaptation via perceptual editing. Note that the vision does not merely overrule the proprioceptive sense of the hand as the behavioral adaptation is gradual (Cressman and Henriques, 2009).

Cortical plasticity

There is reason to believe that cortical reorganization of spatial representation occurred in response to behavioral adaptation to the sensory mismatch induced by displacing prisms. With the lack of visual feedback or lack of interaction with the environment, cortical plasticity does not occur in area 7a (Andersen et al., 1985). However the current data show that the visuomotor spatial representations in area 7a and DP are highly plastic and can be modified with visual feedback. Changes in spatial tuning for all four epochs between pre-prism and prism conditions show that cortical plasticity occurred as a result of prismatic distortion. It was originally hypothesized that upon inserting the prism, the spatial tuning would alter in the opposite direction of the prism shift; the resulting spatial tuning would compensate for the prism shift. However this was not observed. The following are the percentages of the neurons that did not compensate

for the prism shift during the four epochs: baseline (66%), visual (62%), preparatory (70%), and reach (58%). Furthermore, for some neurons spatial tuning altered along the axis orthogonal to the axis perturbed by the prismatic distortion. That is, spatial tuning was altered along the axis that was not manipulated by the prism shift. This was observed in 42% (baseline), 45% (visual), 46% (preparatory), and 53% (reach). These data show that the spatial tuning varied drastically when the response fields of the four epochs were compared during the pre-prism and the prism condition. Such modulations in the response fields of the neurons in area 7a and DP have many explanations, which are discussed next.

Expansion of response fields: It is likely that the response fields of the neurons in areas 7a and DP expand resulting in spatial shifts in various directions. In a non-human primate study using inverting prism, the receptive fields of neurons in V1 were observed to enlarge and respond to visual stimulation in ipsilateral and contralateral visual field (Sugita, 1996). The receptive field sizes in V1 have been shown to alter depending on the visual stimulus properties (Kapadia et al., 1999). Such changes in dimensions of the receptive field properties occur as a result of spatial summation. Spatial integration can occur as a result of cortico-cortical connectivity within V1 or between V1 and other cortical areas via feedback projections. The receptive fields of area 7a neurons are large and bilateral (Motter and Mountcastle, 1981; Andersen et al., 1990). DP neurons have smaller and generally contralateral receptive fields (Andersen et al., 1990). Current data show that neurons in both areas 7a and DP respond to eye-positions, visual stimuli, reach-planning, and reaching bilaterally with the prisms. This implies that the receptive fields

are expanding due to prismatic distortions. The resulting enlargement in the spatial tuning suggests that there is a reorganization of cortical representation of space.

Global effect of perturbation: The prismatic distortions affect the neural properties of area 7a and DP globally, that is, once a prism shift is induced, the spatial tuning of all neurons is affected. Therefore prism shifts in different directions affected each neuron differently. Since four different prism shifts were used in the current experiment, the global effect of the perturbation altered several times leading to the various spatial tuning summations for every neuron. As shown by the current data, not all neurons regained their original tuning properties once the prism was removed. The neurons included in the study may have undergone spatial tuning alterations in a distributed manner as each neuron was affected differently by each prism shift over a period of time. In the current study, such a long-term change could occur as a result of perceptual learning for a length of time (Gilbert et al., 2009).

Attentional and cognitive demands: The visually guided reaching task demanded greater attentional focus under the prism condition. Although the stimulus was always foveated and no overt shift in locus of attention was required, the monkeys received mismatched input between visual (target location) and proprioceptive (hand location) modalities. This mismatch demanded the monkeys to use greater attention while performing the visually guided reaching task under the prism condition. It is likely that this increased attentive state globally altered the spatial tuning of the neurons. Increased cognitive and attentional demands have been shown to modulate receptive field properties of single units in areas 7a (Bushnell et al., 1981; Constantinidis and Steinmetz, 2001a, b; Quraishi et al., 2007) and DP. Raffi and Siegel (2005) have shown that regions

of cortical activation over area 7a and DP vary over time when monkeys covertly direct attention to different locations in visual space. These topographical changes occur without any gross experimental perturbations. The prism condition forces the monkeys to be highly attentive in order to successfully correct the initial erroneous reaches and maintain the corrected reach behavior. It is very likely that this added attentional demand alters the cortical topography of attention and the response field properties of areas 7a and DP in a distributed manner.

Adaptation and perceptual learning: Adapting to an altered sensory input allows primates to interact with their environment successfully. Behavioral adaptation has been tested in humans and non-human primates via prismatic distortions (Healy et al., 1973; Kitazawa and Yin, 2002; Berberovic and Mattingley, 2003; Marotta et al., 2005). In such tasks the visual field is either displaced (Kurata and Hoshi, 2002) or inverted (Sugita, 1996) resulting in a mismatch between the perceived location of the target and the physical location of the target to which the primates must reach. With training, primates modify their behavior and reach to the correct location of the reach target (Sugita, 1996; Kurata and Hoshi, 2002).

Perceptual learning is necessary to successfully complete other perceptual tasks such as those requiring orientation discrimination. For an orientation discrimination task, monkeys are trained to report whether two orientation stimuli are same or different (Yang and Maunsell, 2004; Raiguel et al., 2006). Adaptation and perceptual learning has been shown to alter tuning properties of neurons in many cortical areas (Sugita, 1996; Yang and Maunsell, 2004; Raiguel et al., 2006; Gilbert et al., 2009; Teich and Qian, 2010). Learning also induces dynamic short-term changes in response properties of single

neurons which are affected by attention, cognition, and perceptual task (Gilbert et al., 2009). Although the monkeys were highly trained with the Fresnel prisms in the current experiment, it was necessary to adapt and perceptually learn to correct the reaching movement while reaching with the prisms. The adaptation to the prisms therefore resulted in modulation of the tuning properties of the neurons in areas 7a and DP. Temporal comparison between PRR and PMd suggests that reach activity in the PRR fine-tunes the reach plan (Tanne et al., 1995; Johnson et al., 1996; Boussaoud and Bremmer, 1999; Chang et al., 2009). It is likely that areas 7a and DP are also involved in 'fine tuning' the reach plan which is necessary for executing an accurate reaches under the prism condition.

Do the tuning properties return to the original tuning properties after removing the Fresnel prism?

Depending on the stability of the recording and the motivation of the monkeys, neurons were tested under post-prism condition, i.e., the prism was removed and monkeys were required to do the foveal reaching task. This was done in order to test whether the tuning properties of the neurons returned to the pre-prism properties or remained altered. A pre-prism condition versus post-prism condition comparison for all four epochs showed that for a majority of neurons the tuning properties remained altered after removal of the prism: baseline (83%), visual (86%), preparatory (85%), and reach (80%).

Once the prisms were removed the monkeys initially reached in the opposite direction of the prismatic distortion, but corrected this reach error upon receiving visual feedback at the endpoint location. Similar to the prism condition, the reach error was

rectified within the first five to nine trials. Such a rapid adaptation can be explained by human study that showed that subjects correct their reaching by about 20% between trials (Cheng and Sabes, 2007). This reach error correction occurred due to sensory feedback.

Removing the prisms again caused an alteration of sensory input. The monkeys showed behavioral adaptation in order to reach accurately. Modulation of cortical circuitry is expected along with behavioral adaptation. However for some neurons the alterations did not change enough to match the original circuitry, which can be shown by example neurons for which the spatial tuning was regained but the overall firing rate remained altered. The tuning properties for some neurons changed in a pattern that was distinct from the original circuitry. The change in visuomotor spatial tuning observed thus may be a result of cortical instability due to the perturbed visual field.

Repeated behavior would result in strengthening of synaptic connections within visuomotor spatial maps, based on the assumption that similar behaviors require similar neural networks, whereas drastic changes in behavioral patterns recruit different neural networks. However a study in which neural activity in the PMd and primary motor cortex was recorded (Chestek et al., 2007) showed variability in the spatial tuning when the monkey reached for the target during a repeated behavior reaching task. Even though the monkeys were over-trained for the reaching task, the performance was seldom static; the reach endpoint locations vary with each trial. Although these minor changes in behavior were within the permitted error range to complete the task correctly, they affected the neural response. Thus, if repetitive behavior caused variations in response fields of the neurons, it is likely that intercepting two identical visually guided reaching blocks of trials (pre-prism and post-prism conditions) with the prism condition would yield even

greater variability between pre-prism and post-prism conditions even though the behavior was the same.

Some neurons had very similar spatial tuning properties between pre-prism and post-prism conditions during the preparatory epoch. This suggests that during the planning phase of the task, similar computations occurred during the pre-prism and the post-prism conditions. This could be explained by the compound gain field theory which states that in order to complete a successful reaching movement, the distance between the eye position and the hand position is computed (Chang et al., 2009). During the pre-prism and the post-prism condition, this distance was the same as the eye position and the hand location were identical during these two conditions.

About half of the neurons that had differential spatial tuning during pre-prism and post-prism condition did not have significantly different mean firing rates: 52% (baseline), 53% (visual), 50% (preparatory), 58% (reach). Attentional demands increase during the prism condition. Once the prism was removed (post-prism condition) however, the attentional demands decreased and matched those during the pre-prism condition. Changes in attentional demands have been shown to modulate the firing rate of the neurons (Bushnell et al., 1981; Moran and Desimone, 1985; Connor, 2006; Womelsdorf et al., 2006). Therefore the similarity in attentional demands could explain the lack of difference in firing rate during the pre-prism and post-prism conditions.

Sensorimotor transformation

Modulation of neural response to successive time points, which mark distinct events, suggests that multimodal inputs are integrated in area 7a and DP. After

performing the epoch based analysis, neurons in areas 7a and DP were classified as either type E, ExP, or NS. NS neurons showed no change in response properties as the trial progressed. Type E neurons had different mean firing rates but were not spatially tuned. These neurons were relatively few in EVAR (10%), RVAR (20%), pre-prism (8%), prism (9%), and post-prism (10%). The slightly larger percentages of the neurons with only mean rate change during the RVAR condition can be attributed to the large and bilateral receptive fields of area 7a neurons (Motter and Mountcastle, 1981; Blatt et al., 1990) which can extend the display area.

Between 50% and 60% of all the neurons tested in areas 7a and DP under various conditions (EVAR, RVAR, pre-prism, prism, and post-prism) change their spatial preference across the four epochs (baseline, visual, preparatory, and reach). These ExP type neurons had a particular spatial preference at the beginning of the trial (baseline) which then altered at the onset of the visual stimulus, followed by further alteration as the monkeys prepared and executed the visually guided reach. Substantial changes in response properties were observed between the visual and preparatory epochs. Since there were no overt changes in sensory stimulation or motor behavior, this modulation of spatial preferences can be attributed to spatial attention or planning signals based on various or a combination of multiple coordinate frames (e.g. eye-centered, head-centered, arm-centered) originating from the prefrontal cortex (Pesaran et al., 2006) or other parietal areas (Rozzi et al., 2006). Modulation observed during the reach epoch can be attributed to the sensory stimulation (e.g. visual and proprioceptive) and to the motor signals that are contributed via prefrontal feedback projections (Tanne et al., 1995) or other parietal areas (Breveglieri et al., 2008; Marzocchi et al., 2008).

Other parietal areas such as LIP and PRR are known to have gain field modulations (Cohen and Andersen, 2002) along with motor activity and thus are claimed to be a locus of reference frame transformations. Kurata and Hoshi (2002) observed neurons that responded to both visual stimulation and motor behavior in the PMv. The neurons that responded to visual stimulation did so only when a motor movement was performed. Other studies in the PMv have shown such cells with visual and motor signals combined (Kurata and Tanji, 1986; Kurata and Hoffman, 1994; Mushiake et al., 1997). Based on the current data area 7a and DP neurons also responded to visual stimulation, showed gain field modulation, and responded to movement planning and initiation implying that these areas are involved in sensorimotor transformation.

Therefore the neural response in area 7a and DP could reflect the ongoing processes of integrating the multimodal input from various cortical areas leading to the transformation of sensory signals into a succesfully accurate reach plan. Alterations and shifts in spatial tuning may be a result of feedback from spatially tuned neurons from other cortical areas. These shifts may also be a result of online correction of movement in order to increase reach accuracy. Such an online correction, which can arise form cortico-cortical connection or feedback loops within areas 7a and DP, is especially important while reaching under the prism condition. The rapid adaptation to the prism condition shown in the current behavioral data implies that the reaching is corrected online using proprioceptive input and feedforward motor command (efference copy information) (Lewis et al., 1998) during the reach and visual feedback at the end of the reach. The online adjustment or the ‘fine tuning’ of the reaching movements under visual control is supported by lesion and imaging studies (Desmurget et al., 1999; Pisella et al., 2000).

Online correction and such motor commands can only be formed and updated using multimodal inputs such as visual, proprioceptive and efference copy information.

That the eye position modulates the visual signal (gain field) in areas 7a and DP has been known for over two decades (Andersen et al., 1985; Andersen et al., 1990; Bremmer et al., 1997; Read and Siegel, 1997; Siegel et al., 2003; Siegel et al., 2007). Neural responses are further modulated by the retinotopic location of the visual target (Andersen et al., 1990; Heider et al., 2005). Different variations of the visually guided reaching tasks were used to test the influence of eye position signal on the preparatory and reach activity of the neurons thus investigating the sensorimotor tranformation in areas 7a and DP. To separate the contributions of retinopic and gain field signals, the loci of retinal stimuli and fixation were systematically varied and quantitatively assessed. To explore the gain field dominance on the reach related response, a 12º Fresnel prism was used to introduce a mismatch between the eye position (locus of fixation) and the endpoint hand location.

The quantitative assesment was done using the condition based analysis (Ch.3: EVAR vs RVAR; Ch.4: pre-prism vs prism), which classified neurons in area 7a and DP into three categories: type C, CxP, and NS. Type NS neurons had neither condition nor position effect. Type C neurons had different firing rates for the two conditions compared. After comparing the EVAR and the RVAR conditions, 30% and 27% of the neurons had modulated firing rates during the preparatory and the reach epoch respectively (type C). The spatial tuning of 46% (preparatory epoch) and 54% (reach epoch) of the neurons was found to be different between the EVAR and the RVAR conditions (type CxP). The physical reach location under both EVAR and RVAR

conditions was the same. However reaching under the EVAR condition was foveal and under the RVAR condition was peripheral. Therefore these data imply that the eye position signal differentially affects the neural response during foveal and preipheral reach. The gaze direction affects the planning and preparation of the reaching behavior. Likewise, the retinotopic location of the stimulus affects the preparatory and the reach response of the neurons in area 7a and DP.

After comparing the pre-prism and the prism conditions it was found that 34% (preparatory epoch) and 21% (reach epoch) neurons had different firing rate. The spatial tuning of 53% (preparatory epoch) and 60% (reach epoch) was altered due to the insertion of the Fresnel prism. Introducing the prism resulted in a 12º displacement of the visual field, and thus displaced the gaze direction by 12º. The monkeys were trained to reach to the actual location of the reach target and not the perceptually displaced location. The reach endpoint location was thus identical in both conditions. The current data show that during the planning or the preparatory stage of the task, a majority of neurons had altered tuning properties. Many neurons were thus affected by the displacement of the eye position even during the planning stage implying that eye position plays a crucial role in designing a reach movement. The execution of the reach was also influenced by the gaze direction shown by the majority of the neurons that had altered tuning properties as a result of the displaced eye position. The change in spatial tuning was not necessarily consistent with the shift in eye position; the spatial tuning either altered in the direction of the prism shift, or opposite or orthogonal to it. These dramatic changes in spatial tuning across all measured neural events suggest that there is a range of remapping of the sensorimotor transformations that guide reaching.

A back-propagation programmed neural network shows that area 7a neurons combine information regarding the retinal location of the target and the eye position to compute the exact target location in extrapersonal space (Zipser and Andersen, 1988). Retinocentric and eye position centered reference frames are combined to transform the information into a head centered reference frame. This head centered reference frame is likely to be transformed further into an arm centered reference frame in order to complete an accurate reaching movement. The early phase of this transformation can be observed based on the current results that showed differential activation during the visual, preparatory, and reach epochs of the task. Moreover, this transformation was influenced by the eye position as the preparatory and the reach responses in area 7a and DP neurons with and without prisms were different. Chang et al. (2009) have shown that during a reaching movement, neurons in the PRR compute the distance between the eye and the hand (compound gain field). This compound gain field modulates neural response based on the distance between the locus of fixation and the hand. In the current study, this distance is altered due to the displaced locus of fixation. It is likely that such a computation occurs in area 7a and DP neurons resulting in differential neural response once the eye position (locus of fixation) is displaced. With a maintained hand position and a displaced locus of fixation, the compound gain field is affected.

In both PRR and area 5 reference frame transformation occurs in a time-invariant manner (Buneo et al., 2008). That is, the various stages of sensorimotor transformation do not evolve in time. Once the location of the reach target is visually available, all stages of the transformation occur simultaneously. This allows any changes in information to be updated rapidly thus allowing areas involved in the network to influence other areas of

the network with very little delay. Thus the sensorimotor transformation relies on the eye-centered frame of reference for areas in which neurons predominantly use this reference frame. Since the eye position response is dominant in neurons in areas 7a and DP, the alteration in eye position likely affects the reference frame transformation. This may also explain the drastic variations in spatial tuning with and without prisms.

Summary

Area 7a and DP of the IPL receive multimodal inputs resulting in the heterogeneous tuning properties of the neurons. To examine these properties, single unit activity was recorded while monkeys performed variations of visually guided reaching task. Neural activity was synchronized to various events in the task resulting in four epochs: baseline, visual, preparatory, and reach. A majority of neurons were spatially tuned to each of the four epochs. The angular tuning of the neurons was uniformly distributed indicating that area 7a and DP have a distributed representation of space. As the visually guided reach trial progressed, the spatial tuning of the neurons altered. This temporal alteration in spatial tuning indicates that there is a transformation of extrapersonal space from the sensory representation to a motor representation. Differential reach related responses were observed during foveal and peripheral reaching implying that distinct neural networks are used under these conditions. Likewise, it is possible that different computations regarding the eye and hand distance occur within a neural network while reaching to foveal and peripheral targets. This differential response also indicates that the eye position influences the reach response in area 7a and DP.

The gain fields and the spatial tuning during the preparatory and reach epochs altered once a 12º Fresnel prism was used to displace the visual field thus shifting the eye position. The perturbed visual field resulted in a mismatch between the eye position and the endpoint hand location as the monkeys were required to reach to the actual location of the target and not the perceived location. Thus the alterations of spatial tuning were considered to have occurred due to the displaced eye position. This strongly supports the notion that areas 7a and DP operate using an eye-centered frame of reference. The alteration in spatial tuning during and after prism distortion also implies that areas 7a and DP show plastic changes in their tuning properties. Rapid behavioral adaptation was observed along with cortical plasticity. Differential reach related responses with and without prisms imply that distinct computations occur under the two conditions. The neurons in these two areas compensate for the prismatic distortion by possibly enlarging their response fields. The resulting changes in spatial tuning were not correlated with the direction of the prism shift. Attentional modulation also likely influenced the neural response. After the prism was removed, most neurons did not regain their original spatial tuning suggesting that effects of prismatic distortion linger even after the distortion is removed. This further implies that long-term cortical plasticity occurs as a result of sensory perturbation.

Future directions

The differential response of the neurons during the preparatory epoch implies that neurons in DP and area 7a are involved in the planning phase of the reaching behavior. However, it is not known whether the neural response during the preparatory epoch is

due to reaching or due to a motor behavior. In other words, is this a motor planning response or a reach planning response? This can be tested using a saccade task instead of a reaching task. A similar alteration in tuning properties prior to a saccade would indicate that the neural activity during the preparatory epoch is as a result of planning of a motor behavior. On the other hand, no change in tuning properties during this epoch would indicate that the preparatory neural response is specific for arm movements.

Based on the current data, it would be interesting to investigate whether the reach trajectory is affected due to the perceptual perturbation. A majority of the neurons had different tuning properties during the reach epoch as a result of the prismatic distortion, however, the monkeys adapted to the distortion almost immediately. In order to test whether this different in tuning properties was as a result of behavioral differences, it is essential to explore the kinematic differences as monkeys perform the visually guided reaching task with and without prisms. It is possible that the change in tuning properties was as a result of minor changes in the reach trajectory.

Although the perceptual distortion used was gross, it would be interesting to explore the result of an even more drastic perturbation of the visual field. This could be done via reversing prisms. In the current experiments, the spatial tuning of the neurons altered in various directions when a shifting prism was used to displace the visual field. Reaching with an inverting prism would be even more challenging and require greater attention. It is likely that increasing the attentional demand may result in an even more drastic change in spatial tuning of the neurons. This would further confirm the claim that signals other than the eye position signal modulated the reach responses in DP and area 7a.

Appendix A: Abbreviations

Cortical and subcortical areas

PPC	posterior parietal cortex
IPL	inferior parietal lobe
SPL	superior parietal lobe
V1	primary visual area
V2	secondary visual area
V3A	visual area three A
V4	visual area four
MST	middle superior temporal area
MT	middle temporal area
IT	inferotemporal cortex
STP	superior temporal polysensory area
PO	parieto-occipital area
V6	visual area six
V6A	visual area six A
PRR	parietal reach region
MIP	medial intraparietal area
LIP	lateral intraparietal area
AIP	anterior intraparietal area
VIP	ventral intraparietal area
DP	dorsal prelunate area
PCC	posterior cingulate cortex
PMd	dorsal premotor area
PMv	ventral premotor area
SEF	supplementary eye fields

Sulci

LS	lunate sulcus
STS	superior temporal sulcus
IPS	intraparietal sulcus

Conditions

EVAR eye position varying task

RVAR retinal varying task

Behavioral measurements

RT	reaction time
MVT	movement time

Neural classification

NS	not significant

Epoch based analysis

E	different mean firing rates
ExP	different spatial tuning

Condition based analysis

C	different mean firing rates
CxP	different spatial tuning

Appendix B: Complete description of categorical regression analysis

Objective

The objective of the current experiments was to test the spatial properties of the neurons during various conditions. In order to do this successfully, derivation of the best fitting model was necessary. The spatial tuning of a neuron was defined by the best fitting model derived using stepwise regression analysis.

Benefit of stepwise regression

Multiple samples of data (neural responses during two conditions) are considered at once. The benefit of fitting multiple samples using one model is to gain the ability to test for different slopes and intercepts in the samples. Additionally, more degrees of freedom are available for analysis. The combined ability to test different slopes and intercepts and the availability of a large number of degrees of freedom enables the best fitting of the data. The regression analysis uses qualitative variables to derive different best fitting models from a single best fitting model.

General procedure

The general linear model procedure is first used to construct a design matrix. Stepwise regression, a multistep method of analysis, is then used to fit the data with the best fitting model. A ‘dummy variable’ is used to differentiate between different samples; this allows each sample to have a different intercept value. The ‘dummy variable’ in the

current analysis has two values (0 and 1): one for each condition (condition based analysis). The stepwise regression method begins without any parameters in the model. The parameters are added based on their significance, which is tested using the *f*-test. Each variable is tested for a significance level of $p < 0.05$. Therefore, if the value of the estimated parameter is significantly different from zero, it is added to the model. Upon considering a new variable, previously added parameters are also retested. If upon retesting a variable is found to be non-significant (not necessary to define the model), it is deleted from the model. A criterion for a parameter to be kept in the model is that its *p*-value must be less than 0.05. Thus at the completion of stepwise regression analysis on a particular data set, only the significant parameters are maintained in the model that is used to fit the data. The values of these parameters are the estimated regression coefficients for the model. Significant parameters in a model can then be used to derive separate fits for all the samples in the data set. The different estimates of the significant parameters indicate that those parameters are essential in defining the fit and that the samples considered are different from each other. In the current experiments this implies that the neurons' spatial tuning is different for the two conditions (two samples).

Criteria to choose the best model

R-squared criterion

A model is chosen based on the R^2 value and Mallow's C_p (Mallow, 1973) value. Based on the R^2 value (derived from simple linear regression of a sample), the independent variable that best predicts the dependent variable in a given sample can be found. Number of independent variables to be included in a 'subset' can be arbitrarily

specified. For the current analysis, the number of independent variables in a subset varied depending on how many parameters were in the model.

Mallow's C_p criterion

The addition of too many parameters in a model results in 'over-fitting' of the data. A model that over-fits the data set has a low probability of predictive performance. Over-fitting occurs when an extremely complex model is used to define the data set. Such a model fits the errors and noise, thus decreasing its ability to predict accurately. To avoid over-fitting, Mallow's C_p criterion is used to minimize the number of parameters included in the model. The C_p value is the measure of total squared error of the sample and is defined by the following equation (SAS/STAT 9.1 User Guide):

$$\mathrm{C}_p = \frac{SSE_p}{s^2} - (N - 2p)$$

Where s^2 is the mean squared error of the model being tested and the SSE_p is the sum of squared error for the model with p parameters, including the intercept. N refers to the number of observances.

A combination of greatest R^2 value and lowest C_p value defines the best model to fit a data set. An overall significant *f*-test ($p < 0.05$) for the model chosen by the greatest and the least R^2 and C_p values respectively indicate that the intercept and the coefficients of the parameters of each model are significantly different from zero.

An example of the stepwise regression analysis for one neuron

The goal here was to test whether the spatial tuning of the neuron was the same or different when the monkeys performed the visually guided reaching task with (prism condition) and without (pre-prism condition) the prism. The analysis was conducted using the GLMOD and REG procedures in the SAS statistical software (SAS Institute Inc., Cary, NC).

The following information was submitted to the analysis software: condition, *x*-position of the stimulus, *y*-position of the stimulus, and firing rate. The firing rate (rate L) of the neuron was the dependent variable. There were two categorical values, 0 and 1, denoting pre-prism and prism conditions respectively. Since information for both conditions was fed into the program at once, the values for the dummy variable for these two samples were: 0 (pre-prism) and 1 (prism). The dummy variable will be used later to derive separate intercept and spatial parameter estimates. The following parameters will be tested: x, y, x^2, y^2, and the intercept to find the best fitting model for each type. The GLMOD procedure is used to define the parameters and design the matrix. The following are the definitions of the parameters:

```
The GLMMOD Procedure
Class Level Information
Class         Levels    Values
type               2    0 1
Number of Observations Read         181
Number of Observations Used         181

The GLMMOD Procedure: Parameter definitions
Column Number  Associated Effect   CLASS Variable values type
1              Intercept
2              Type               0
3              Type               1
4              xposL
```

5	yposL	
6	xyposL	
7	xxposL	
8	yyposL	
9	xposL*type	0
10	xposL*type	1
11	yposL*type	0
12	yposL*type	1
13	xyposL*type	0
14	xyposL*type	1
15	xxposL*type	0
16	xxposL*type	1
17	yyposL*type	0
18	yyposL*type	1

Only the significant parameters will be included in the model.

The GLMMOD procedure then deigns the matrix using the data set and the parameters defined above. The following is an example of part of the matrix:

N	R L	1	2	3	4	5	6	7	8	9	10	11	12	13	14	15	16	17	18
1	20	1	0	1	10	2	20	100	4	0	10	0	2	0	20	0	100	0	4
2	34	1	0	1	-10	12	-120	100	144	0	-10	0	12	0	-120	0	100	0	144
3	8	1	0	1	0	12	0	0	144	0	0	0	12	0	0	0	0	0	144
4	10	1	0	1	10	22	220	100	484	0	10	0	22	0	220	0	100	0	484
5	12	1	0	1	-10	22	-220	100	484	0	-10	0	22	0	-220	0	100	0	484
6	24	1	0	1	0	2	0	0	4	0	0	0	2	0	0	0	0	0	4
7	32	1	0	1	-10	2	-20	100	4	0	-10	0	2	0	-20	0	100	0	4
8	18	1	0	1	10	12	120	100	144	0	10	0	12	0	120	0	100	0	144
9	16	1	0	1	0	22	0	0	484	0	0	0	22	0	0	0	0	0	484
10	22	1	0	1	-10	12	-120	0	144	0	-10	0	12	0	-120	0	100	0	144

In the above matrix, the first column (N) contains the observation number (one trial per line). Column two (R L) lists the firing rate of the neuron for that trial. Following columns (1 – 18) correspond to the respective parameters defined above.

Based on this matrix, the REG procedure estimates values for the parameters beginning with the intercept and a spatial parameter that has a $p < 0.05$ at the entry level (entry into the model). This model is then tested for the goodness of fit using the ANOVA, R^2-value, and C_p-value. The following is the summary of the first step:

Stepwise Selection: Step 1
GROUP5 Entered: R-Square = 0.1835 and C(p) = 49.1368
Analysis of Variance

DF	Sum of Squares	Mean Square	F Value	Pr>F	Source
2	3859.87103	1929.93551	20.00	<.0001	Model
178	17180	96.51609			Error
180	21040				Corrected Total

The summary statement above is a result of testing the model with the following parameters. These parameters were added to the model because their *p*-value at the entry level was less than 0.05.

Parameter Estimate	Standard Error	Type II SS	F Value	Pr > F	Variable
26.52286	1.14212	52050	539.28	<.0001	Intercept
		3859.87103	20.00	<.0001	GROUP5
-0.02749	0.00454	3534.48278	36.62	<.0001	yypos
-0.04407	0.01572	758.25962	7.86	0.0056	yytp0

Here, the y^2 (group 5) parameter was included in the model in addition to the intercept parameter. As shown by the overall *f*-test of the entire group 5, $p < 0.0001$. The parameters *yypos* ($p < 0.0001$) and *yytp0* ($p = 0.0056$) are both individually significant. The first column 'parameter estimate' is the estimated value of the parameter in this model. This value may change once more parameters are added and the model is retested.

In the second step, another parameter with significance at the entry level is added to the model. The whole model is then tested again. The summary of this step is reproduced below:

Stepwise Selection: Step 2
GROUP1 Entered: R-Square = 0.2620 and C(p) = 29.5764
Analysis of Variance

DF	Sum of Squares	Mean Square	F Value	Pr>F	Source
3	5512.45386	1837.48462	20.95	<.0001	Model
177	15527	87.72475			Error
180	21040				Corrected Total

Based on the R^2 and the C_p value, it can be seen that this model fits the data better than the model tested in step one. The parameter results included in this model are reproduced below:

Parameter Estimate	Standard Error	Type II SS	F Value	Pr > F	Variable
30.42563	1.41215	40723	464.21	<.0001	Intercept
		1652.58283	18.84	<.0001	GROUP1
-9.62563	2.21773	1652.58283	18.84	<.0001	tp0
		5148.29952	29.34	<.0001	GROUP5
-0.03716	0.00487	5107.21063	58.22	<.0001	yypos
0.02283	0.02150	98.87850	1.13	0.2898	yytp0

Although *yytp0* is now non-significant ($p = 0.2898$), due to the overall significant value of group 5, the parameter is maintained in the model.

The summary and the parameters included in the third step are reproduced below:

Stepwise Selection: Step 3
GROUP2 Entered: R-Square = 0.3231 and C(p) = 16.7917
Analysis of Variance

DF	Sum of Squares	Mean Square	F Value	Pr>F	Source
5	6798.98719	1359.79744	16.71	<.0001	Model
175	14241	81.37570			Error
180	21040				Corrected Total

Parameter Estimate	Standard Error	Type II SS	F Value	Pr > F	Variable
30.42563	1.36009	40723	500.43	<.0001	Intercept
		1652.58283	20.31	<.0001	GROUP1
-9.62563	2.13597	1652.58283	20.31	<.0001	tp0
		1286.53333	7.90	0.0005	GROUP2
-0.45667	0.11646	1251.26667	15.38	0.0001	xpos
0.53333	0.16470	853.33333	10.49	0.0014	xtp0
		5148.29952	31.63	<.0001	GROUP5
-0.03716	0.00469	5107.21063	62.76	<.0001	yypos
0.02283	0.02071	98.87850	1.22	0.2718	yytp0

Based on the R^2 and the C_p value, it can be seen that this model fits the data better than the model tested in step one. The overall significance of group 5 allows the yytp0 parameter to be maintained in the model. Thus far the best fitting model consists of *x* and the y^2 parameters in addition to the intercept.

Group 3 entered the model in the fourth step. The following is the summary and the parameters included in the model during step four:

Stepwise Selection: Step 4
GROUP3 Entered: R-Square = 0.3720 and C(p) = 7.3841
Analysis of Variance

DF	Sum of Squares	Mean Square	F Value	Pr>F	Source
7	7826.66384	1118.09483	14.64	<.0001	Model
173	13213	76.37613			Error
180	21040				Corrected Total

Parameter Estimate	Standard Error	Type II SS	F Value	Pr > F	Variable
34.02383	2.19599	18334	240.05	<.0001	Intercept
		1812.62541	23.73	<.0001	GROUP1
-13.22383	2.71445	1812.62541	23.73	<.0001	tp0
		1286.53333	8.42	0.0003	GROUP2
-0.45667	0.11282	1251.26667	16.38	0.0001	xpos
0.53333	0.15956	853.33333	11.17	0.0010	xtp0
		1027.67665	6.73	0.0015	GROUP3
-0.98297	0.47992	320.40998	4.20	0.0421	ypos
-0.63963	0.49300	128.56662	1.68	0.1962	ytp0
		41.64026	0.27	0.7617	GROUP5
0.00166	0.01949	0.55137	0.01	0.9324	yypos
-0.01599	0.02760	25.63451	0.34	0.5631	yytp0

This model, which includes the x, y, and y^2 parameters in addition to the intercept, is the best fitting model thus far. However, with the inclusion of the y parameter, group5 is observed to be non significant ($p = 0.7617$).

Since group 5 is not significant to describe the model, in step five group5 will be removed and the model will be tested again. Thus this model will now include the x (group 2) and y (group 3) parameters in addition to the intercept. The results are reproduced below:

Stepwise Selection: Step 4
GROUP5 Removed: R-Square = 0.3700 and C(p) = 3.9274
Analysis of Variance

DF	Sum of Squares	Mean Square	F Value	Pr>F	Source
5	7785.02358	1557.00472	20.56	<.0001	Model
175	13255	75.74121			Error
180	21040			Corrected Total	

Parameter Estimate	Standard Error	Type II SS	F Value	Pr > F	Variable
33.89744	1.60874	33628	443.98	<.0001	Intercept
		4361.40965	57.58	<.0001	GROUP1
-14.05300	1.85192	4361.40965	57.58	<.0001	tp0
		1286.53333	8.49	0.0003	GROUP2
-0.45667	0.11235	1251.26667	16.52	<.0001	xpos
0.53333	0.15889	853.33333	11.27	0.0010	xtp0
		6134.33590	40.50	<.0001	GROUP3
-0.94332	0.11144	5427.06923	71.65	<.0001	ypos
0.59998	0.15825	1088.76294	14.37	0.0002	ytp0

The model without the group 5 parameters is observed to be the best fitting model (R^2 = 0.3700; C_p = 3.9274) for the data set. Only *x* and *y* parameters remain in the model in addition to the intercept. These parameters maintained a *p*-value of less than 0.05 throughout the steps of regression. Below is the summary of the entire analysis followed by the resulting model:

```
All groups of variables left in the model are significant at the 0.0500
level.

No other group of variables met the 0.0500 significance level for entry
into the model.
```

Summary of Stepwise Selection

Step	Group Entered	Group Removed	Number Vars In	Part R-Sq	Model R-Sq	C(p)	F Value	Pr > F
1	GROUP5		2	0.1835	0.1835	49.1368	20.00	<.0001
2	GROUP1		3	0.0785	0.2620	29.5764	18.84	<.0001
3	GROUP2		5	0.0611	0.3231	16.7917	7.90	0.0005
4	GROUP3		7	0.0488	0.3720	7.3841	6.73	0.0015
5		GROUP5	5	0.0020	0.3700	3.9274	0.27	0.7617

MODEL	_TYPE_	_DEPVAR_	_RMSE_	Intercept	tp0
MODEL1	PARMS	rateL	8.70294	33.8974	-14.0530

tp1	xpos	xtp0	xtp1	ypos	ytp0	ytp1
.	-0.45667	0.53333	.	-0.94332	0.59998	.

xxpos	xxtp0	xxtp1	yypos	yytp0	yytp1
.	.	.	.	.	.

Each dot in the model represents 0. Since the parameters *xxpos* and *yypos* did not have significant values, i.e., the estimated values of these parameters were not

significantly different from 0, these parameters were excluded from the model. Based on this model, the following are the definitions for the rate of the neuron in the absence (pre-prism condition) and the presence (prism condition) of the prism:

Pre-prism condition (type 0): $rate = 0.077x - 0.343y + 19.8$

Prism condition (type 1): $rate = -0.457x - 0.943y + 33.9$

Since only significant parameters are maintained in the model, the two model statements above are considered different from each other. The *x* and *y* parameters correspond to the horizontal and vertical spatial components. This indicates that the spatial tuning of this neuron is different for the two conditions; the slopes of the response fields of this neuron are different with and without the prism. The intercept values of the population during pre-prism and prism conditions are compared using paired *t*-test. The linear spatial components for each condition are used to derive the direction and amplitude of the spatial tuning. These were then statistically compared using circular statistics to determine the whether the sample pool consisted of a mean direction. All significant levels, for both *t*-tests and *f*-tests were set to $p < 0.05$.

Appendix C: Two way analysis of variance

Two-way analysis of variance (ANOVA) was used to test whether neurons in DP and area 7a respond differentially to the onset of the visual stimulus (visual response) change in visual stimulus, and the initiation of the reaching movement (reach response). The firing rate was the dependent variable and the position of the visual stimulus and the event were the independent variables.

In order to test the visual response, neural activity during the 500 ms time interval after the onset of the visual stimulus was compared to the neural activity during 500 ms immediately prior to this event. Similarly to investigate the preparatory response, the neural response during 500 ms time interval after the change in stimulus was compared to the response during 500 ms time interval prior to the event. However, since the motion of the stimulus changes, this change in neural response is confounded by the change in visual input. Lastly neural response during the 500 ms time interval before and after the lift hand event was compared to investigate the reach response. Since the visual stimulus is constant (unstructured) before and after the initiation of the reach, any change in neural response detected during this time interval is a result of the reaching movement. The significance level was set to $p < 0.05$. Data for DP and area 7a was combined for the analysis.

Based on the results of the ANOVA, the neurons were classified into four categories: interactive, position, intercept, and not significant (NS). The interactive classified neurons were those that altered their firing rate at the onset of the event dependant on the position of the stimulus. These neurons were position selective and were thus spatially tuned. These neurons altered their spatial tuning as well as their firing

rate at the onset of the event. The neurons classified as position neurons were sensitive for the position of the visual stimulus. These neurons did not alter their firing rate at the onset of the event. The intercept neurons had different firing rates before and after the event however these neurons were not spatially tuned. The non significant neurons (NS) did not show any effect.

For the EVAR condition (Fig. A1), 54/164 (33%, visual); 35/164 (21%, preparatory); and 50/164 (30%, reach) neurons were classified as having an interactive effect. These neurons had a selective response to the position of the stimulus at the onset of the visual stimulus, change in the stimulus, and initiation of the reach. About 21% (34/164, visual); 38% (62/164, preparatory); and 32% (52/164, reach) neurons were classified as 'position' neurons. These neurons were spatially tuned however, the overall firing rate of the neurons was maintained before and the after the event occurrence. This implies that neurons in DP and area 7a have gain fields and are spatially selective during the planning and reaching phase of the behavioral task. About 11% (18/164, visual); 12% (20/164, preparatory); and 12% (19/164, reach) neurons were not spatially tuned, however, altered their firing rates at the onset of an event. The overall firing rate before and after the event was different. Therefore a total of

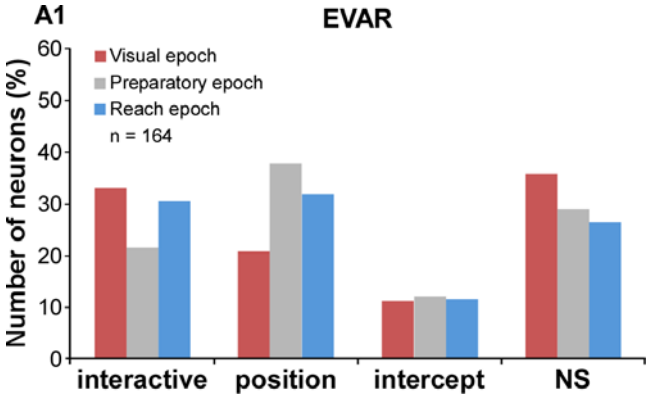


Figure A1: Population distribution of EVAR condition. Interactive, neurons that had alteration in their firing rate and spatial tuning – both event and position effect; position, neurons with change in only spatial tuning – position of the stimulus effect; intercept, neuron with change in only the firing rate – event effect; NS, non-significant neurons – neither event nor position effect.

44% (visual), 33% (preparatory), and 42% (reach) neurons had different tuning properties during the time interval before and after an event. This indicates that DP and area 7a have gain fields and are involved in the reach circuitry during foveal reaching. Neurons in these two areas are involved in both the preparation and the initiation of the reaching behavior when reaching foveally. Lastly, 58/164 (35%, visual); 47/164 (29%, preparatory); and 43/164 (26%, reach) neurons were not spatially tuned and did not have different firing rates during the time intervals before and after the events. These neurons were considered to be NS.

The following are the results for the RVAR condition (Fig. A2). About 29% (34/119, visual); 17% (21/119, preparatory); and 29% (35/119, reach) neurons altered their spatial tuning and firing rates at the onset of either visual, preparatory, or reach event. Four out of 119 (3%, visual); 39/119 (33%, preparatory); and 32/119 (27%, reach) neurons had different spatial tuning properties but no difference in their overall firing rate between the time interval before and after a particular event occurrence. These neurons were sensitive to the position of the visual stimulus. About 22/119 (18%, visual); 8/119 (7%, preparatory); and 11/119 (9%, reach) neurons had different firing rates between the time interval before and after

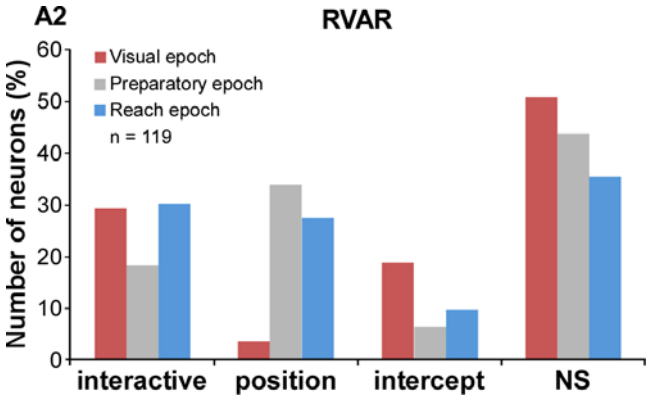


Figure A2: Population distribution of EVAR condition. Interactive, neurons that had alteration in their firing rate and spatial tuning – both event and position effect; position, neurons with change in only spatial tuning – position of the stimulus effect; intercept, neuron with change in only the firing rate – event effect; NS, non-significant neurons – neither event nor position effect.

an event, however, the spatial tuning of these neurons did not alter. A total of 47% (visual), 24% (preparatory), and 38% (reach) neurons altered their tuning properties as a result of the occurrence of an event. This indicates that neurons in DP and area 7a are retinotopic and involved in preparation and initiation of the reaching behavior during peripheral reaching. Lastly, 50% (59/119, visual); 43% (51/119, preparatory); and 34% (41/119, reach) neurons did not have an effect of the event or the position of the stimulus, and therefore were classified as NS.

References

Allard T, Clark SA, Jenkins WM, Merzenich MM (1991) Reorganization of somatosensory area 3b representations in adult owl monkeys after digital syndactyly. J Neurophysiol 66:1048-1058.

Andersen RA (1997) Multimodal integration for the representation of space in the posterior parietal cortex. Philos Trans R Soc Lond B Biol Sci 352:1421-1428.

Andersen RA, Buneo CA (2002) Intentional maps in posterior parietal cortex. Annu Rev Neurosci 25:189-220.

Andersen RA, Cui H (2009) Intention, action planning, and decision making in parietal-frontal circuits. Neuron 63:568-583.

Andersen RA, Essick GK, Siegel RM (1985) Encoding of spatial location by posterior parietal neurons. Science 230:456-458.

Andersen RA, Asanuma C, Essick G, Siegel RM (1990) Corticocortical connections of anatomically and physiologically defined subdivisions within the inferior parietal lobule. The Journal of comparative neurology 296:65-113.

Andersen RA, Snyder LH, Bradley DC, Xing J (1997) Multimodal representation of space in the posterior parietal cortex and its use in planning movements. Annu Rev Neurosci 20:303-330.

Andersen RA, Snyder LH, Batista AP, Buneo CA, Cohen YE (1998) Posterior parietal areas specialized for eye movements (LIP) and reach (PRR) using a common coordinate frame. Novartis Found Symp 218:109-122; discussion 122-108, 171-105.

Anderson KC, Siegel RM (1999) Optic flow selectivity in the anterior superior temporal polysensory area, STPa, of the behaving monkey. J Neurosci 19:2681-2692.

Asanuma C, Andersen RA, Cowan WM (1985) The thalamic relations of the caudal inferior parietal lobule and the lateral prefrontal cortex in monkeys: divergent cortical projections from cell clusters in the medial pulvinar nucleus. The Journal of comparative neurology 241:357-381.

Baizer JS, Ungerleider LG, Desimone R (1991) Organization of visual inputs to the inferior temporal and posterior parietal cortex in macaques. J Neurosci 11:168-190.

Bàlint R (1909) Seelenlähmung des "Schauens", optische Ataxie und räumliche Störung der Aufmerksamkeit. Monatsschrift für Psychiatrie und Neurologie 25:51-81.

Barrash J (1998) A historical review of topographical disorientation and its neuroanatomical correlates. J Clin Exp Neuropsychol 20:807-827.

Barrash J, Damasio H, Adolphs R, Tranel D (2000) The neuroanatomical correlates of route learning impairment. Neuropsychologia 38:820-836.

Batista AP, Andersen RA (2001) The parietal reach region codes the next planned movement in a sequential reach task. J Neurophysiol 85:539-544.

Batista AP, Buneo CA, Snyder LH, Andersen RA (1999) Reach plans in eye-centered coordinates. Science 285:257-260.

Batista AP, Santhanam G, Yu BM, Ryu SI, Afshar A, Shenoy KV (2007) Reference frames for reach planning in macaque dorsal premotor cortex. J Neurophysiol 98:966-983.

Battaglia-Mayer A, Caminiti R (2002) Optic ataxia as a result of the breakdown of the global tuning fields of parietal neurones. Brain 125:225-237.

Battaglia-Mayer A, Mascaro M, Caminiti R (2007) Temporal evolution and strength of neural activity in parietal cortex during eye and hand movements. Cereb Cortex 17:1350-1363.

Battaglia-Mayer A, Mascaro M, Brunamonti E, Caminiti R (2005) The over-representation of contralateral space in parietal cortex: a positive image of directional motor components of neglect? Cereb Cortex 15:514-525.

Battaglia-Mayer A, Ferraina S, Mitsuda T, Marconi B, Genovesio A, Onorati P, Lacquaniti F, Caminiti R (2000) Early coding of reaching in the parietooccipital cortex. J Neurophysiol 83:2374-2391.

Battaglia-Mayer A, Ferraina S, Genovesio A, Marconi B, Squatrito S, Molinari M, Lacquaniti F, Caminiti R (2001) Eye-hand coordination during reaching. II. An analysis of the relationships between visuomanual signals in parietal cortex and parieto-frontal association projections. Cereb Cortex 11:528-544.

Battaglia Mayer A, Ferraina S, Marconi B, Bullis JB, Lacquaniti F, Burnod Y, Baraduc P, Caminiti R (1998) Early motor influences on visuomotor transformations for reaching: a positive image of optic ataxia. Exp Brain Res 123:172-189.

Bender DB, Youakim M (2001) Effect of attentive fixation in macaque thalamus and cortex. J Neurophysiol 85:219-234.

Berberovic N, Mattingley JB (2003) Effects of prismatic adaptation on judgements of spatial extent in peripersonal and extrapersonal space. Neuropsychologia 41:493-503.

Beurze SM, de Lange FP, Toni I, Medendorp WP (2007) Integration of target and effector information in the human brain during reach planning. J Neurophysiol 97:188-199.

Biguer B, Jeannerod M, Prablanc C (1982) The coordination of eye, head, and arm movements during reaching at a single visual target. Exp Brain Res 46:301-304.

Blatt GJ, Andersen RA, Stoner GR (1990) Visual receptive field organization and cortico-cortical connections of the lateral intraparietal area (area LIP) in the macaque. The Journal of comparative neurology 299:421-445.

Blum B (1985) Manipulation reach and visual reach neurons in the inferior parietal lobule of the rhesus monkey. Behav Brain Res 18:167-173.

Boussaoud D, Wise SP (1993) Primate frontal cortex: effects of stimulus and movement. Exp Brain Res 95:28-40.

Boussaoud D, Bremmer F (1999) Gaze effects in the cerebral cortex: reference frames for space coding and action. Exp Brain Res 128:170-180.

Boussaoud D, Barth TM, Wise SP (1993) Effects of gaze on apparent visual responses of frontal cortex neurons. Exp Brain Res 93:423-434.

Boussaoud D, Jouffrais C, Bremmer F (1998) Eye position effects on the neuronal activity of dorsal premotor cortex in the macaque monkey. J Neurophysiol 80:1132-1150.

Bremmer F, Distler C, Hoffmann KP (1997) Eye position effects in monkey cortex. II. Pursuit- and fixation-related activity in posterior parietal areas LIP and 7A. J Neurophysiol 77:962-977.

Breveglieri R, Galletti C, Monaco S, Fattori P (2008) Visual, somatosensory, and bimodal activities in the macaque parietal area PEc. Cereb Cortex 18:806-816.

Breveglieri R, Galletti C, Gamberini M, Passarelli L, Fattori P (2006) Somatosensory cells in area PEc of macaque posterior parietal cortex. J Neurosci 26:3679-3684.

Britten KH, Van Wezel RJ (2002) Area MST and heading perception in macaque monkeys. Cereb Cortex 12:692-701.

Bruce C, Desimone R, Gross CG (1981) Visual properties of neurons in a polysensory area in superior temporal sulcus of the macaque. J Neurophysiol 46:369-384.

Buneo CA, Andersen RA (2006) The posterior parietal cortex: sensorimotor interface for the planning and online control of visually guided movements. Neuropsychologia 44:2594-2606.

Buneo CA, Jarvis MR, Batista AP, Andersen RA (2002) Direct visuomotor transformations for reaching. Nature 416:632-636.

Buneo CA, Jarvis MR, Batista AP, Andersen RA (2003) Properties of spike train spectra in two parietal reach areas. Exp Brain Res 153:134-139.

Buneo CA, Batista AP, Jarvis MR, Andersen RA (2008) Time-invariant reference frames for parietal reach activity. Exp Brain Res 188:77-89.

Burnod Y, Baraduc P, Battaglia-Mayer A, Guigon E, Koechlin E, Ferraina S, Lacquaniti F, Caminiti R (1999) Parieto-frontal coding of reaching: an integrated framework. Exp Brain Res 129:325-346.

Bushnell MC, Goldberg ME, Robinson DL (1981) Behavioral enhancement of visual responses in monkey cerebral cortex. I. Modulation in posterior parietal cortex related to selective visual attention. J Neurophysiol 46:755-772.

Caminiti R, Ferraina S, Johnson PB (1996) The sources of visual information to the primate frontal lobe: a novel role for the superior parietal lobule. Cereb Cortex 6:319-328.

Cavada C, Goldman-Rakic PS (1989a) Posterior parietal cortex in rhesus monkey: II. Evidence for segregated corticocortical networks linking sensory and limbic areas with the frontal lobe. The Journal of comparative neurology 287:422-445.

Cavada C, Goldman-Rakic PS (1989b) Posterior parietal cortex in rhesus monkey: I. Parcellation of areas based on distinctive limbic and sensory corticocortical connections. The Journal of comparative neurology 287:393-421.

Celebrini S, Newsome WT (1994) Neuronal and psychophysical sensitivity to motion signals in extrastriate area MST of the macaque monkey. J Neurosci 14:4109-4124.

Chang SW, Snyder LH (2010) Idiosyncratic and systematic aspects of spatial representations in the macaque parietal cortex. Proc Natl Acad Sci U S A 107:7951-7956.

Chang SW, Papadimitriou C, Snyder LH (2009) Using a compound gain field to compute a reach plan. Neuron 64:744-755.

Cheng S, Sabes PN (2007) Calibration of visually guided reaching is driven by error-corrective learning and internal dynamics. J Neurophysiol 97:3057-3069.

Chestek CA, Batista AP, Santhanam G, Yu BM, Afshar A, Cunningham JP, Gilja V, Ryu SI, Churchland MM, Shenoy KV (2007) Single-neuron stability during repeated reaching in macaque premotor cortex. J Neurosci 27:10742-10750.

Churchland MM, Santhanam G, Shenoy KV (2006) Preparatory activity in premotor and motor cortex reflects the speed of the upcoming reach. J Neurophysiol 96:3130-3146.

Clavagnier S, Prado J, Kennedy H, Perenin MT (2007) How humans reach: distinct cortical systems for central and peripheral vision. Neuroscientist 13:22-27.

Clower DM, West RA, Lynch JC, Strick PL (2001) The inferior parietal lobule is the target of output from the superior colliculus, hippocampus, and cerebellum. J Neurosci 21:6283-6291.

Clower DM, Hoffman JM, Votaw JR, Faber TL, Woods RP, Alexander GE (1996) Role of posterior parietal cortex in the recalibration of visually guided reaching. Nature 383:618-621.

Cohen YE, Andersen RA (2000) Reaches to sounds encoded in an eye-centered reference frame. Neuron 27:647-652.

Cohen YE, Andersen RA (2002) A common reference frame for movement plans in the posterior parietal cortex. Nat Rev Neurosci 3:553-562.

Colby CL, Gattass R, Olson CR, Gross CG (1988) Topographical organization of cortical afferents to extrastriate visual area PO in the macaque: a dual tracer study. The Journal of comparative neurology 269:392-413.

Connor CE (2006) Attention: beyond neural response increases. Nat Neurosci 9:1083-1084.

Coull JT, Jones ME, Egan TD, Frith CD, Maze M (2004) Attentional effects of noradrenaline vary with arousal level: selective activation of thalamic pulvinar in humans. Neuroimage 22:315-322.

Cressman EK, Henriques DY (2009) Sensory recalibration of hand position following visuomotor adaptation. J Neurophysiol 102:3505-3518.

Crist RE, Li W, Gilbert CD (2001) Learning to see: experience and attention in primary visual cortex. Nat Neurosci 4:519-525.

Critchley M (1953) The parietal lobes. New York: Hafner Press.

Darian-Smith C, Gilbert CD (1995) Topographic reorganization in the striate cortex of the adult cat and monkey is cortically mediated. J Neurosci 15:1631-1647.

Dean HL, Crowley JC, Platt ML (2004) Visual and saccade-related activity in macaque posterior cingulate cortex. J Neurophysiol 92:3056-3068.

Desmurget M, Grafton S (2000) Forward modeling allows feedback control for fast reaching movements. Trends Cogn Sci 4:423-431.

Desmurget M, Epstein CM, Turner RS, Prablanc C, Alexander GE, Grafton ST (1999) Role of the posterior parietal cortex in updating reaching movements to a visual target. Nat Neurosci 2:563-567.

Fattori P, Gamberini M, Kutz DF, Galletti C (2001) 'Arm-reaching' neurons in the parietal area V6A of the macaque monkey. Eur J Neurosci 13:2309-2313.

Fattori P, Kutz DF, Breveglieri R, Marzocchi N, Galletti C (2005) Spatial tuning of reaching activity in the medial parieto-occipital cortex (area V6A) of macaque monkey. Eur J Neurosci 22:956-972.

Faugier-Grimaud S, Frenois C, Peronnet F (1985) Effects of posterior parietal lesions on visually guided movements in monkeys. Exp Brain Res 59:125-138.

Felleman DJ, Van Essen DC (1991) Distributed hierarchical processing in the primate cerebral cortex. Cereb Cortex 1:1-47.

Ferraina S, Battaglia-Mayer A, Genovesio A, Marconi B, Onorati P, Caminiti R (2001) Early coding of visuomanual coordination during reaching in parietal area PEc. J Neurophysiol 85:462-467.

Ferraina S, Garasto MR, Battaglia-Mayer A, Ferraresi P, Johnson PB, Lacquaniti F, Caminiti R (1997) Visual control of hand-reaching movement: activity in parietal area 7m. Eur J Neurosci 9:1090-1095.

Flook JP, McGonigle BO (1977) Serial adaptation to conflicting prismatic rearrangement effects in monkey and man. Perception 6:15-29.

Fogassi L, Gallese V, Fadiga L, Luppino G, Matelli M, Rizzolatti G (1996) Coding of peripersonal space in inferior premotor cortex (area F4). J Neurophysiol 76:141-157.

Fogassi L, Gallese V, Buccino G, Craighero L, Fadiga L, Rizzolatti G (2001) Cortical mechanism for the visual guidance of hand grasping movements in the monkey: A reversible inactivation study. Brain 124:571-586.

Galletti C, Battaglini PP, Fattori P (1995) Eye position influence on the parieto-occipital area PO (V6) of the macaque monkey. Eur J Neurosci 7:2486-2501.

Galletti C, Fattori P, Kutz DF, Battaglini PP (1997) Arm movement-related neurons in the visual area V6A of the macaque superior parietal lobule. Eur J Neurosci 9:410-413.

Galletti C, Fattori P, Battaglini PP, Shipp S, Zeki S (1996) Functional demarcation of a border between areas V6 and V6A in the superior parietal gyrus of the macaque monkey. Eur J Neurosci 8:30-52.

Gardner EP, Babu KS, Reitzen SD, Ghosh S, Brown AS, Chen J, Hall AL, Herzlinger MD, Kohlenstein JB, Ro JY (2007) Neurophysiology of prehension. I. Posterior parietal cortex and object-oriented hand behaviors. J Neurophysiol 97:387-406.

Gilbert CD (1996a) Learning and receptive field plasticity. Proc Natl Acad Sci U S A 93:10546-10547.

Gilbert CD (1996b) Plasticity in visual perception and physiology. Curr Opin Neurobiol 6:269-274.

Gilbert CD, Li W, Piech V (2009) Perceptual learning and adult cortical plasticity. J Physiol 587:2743-2751.

Goldberg ME, Bruce CJ (1990) Primate frontal eye fields. III. Maintenance of a spatially accurate saccade signal. J Neurophysiol 64:489-508.

Graziano MS, Gross CG (1998) Visual responses with and without fixation: neurons in premotor cortex encode spatial locations independently of eye position. Exp Brain Res 118:373-380.

Graziano MS, Andersen RA, Snowden RJ (1994) Tuning of MST neurons to spiral motions. J Neurosci 14:54-67.

Gregoriou GG, Savaki HE (2003) When vision guides movement: a functional imaging study of the monkey brain. Neuroimage 19:959-967.

Gregoriou GG, Luppino G, Matelli M, Savaki HE (2005) Frontal cortical areas of the monkey brain engaged in reaching behavior: a (14)C-deoxyglucose imaging study. Neuroimage 27:442-464.

Gribble PL, Everling S, Ford K, Mattar A (2002) Hand-eye coordination for rapid pointing movements. Arm movement direction and distance are specified prior to saccade onset. Exp Brain Res 145:372-382.

Healy MH, Symmes D, Ommaya AK (1973) Visual discordance cues induce prism adaptation in normal monkeys. Percept Mot Skills 37:683-693.

Heider B, Jando G, Siegel RM (2005) Functional architecture of retinotopy in visual association cortex of behaving monkey. Cereb Cortex 15:460-478.

Henriques DY, Crawford JD (2000) Direction-dependent distortions of retinocentric space in the visuomotor transformation for pointing. Exp Brain Res 132:179-194.

Henriques DY, Klier EM, Smith MA, Lowy D, Crawford JD (1998) Gaze-centered remapping of remembered visual space in an open-loop pointing task. J Neurosci 18:1583-1594.

Hoshi E, Tanji J (2000) Integration of target and body-part information in the premotor cortex when planning action. Nature 408:466-470.

Hoshi E, Tanji J (2006) Differential involvement of neurons in the dorsal and ventral premotor cortex during processing of visual signals for action planning. J Neurophysiol 95:3596-3616.

Hyvarinen J, Poranen A (1974) Function of the parietal associative area 7 as revealed from cellular discharges in alert monkeys. Brain 97:673-692.

Johnson PB, Ferraina S, Bianchi L, Caminiti R (1996) Cortical networks for visual reaching: physiological and anatomical organization of frontal and parietal lobe arm regions. Cereb Cortex 6:102-119.

Jouffrais C, Boussaoud D (1999) Neuronal activity related to eye-hand coordination in the primate premotor cortex. Exp Brain Res 128:205-209.

Kaas JH, Krubitzer LA, Chino YM, Langston AL, Polley EH, Blair N (1990) Reorganization of retinotopic cortical maps in adult mammals after lesions of the retina. Science 248:229-231.

Kalaska JF (1988) The representation of arm movements in postcentral and parietal cortex. Can J Physiol Pharmacol 66:455-463.

Kapadia MK, Westheimer G, Gilbert CD (1999) Dynamics of spatial summation in primary visual cortex of alert monkeys. Proc Natl Acad Sci U S A 96:12073-12078.

Kitazawa S, Yin PB (2002) Prism adaptation with delayed visual error signals in the monkey. Exp Brain Res 144:258-261.

Kobayashi Y, Amaral DG (2007) Macaque monkey retrosplenial cortex: III. Cortical efferents. The Journal of comparative neurology 502:810-833.

Kurata K (1991) Corticocortical inputs to the dorsal and ventral aspects of the premotor cortex of macaque monkeys. Neurosci Res 12:263-280.

Kurata K (2007) Laterality of movement-related activity reflects transformation of coordinates in ventral premotor cortex and primary motor cortex of monkeys. J Neurophysiol 98:2008-2021.

Kurata K, Tanji J (1986) Premotor cortex neurons in macaques: activity before distal and proximal forelimb movements. J Neurosci 6:403-411.

Kurata K, Hoffman DS (1994) Differential effects of muscimol microinjection into dorsal and ventral aspects of the premotor cortex of monkeys. J Neurophysiol 71:1151-1164.

Kurata K, Hoshi E (1999) Reacquisition deficits in prism adaptation after muscimol microinjection into the ventral premotor cortex of monkeys. J Neurophysiol 81:1927-1938.

Kurata K, Hoshi E (2002) Movement-related neuronal activity reflecting the transformation of coordinates in the ventral premotor cortex of monkeys. J Neurophysiol 88:3118-3132.

Kutz DF, Fattori P, Gamberini M, Breveglieri R, Galletti C (2003) Early- and late-responding cells to saccadic eye movements in the cortical area V6A of macaque monkey. Exp Brain Res 149:83-95.

Lacquaniti F, Guigon E, Bianchi L, Ferraina S, Caminiti R (1995) Representing spatial information for limb movement: role of area 5 in the monkey. Cereb Cortex 5:391-409.

Lamotte RH, Acuna C (1978) Defects in accuracy of reaching after removal of posterior parietal cortex in monkeys. Brain Res 139:309-326.

Lewis JW, Van Essen DC (2000) Corticocortical connections of visual, sensorimotor, and multimodal processing areas in the parietal lobe of the macaque monkey. The Journal of comparative neurology 428:112-137.

Lewis RF, Gaymard BM, Tamargo RJ (1998) Efference copy provides the eye position information required for visually guided reaching. J Neurophysiol 80:1605-1608.

Li CY, Tanaka M, Creutzfeldt OD (1989) Attention and eye movement related activation of neurons in the dorsal prelunate gyrus (area DP). Brain Res 496:307-313.

Li W, Piech V, Gilbert CD (2004) Perceptual learning and top-down influences in primary visual cortex. Nat Neurosci 7:651-657.

Luaute J, Schwartz S, Rossetti Y, Spiridon M, Rode G, Boisson D, Vuilleumier P (2009) Dynamic changes in brain activity during prism adaptation. J Neurosci 29:169-178.

Luppino G, Hamed SB, Gamberini M, Matelli M, Galletti C (2005) Occipital (V6) and parietal (V6A) areas in the anterior wall of the parieto-occipital sulcus of the macaque: a cytoarchitectonic study. Eur J Neurosci 21:3056-3076.

MacKay WA (1992) Properties of reach-related neuronal activity in cortical area 7A. J Neurophysiol 67:1335-1345.

Mallow, CL (1973) Some comments on Cp. Technometrics 15:661-675.

Marotta JJ, Keith GP, Crawford JD (2005) Task-specific sensorimotor adaptation to reversing prisms. J Neurophysiol 93:1104-1110.

Marzocchi N, Breveglieri R, Galletti C, Fattori P (2008) Reaching activity in parietal area V6A of macaque: eye influence on arm activity or retinocentric coding of reaching movements? Eur J Neurosci 27:775-789.

McGonigle BO, Flook J (1978) Long-term retention of single and multistate prismatic adaptation by humans. Nature 272:364-366.

Merchant H, Battaglia-Mayer A, Georgopoulos AP (2001) Effects of optic flow in motor cortex and area 7a. J Neurophysiol 86:1937-1954.

Moran DW, Schwartz AB (1999) Motor cortical representation of speed and direction during reaching. J Neurophysiol 82:2676-2692.

Moran J, Desimone R (1985) Selective attention gates visual processing in the extrastriate cortex. Science 229:782-784.

Motter BC, Mountcastle VB (1981) The functional properties of the light-sensitive neurons of the posterior parietal cortex studied in waking monkeys: foveal sparing and opponent vector organization. J Neurosci 1:3-26.

Mountcastle VB, Andersen RA, Motter BC (1981) The influence of attentive fixation upon the excitability of the light- sensitive neurons of the posterior parietal cortex. JNeurosci 1:1218-1225.

Mountcastle VB, Motter BC, Steinmetz MA, Sestokas AK (1987a) Common and differential effects of attentive fixation on the excitability of parietal and prestriate (V4) cortical visual neurons in the macaque monkey. J Neurosci 7:2239-2255.

Mountcastle VB, Motter BC, Steinmetz MA, Sestokas AK (1987b) Common and differential effects of attentive fixation on the excitability of parietal and prestriate (V4) cortical visual neurons in the macaque monkey. Journal of Neuroscience 7:2239-2255.

Mountcastle VB, Lynch JC, Georgopoulos A, Sakata H, Acuna C (1975) Posterior parietal association cortex of the monkey: command functions for operations within extrapersonal space. J Neurophysiol 38:871-908.

Muakkassa KF, Strick PL (1979) Frontal lobe inputs to primate motor cortex: evidence for four somatotopically organized 'premotor' areas. Brain Res 177:176-182.

Mushiake H, Tanatsugu Y, Tanji J (1997) Neuronal activity in the ventral part of premotor cortex during target-reach movement is modulated by direction of gaze. J Neurophysiol 78:567-571.

Nakamura K, Chung HH, Graziano MS, Gross CG (1999) Dynamic representation of eye position in the parieto-occipital sulcus. J Neurophysiol 81:2374-2385.

Neal JW, Pearson RC, Powell TP (1988) The cortico-cortical connections within the parieto-temporal lobe of area PG,7a, in the monkey. Brain Res 438:343-350.

Olson CR, Musil SY, Goldberg ME (1996) Single neurons in posterior cingulate cortex of behaving macaque: eye movement signals. J Neurophysiol 76:3285-3300.

Pandya DN, Seltzer B (1982) Intrinsic connections and architectonics of posterior parietal cortex in the rhesus monkey. The Journal of comparative neurology 204:196-210.

Pesaran B, Nelson MJ, Andersen RA (2006) Dorsal premotor neurons encode the relative position of the hand, eye, and goal during reach planning. Neuron 51:125-134.

Peterhans E, Heider B, Baumann R (2005) Neurons in monkey visual cortex detect lines defined by coherent motion of dots. Eur J Neurosci 21:1091-1100.

Pisella L, Grea H, Tilikete C, Vighetto A, Desmurget M, Rode G, Boisson D, Rossetti Y (2000) An 'automatic pilot' for the hand in human posterior parietal cortex: toward reinterpreting optic ataxia. Nat Neurosci 3:729-736.

Polley DB, Steinberg EE, Merzenich MM (2006) Perceptual learning directs auditory cortical map reorganization through top-down influences. J Neurosci 26:4970-4982.

Prablanc C, Pelisson D, Goodale MA (1986) Visual control of reaching movements without vision of the limb. I. Role of retinal feedback of target position in guiding the hand. Exp Brain Res 62:293-302.

Prado J, Clavagnier S, Otzenberger H, Scheiber C, Kennedy H, Perenin MT (2005) Two cortical systems for reaching in central and peripheral vision. Neuron 48:849-858.

Prud'homme MJ, Kalaska JF (1994) Proprioceptive activity in primate primary somatosensory cortex during active arm reaching movements. J Neurophysiol 72:2280-2301.

Quraishi S, Heider B, Siegel RM (2006) Attentional Modulation of Receptive Field Structure in Area 7a of the Behaving Monkey. Cereb Cortex.

Quraishi S, Heider B, Siegel RM (2007) Attentional modulation of receptive field structure in area 7a of the behaving monkey. Cereb Cortex 17:1841-1857.

Raffi M, Siegel RM (2005) Functional architecture of spatial attention in the parietal cortex of the behaving monkey. J Neurosci 25:5171-5186.

Raffi M, Siegel RM (2007) A functional architecture of optic flow in the inferior parietal lobule of the behaving monkey. PLoS ONE 2:e200.

Raiguel S, Vogels R, Mysore SG, Orban GA (2006) Learning to see the difference specifically alters the most informative V4 neurons. J Neurosci 26:6589-6602.

Raos V, Umilta MA, Murata A, Fogassi L, Gallese V (2006) Functional properties of grasping-related neurons in the ventral premotor area F5 of the macaque monkey. J Neurophysiol 95:709-729.

Read HL, Siegel RM (1997) Modulation of responses to optic flow in area 7a by retinotopic and oculomotor cues in monkey. Cereb Cortex 7:647-661.

Redding GM, Wallace B (1988) Components of prism adaptation in terminal and concurrent exposure: organization of the eye-hand coordination loop. Percept Psychophys 44:59-68.

Redding GM, Wallace B (1996) Adaptive spatial alignment and strategic perceptual-motor control. J Exp Psychol Hum Percept Perform 22:379-394.

Redding GM, Clark SE, Wallace B (1985) Attention and prism adaptation. Cogn Psychol 17:1-25.

Redding GM, Rossetti Y, Wallace B (2005) Applications of prism adaptation: a tutorial in theory and method. Neurosci Biobehav Rev 29:431-444.

Reep RL, Corwin JV (2009) Posterior parietal cortex as part of a neural network for directed attention in rats. Neurobiol Learn Mem 91:104-113.

Richter H, Magnusson S, Imamura K, Fredrikson M, Okura M, Watanabe Y, Langstrom B (2002) Long-term adaptation to prism-induced inversion of the retinal images. Exp Brain Res 144:445-457.

Rizzolatti G, Matelli M (2003) Two different streams form the dorsal visual system: anatomy and functions. Exp Brain Res 153:146-157.

Rode G, Pisella L, Rossetti Y, Farne A, Boisson D (2003) Bottom-up transfer of sensory-motor plasticity to recovery of spatial cognition: visuomotor adaptation and spatial neglect. Prog Brain Res 142:273-287.

Rossetti Y, Koga K, Mano T (1993) Prismatic displacement of vision induces transient changes in the timing of eye-hand coordination. Percept Psychophys 54:355-364.

Rossetti Y, Rode G, Pisella L, Farne A, Li L, Boisson D, Perenin MT (1998) Prism adaptation to a rightward optical deviation rehabilitates left hemispatial neglect. Nature 395:166-169.

Rozzi S, Ferrari PF, Bonini L, Rizzolatti G, Fogassi L (2008) Functional organization of inferior parietal lobule convexity in the macaque monkey: electrophysiological characterization of motor, sensory and mirror responses and their correlation with cytoarchitectonic areas. Eur J Neurosci 28:1569-1588.

Rozzi S, Calzavara R, Belmalih A, Borra E, Gregoriou GG, Matelli M, Luppino G (2006) Cortical connections of the inferior parietal cortical convexity of the macaque monkey. Cereb Cortex 16:1389-1417.

Rushworth MF, Nixon PD, Passingham RE (1997a) Parietal cortex and movement. II. Spatial representation. Exp Brain Res 117:311-323.

Rushworth MF, Nixon PD, Passingham RE (1997b) Parietal cortex and movement. I. Movement selection and reaching. Exp Brain Res 117:292-310.

Scheidt RA, Conditt MA, Secco EL, Mussa-Ivaldi FA (2005) Interaction of visual and proprioceptive feedback during adaptation of human reaching movements. J Neurophysiol 93:3200-3213.

Scherberger H, Andersen RA (2007) Target selection signals for arm reaching in the posterior parietal cortex. J Neurosci 27:2001-2012.

Scherberger H, Jarvis MR, Andersen RA (2005) Cortical local field potential encodes movement intentions in the posterior parietal cortex. Neuron 46:347-354.

Schummers J, Sharma J, Sur M (2005) Bottom-up and top-down dynamics in visual cortex. Prog Brain Res 149:65-81.

Shipp S (2004) The brain circuitry of attention. Trends Cogn Sci 8:223-230.

Shipp S, Blanton M, Zeki S (1998) A visuo-somatomotor pathway through superior parietal cortex in the macaque monkey: cortical connections of areas V6 and V6A. Eur J Neurosci 10:3171-3193.

Siegel RM, Read HL (1997) Analysis of optic flow in the monkey parietal area 7a. Cereb Cortex 7:327-346.

Siegel RM, Duann JR, Jung TP, Sejnowski T (2007) Spatiotemporal dynamics of the functional architecture for gain fields in inferior parietal lobule of behaving monkey. Cereb Cortex 17:378-390.

Siegel RM, Raffi M, Phinney RE, Turner JA, Jando G (2003) Functional architecture of eye position gain fields in visual association cortex of behaving monkey. J Neurophysiol 90:1279-1294.

Snyder LH, Batista AP, Andersen RA (1997) Coding of intention in the posterior parietal cortex. Nature 386:167-170.

Snyder LH, Batista AP, Andersen RA (2000) Saccade-related activity in the parietal reach region. J Neurophysiol 83:1099-1102.

Snyder LH, Dickinson AR, Calton JL (2006) Preparatory delay activity in the monkey parietal reach region predicts reach reaction times. J Neurosci 26:10091-10099.

Stepniewska I, Collins CE, Kaas JH (2005) Reappraisal of DL/V4 boundaries based on connectivity patterns of dorsolateral visual cortex in macaques. Cereb Cortex 15:809-822.

Stepniewska I, Preuss TM, Kaas JH (2006) Ipsilateral cortical connections of dorsal and ventral premotor areas in New World owl monkeys. The Journal of comparative neurology 495:691-708.

Stricanne B, Andersen RA, Mazzoni P (1996) Eye-centered, head-centered, and intermediate coding of remembered sound locations in area LIP. J Neurophysiol 76:2071-2076.

Sugita Y (1996) Global plasticity in adult visual cortex following reversal of visual input. Nature 380:523-526.

Tanaka M, Lindsley E, Lausmann S, Creutzfeldt OD (1990) Afferent connections of the prelunate visual association cortex (areas V4 and DP). Anat Embryol (Berl) 181:19-30.

Tanne-Gariepy J, Rouiller EM, Boussaoud D (2002) Parietal inputs to dorsal versus ventral premotor areas in the macaque monkey: evidence for largely segregated visuomotor pathways. Exp Brain Res 145:91-103.

Tanne J, Boussaoud D, Boyer-Zeller N, Rouiller EM (1995) Direct visual pathways for reaching movements in the macaque monkey. Neuroreport 7:267-272.

Teich AF, Qian N (2010) V1 orientation plasticity is explained by broadly tuned feedforward inputs and intracortical sharpening. Vis Neurosci:1-17.

Ungerleider LG, Galkin TW, Desimone R, Gattass R (2008) Cortical connections of area V4 in the macaque. Cereb Cortex 18:477-499.

Vercher JL, Magenes G, Prablanc C, Gauthier GM (1994) Eye-head-hand coordination in pointing at visual targets: spatial and temporal analysis. Exp Brain Res 99:507-523.

Vetter P, Goodbody SJ, Wolpert DM (1999) Evidence for an eye-centered spherical representation of the visuomotor map. J Neurophysiol 81:935-939.

Wang X, Zhang M, Cohen IS, Goldberg ME (2007) The proprioceptive representation of eye position in monkey primary somatosensory cortex. Nat Neurosci 10:640-646.

Welch RB, Choe CS, Heinrich DR (1974) Evidence for a three-component model of prism adaptation. J Exp Psychol 103:700-705.

Wilkinson DA (1971) Visual-motor control loop: a linear system? J Exp Psychol 89:250-257.

Wise SP, Boussaoud D, Johnson PB, Caminiti R (1997) Premotor and parietal cortex: corticocortical connectivity and combinatorial computations. Annu Rev Neurosci 20:25-42.

Womelsdorf T, Anton-Erxleben K, Pieper F, Treue S (2006) Dynamic shifts of visual receptive fields in cortical area MT by spatial attention. Nat Neurosci 9:1156-1160.

Xing J, Andersen RA (2000) Models of the posterior parietal cortex which perform multimodal integration and represent space in several coordinate frames. J Cogn Neurosci 12:601-614.

Yang T, Maunsell JH (2004) The effect of perceptual learning on neuronal responses in monkey visual area V4. J Neurosci 24:1617-1626.

Yin PB, Kitazawa S (2001) Long-lasting aftereffects of prism adaptation in the monkey. Exp Brain Res 141:250-253.

Youakim M, Bender DB, Baizer JS (2001) Vertical meridian representation on the prelunate gyrus in area V4 of macaque. Brain Res Bull 56:93-100.

Zeki S, Perry RJ, Bartels A (2003) The processing of kinetic contours in the brain. Cereb Cortex 13:189-202.

Zipser D, Andersen RA (1988) A back-propagation programmed network that simulates response properties of a subset of posterior parietal neurons. Nature 331:679-684.

Curriculum vitae

1984	Born on October 18th in Mumbai, Maharashtra, India
2002	Graduated from Edison High School, Edison, NJ
2004 – 2005	Undergraduate research assistant, Rutgers University, Newark, NJ Advisor: Kent Harber, Ph.D., Department of Psychology, Topic: Effects of social ostracism on perception and sensation of physical discomfort.
2005	PSI CHI – The National Honor Society of Psychology
2005 – 2006	Undergraduate research assistant, Rutgers University, Newark, NJ Advisor: Ralph M. Siegel, Ph.D., Center for Molecular and Behavioral Neuroscience, Thesis topic: Effects of reversing prisms on 3D perception in primates.
2006	B.A. Psychology, Rutgers University, Newark, NJ
2006 – 2010	Graduate Fellowship, Integrative neuroscience, Rutgers University, Newark, NJ
Sept. 2008	Summer Fellowship,Visual Neuroscience: From Spikes to Awareness, Schloss Rauischholzhausen, Hessia, Germany.
Sept. 2008	Invited oral presentation, University of Oxford, UK. Host: Oliver Braddick, Ph.D., Department of Experimental Psychology.
Sept. 2008	Invited oral presentation, University of Bologna, Italy. Host: Milena Raffi, Ph.D., Department of Physiology.
Jun-Jul. 2009	Visiting researcher, Salk Institute, La Jolla, CA Mentor: Ali Cetin, PhD., & Ed Callaway, PhD. Designed and produced adeno associated viral vectors with Ca^{+2} sensors.
2010	Ph.D. in Neuroscience, Rutgers University, Newark, NJ Advisor: Ralph M. Siegel, Ph.D., Center for Molecular and Behavioral Neuroscience. Thesis topic: An adaptive sensorimotor representation for reaching in the inferior parietal lobule of behaving monkeys.